SEISMIC AND RESISTIVITY METHODS OF GEOPHYSICAL EXPLORATION

TECHNICAL RELEASE NO. 44

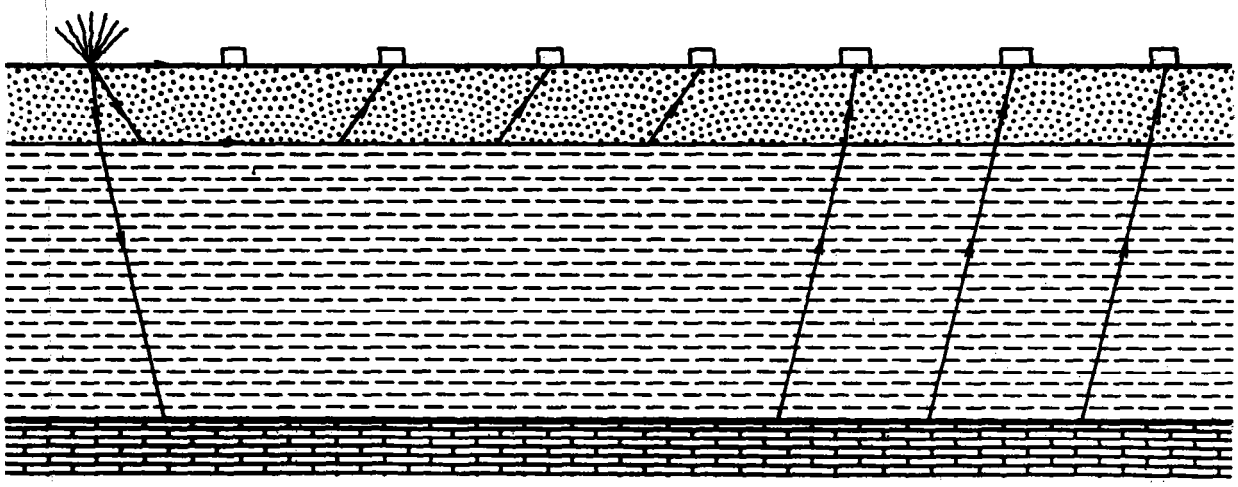

UNITED STATES DEPARTMENT OF AGRICULTURE
SOIL CONSERVATION SERVICE
ENGINEERING DIVISION

by

O.J. Henbest
D.C. Erinakes
D.H. Hixson

PREFACE

This Technical Release, Seismic and Resistivity Methods of Geophysical Exploration, was prepared principally be SCS geologists O. J. Henbest, Forth Worth, Texas, D.C. Erinakes, Orono, Maine, and D.H. Hixson, Hyattsville, Maryland. The following Service personnel (listed in alphabetical order) made many valuable contributions: R.C. Boyce, Upper Darby, Pennsylvania; G.M. Brune, Fort Worth, Texas; R.F. Fonner, Upper Darby, Pennsylvania; A.F. Geiger, Washington, D.C.; D.H. Griswold, Portland, Oregon; J.N. Holeman, Hyattsville, Maryland; J.L. Holland, Portland, Oregon; P.V. Patterson, Portland, Oregon; and O.J. Scherer, Lincoln, Nebraska.

In the preparation of this Technical Release valuable information was obtained through attendance at demonstrations given by manufacturers or distributors, and also through their discussions at SCS training workshops. The literature provided by them and the training received from Soiltest at Baraboo, Wisconsin have been particularly valuable to SCS geologists.

Grateful acknowledgement is extended to Soiltest for permission to make liberal use of figures and text from their Earth Resistivity Manual.

Comments for improvement or correction are welcome and should be sent to the Engineering Division, Washington, D.C.

This issue is for in-Service use and material contained herein is not released for publication.

Washington, D.C. December 1969

Reprinted with minor revisions and corrections August 1971

TECHNICAL RELEASE

NUMBER 44

SEISMIC AND RESISTIVITY METHODS OF GEOPHYSICAL EXPLORATION

Table of Contents

CHAPTER 1. INTRODUCTION

This is intended as a general guide to the selection and use of portable seismic and resistivity geophysical equipment owned by the SCS or which has been observed as suitable for its needs. Trade names are used solely to provide specific information. Mention of a trade name does not constitute a guarantee of the product by the U. S. Department of Agriculture nor does it imply an endorsement by the Department of Agriculture over comparable products that are not named.

Purpose and Scope

This guide is designed to acquaint geologists, engineers, and soil scientists with the types of seismic and resistivity equipment adaptable to SCS use and the results and application that can be expected from the equipment. Other geophysical methods such as; nuclear moisture-density, magnetic, gravity, electro-mechanical, etc. will not be discussed in this guide. It should be understood that geophysical equipment alone will not provide the detailed conclusive data needed on geologic conditions and engineering interpretations. It is necessary to correlate detailed geophysical exploration with accurate data obtained with power equipment; however, the geophysical methods are especially useful in areas where accessibility or economy prohibit or limit the use of heavy equipment. Properly used they may save a great deal of time and expense.

Several types of portable seismographs and electrical resistivity equipment are described. Procedures are described for general operation of the equipment, plotting and computing the results, and making interpretations. Specific step by step operation, calibration and maintenance procedures are obtained from the manuals furnished with each instrument by the manufacturers.

New types of equipment and improvements of earlier models are being marketed in increasing numbers. There are no adequate textbooks or guides available which give the necessary information on the use and capabilities of geophysical equipment and interpretation of the results. The reference list includes several reports and studies by consultants, the description and use of equipment by the manufacturers, and other useful information on geophysical studies.

It is advisable to get brochures and specifications of the equipment desired before ordering. Arrangements may sometimes be made for representatives to demonstrate equipment and train personnel in its use. The E&WP Units will provide assistance in recommending and evaluating equipment.

Applicability to SCS Work

The methods of electrical resistivity and seismic refraction are particularly applicable to SCS work. They offer a means of relatively fast and inexpensive subsurface investigation that will in many cases locate boundaries between different materials and permit interpretation of material types. By the use of these techniques subsurface conditions and/or the location of troublesome areas can be assumed prior to detailed drilling or test pitting. Detailed investigation with drilling and auger equipment remains necessary; however, the amount of detailed drilling work is usually lessened and concentrated in areas where problems occur. The information gained by geophysical methods can be utilized in much the same manner as that gained by mechanical means of investigation. It should be understood however that there may be circumstances where the geophysical methods cannot be utilized and only actual exploration will produce usable results. There are also circumstances where mechanical methods cannot be used and only geophysical equipment is suitable.

TECHNICAL RELEASE

NUMBER 44

SEISMIC AND RESISTIVITY METHODS OF GEOPHYSICAL EXPLORATION

CHAPTER 2. SEISMIC REFRACTION METHODS

Contents

Contents (Continued)

Figures

Tables

CHAPTER 2. SEISMIC REFRACTION METHODS

Refraction is based on the principle that shock waves are bent or refracted upon entering a material of different elasticity in much the same way that light waves are bent in passing from air into water. Reflection is the bouncing of shock waves from the surfaces of different media in the same way that light is reflected from a mirror, and is applicable to deep seismic surveys (50'+).

The discussions in this section of the guide deal only with shallow refraction seismology.

Theory

Seismic investigation depends on the propagation of waves in an elastic medium. In the theoretical circumstance, soil and rock will be considered to be a homogeneous, isotropic, elastic media. In field seismic investigations any deviation from this assumed homogeneous, isotropic condition can be interpreted to indicate changes in depth and nature of the subsurface geologic units. The following discussion will explain the relationship of elastic properties to the refracted seismic wave.

Elastic Constants

The elastic properties of rocks can be described by elastic constants such as Young's modulus (E), Bulk modulus (k), Rigidity or shear modulus (η), Poisson's ratio (σ), and Lame's constants (λ and μ).

These elastic constants are ratios of stress to strain with the different constants defined in terms of different stress, such as tension, compression, pressure or shear, and the deformation or strain produced.

Young's Modulus (E)

Young's modulus is the stress-strain ratio in simple tension or compression. The force or stress applied per unit area divided by the unit shortening or lengthening defines Young's modulus (Nettleton, 1940).

$$\text{Stress} = \frac{\vec{F}\ \text{(force)}}{A\ \text{(area)}}$$

$$\text{Strain} = \frac{\Delta L\ \text{(change in length)}}{L\ \text{(original length)}}$$

$$E = \frac{F/A}{\Delta L/L} = \frac{FL}{A\Delta L}$$

E has the units of force per unit area, commonly pounds per square inch (psi).

Bulk Modulus (k)

The Bulk modulus is the stress-strain ratio under uniform compressive stress in all directions. The stress is force per unit area and the strain is the proportional change in volume.

$$\text{Stress} = \frac{F}{A} \frac{\text{(force)}}{\text{(area)}}$$

$$\text{Strain} = \frac{\Delta V}{V} \frac{\text{(change in volume)}}{\text{(original volume)}}$$

$$k = \frac{F/A}{\Delta V/V} = \frac{FV}{A\Delta V}$$

k has the units of force per unit area, commonly psi.

Rigidity or Shear Modulus (η)

The rigidity or shear modulus is the stress-strain ratio for direct shear. It is determined as the shearing stress (F/A) which is the force tangential to the surface displaced per shearing strain ($\Delta L/L$) which is the displacement (ΔL) in the line of force per unit length (L) perpendicular to the line of force.

$$\eta = \frac{F/A}{\Delta L/L} = \frac{FL}{\Delta LA}$$

It also has units of force per unit area, commonly psi.

Poisson's Ratio (σ)

Poisson's ratio is the ratio of the change in shape of a body due to applied force. If a compressive force is applied to a body, a decrease in length of the body will occur in the direction parallel to the force and an increase in width will occur perpendicular to the force. If the applied force is tension the opposite change in dimensions will occur.

If the body has a length L and a width W, Poisson's ratio (σ) is defined as:

$$\sigma = \frac{\Delta W/W}{\Delta L/L}$$

where ΔW and ΔL are changes in width and length due to the applied force.

Lame's Constants (λ and μ)

Lame's constants are two additional elastic constants that are at times convenient to use. They are defined as:

$$\lambda = \frac{\sigma E}{(1 + \sigma)(1 - 2\sigma)}$$

λ has the same units as Young's modulus (psi).

The constant μ is the same as shear modulus defined previously and has units of psi.

Relationship of Elastic Constants

The various elastic constants are mathematically related as shown in the following equations (Nettleton, 1940):

$$k = \frac{E}{3(1 - 2\sigma)}$$

$$k = \lambda + 2/3\mu$$

$$\eta = \frac{E}{2(1 + \sigma)}$$

$$\mu = \frac{E}{2(1 + \sigma)}$$

$$\lambda = \frac{\sigma E}{(1 + \sigma)(1 - 2\sigma)}$$

$$\lambda = k - 2/3\eta$$

$$\sigma = \frac{3k - 2\eta}{6k + 2\eta}$$

$$\sigma = \frac{E}{2\mu} - 1$$

$$\sigma = \frac{\lambda}{2(\lambda + \mu)}$$

Types of Elastic Waves

The application of mechanical energy to material particles creates several types of elastic waves. The propagation of these waves is governed by their behavior in accordance with the previously mentioned parameters of elasticity. The two types of waves involved in seismic exploration work are the longitudinal, primary, or compressional wave and the transverse, secondary, or shear wave. Rayleigh waves and Love waves are two additional types of waves that will be mentioned briefly.

Longitudinal, Compressional, or Primary Waves (V_p)

Longitudinal waves have the greatest velocity of propagation of any elastic wave in the same medium. The motion of the particles of the medium are parallel to the direction of propagation, hence, the name longitudinal. This oscillation creates minute vertical motions which spread in rapid waves similar to those created by an object dropped in water. The velocity of propagation can be calculated from the following equations in which ρ is the density of the elastic medium:

$$V_P = \sqrt{\frac{k + 4/3\eta}{\rho}} = \sqrt{\frac{\lambda + 2\mu}{\rho}}$$

$$= \sqrt{\frac{E}{\rho}\left[1 + \left(\frac{2\sigma^2}{1 - \sigma - 2\sigma^2}\right)\right]}$$

$$= \sqrt{\frac{E}{\rho}\left[\frac{1 - \sigma}{(1 - 2\sigma)(1 + \sigma)}\right]}$$

Transverse, Secondary, or Shear Waves (V_s)

The motion of the particles of the medium for shear waves are perpendicular to the direction of propagation. The deformation is a shearing motion, hence the name shear waves. The speed of propagation can be calculated from the following equations:

$$V_s = \sqrt{\frac{\eta}{\rho}} = \sqrt{\frac{E}{\rho}\ \frac{1}{2(1 + \sigma)}}$$

Rayleigh and Love Waves

Rayleigh and Love waves are two additional types of elastic waves. Both have slower velocities than either longitudinal or shear waves.

Rayleigh waves are transmitted with an elliptical motion that is a combination of both longitudinal and shear waves. The waves are at the free surface of an elastic solid.

Love waves are a type of transverse wave of variable velocity transmitted at the surface when there is an underlying higher speed layer. These waves are propagated by multiple reflection between the upper and lower layer and their velocity varies between the velocity of the upper and lower layer.

Relationship of Velocity and Elastic Constants

The velocities of the longitudinal and shear waves are mathematically related to the elastic constants. In the following equation illustrating this relationship, ρ is the density of the elastic medium.

$$\sigma = \frac{1/2\ (V_p/V_s)^2 - 1}{(V_p/V_s)^2 - 1}$$

$$E = \rho V_s^2\ \frac{(3V_p^2 - 4V_s^2)}{(V_p^2 - V_s^2)}$$

$$\eta = \rho V_s^2$$

$$\lambda = \rho V_s^2[(V_p/V_s)^2 - 2] \text{ or } \rho(V_p^2 - 2V_s^2)$$

$$k = \rho V_s^2[(V_p/V_s)^2 - 4/3]$$

General Principles of Wave Travel

Seismic waves follow the same basic principles of propagation, reflection, and refraction as light waves.

Seismic waves emanating from a point source in a homogeneous isotropic medium are considered to travel as spherical wave fronts.

A ray is normal to the wave front. A ray always reaches a point from a source by a minimum time path which is not necessarily the shortest distance.

Snell's Law

An elastic (seismic) wave (or ray) crossing the boundary between media with different velocities of propagation (V_1 and V_2) is refracted so that:

$$\frac{\sin i}{\sin r} = \frac{V_1}{V_2}$$

where i is the angle of incidence of the ray in medium V_1, and r is the angle of refraction of the ray in medium V_2. The angle of incidence and angle of refraction are measured between the ray and a normal to the boundary between the media. See Figure 2-1.

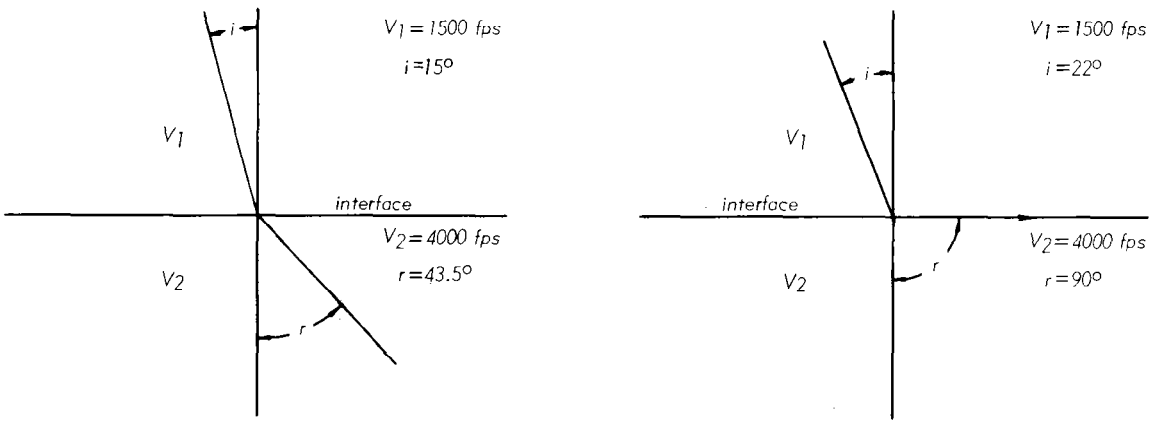

Figure 2–1. – Snells Law.

When a ray in a low speed medium strikes the boundary of a higher speed medium there is a critical angle of incidence where the angle of refraction is 90° and the ray travels along the surface of the higher speed medium.

Since

$$\sin 90° = 1$$

the critical angle of incidence, according to the equation of Snell's Law is:

$$\frac{\sin i}{\sin 90°} = \frac{\sin i}{1} = \frac{V_1}{V_2}$$

where V_2 is greater than V_1.

At angles of incidence less than the critical angle, the ray is refracted but at angles less than 90° and travels within the V_2 medium. At angles of incidence greater than the critical angle the ray is totally reflected.

For the case of seismic refraction, (angle of refraction = 90°) the refracted wave travels along the interface of V_1 and V_2 producing new waves (according to Huygens Principle) that return through the V_1 material to the surface. The wave front generated by these new waves travels to the surface and activates the geophones. Since V_2 must be greater than V_1, at some time after initiation of the original shock wave, the refracted wave front will reach the geophones at the same time or sooner than the non-refracted wave traveling through the surface material.

Figure 2-2 is a graphical model and shows the position of the direct and refracted waves at time increments of 2 through 10 milliseconds after initiation of a seismic wave. The known subsurface conditions depicted in these sketches are two parallel laye with the velocity of the first (V_1) layer 5000 feet per second, the velocity of the second V_2) layer 8000 feet per second and the depth to the second layer 11 feet.

Figure 2-2A shows the position of the wave front at two milliseconds. It is still totally within the V_1 layer, has a radius of 10 feet and has arrived at the first geophone. At 3 milliseconds (Figure 2-2B) the wave front in the V_1 material has a radius of 15 feet, however, it has also reached the V_2 material. One ray at the critical angle determined from Snell's law

$$\frac{\sin i}{1} = \frac{5000}{8000} = 38.6°$$

is refracted along the interface. This refracted wave also generates a wave front as shown and it is only slightly ahead of the V_1 wave. At 4 milliseconds (Figure 2-2C) the V_1 wave front has arrived at the second geophone.

According to Huygen's Principle, any point on a wave front is the source of a new wave front. There are an infinite number of new wave fronts being generated along the interface. The position of the refracted wave at 4 milliseconds is the source of one new wave front and at 5 milliseconds has advanced to the position shown in Figure 2-2D. The position of the original wave front, the refracted wave and new refracted wave fronts at 1 millisecond intervals are shown in Figure 2-2E, through I.

The critical distance is the point where the original V_1 wave and the maximum wave front generated by the V_1 - V_2 refracted wave through the V_1 - V_2 media reach the same point on the ground surface at the same time. A line drawn tangent to the new wave front at any time interval shows the position of the maximum wave front (Figure 2-2H & I). A ray is perpendicular to this wave front. In Figure 2-2H, the point where the ray and the wave front intersect the ground surface is behind the V_1 wave. In Figure 2-2I this point is ahead of the V_1 wave. Therefore, the refracted ray and the V_1 wave front intersect the ground surface at the same point (and time) between 45 and 50 feet (and 9 and 10 milliseconds).

Figure 2-3 is a graphical method of interpolation to find the critical distance. At 9 milliseconds (Figure 2-2H) the surface (V_1) wave is at 45 feet and the maximum wave front intersects the ground surface at 44.5 feet. At 10 milliseconds (Figure 2-2I) the surface wave is at 50 feet and the maximum wave front intersects the ground surface at 52.7 feet. These four points are plotted on rectangular coordinate paper with distance as the abscissa and time the ordinate. The intersection of the lines connecting the points of the surface wave and refracted ray is the critical distance (45.8 feet) and time (9.2 milliseconds).

Checking this graphical representation with the formula on page 2-38.

$$H_1 = \frac{D_1}{2}\sqrt{\frac{V_2 - V_1}{V_2 + V_1}}$$

$$H_1 = \frac{45.8}{2}\sqrt{\frac{8000 - 5000}{8000 + 5000}}$$

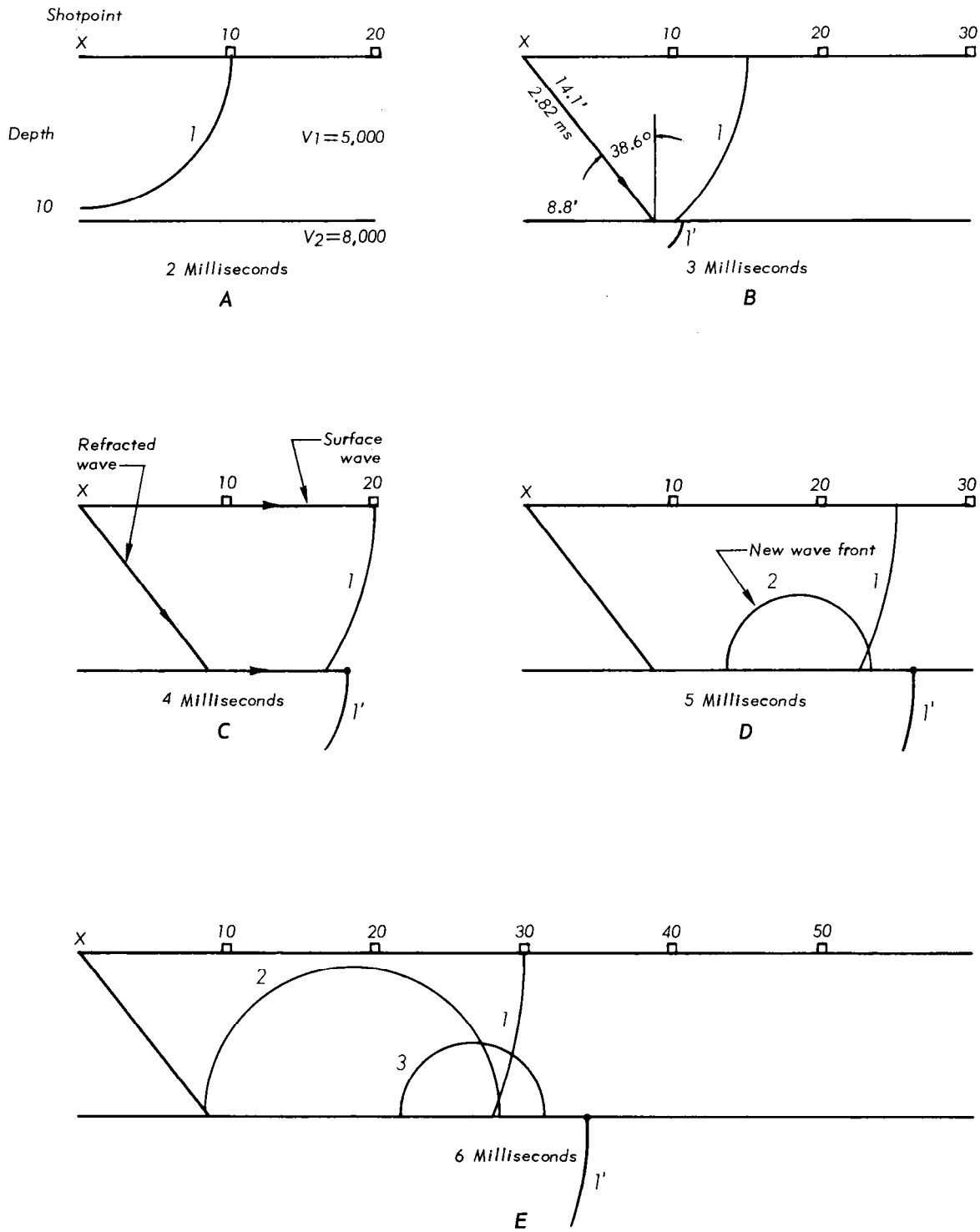

Figure 2–2.– Refracted Waves.

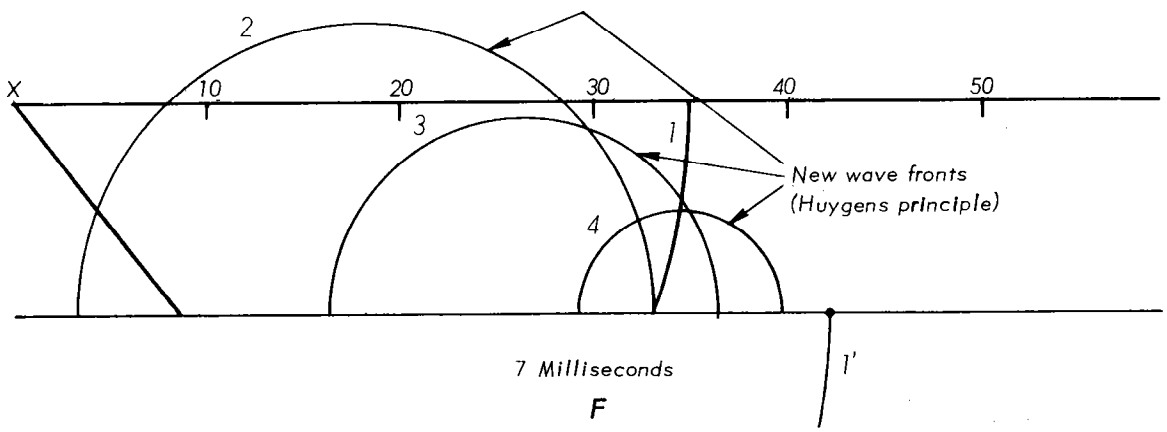

F

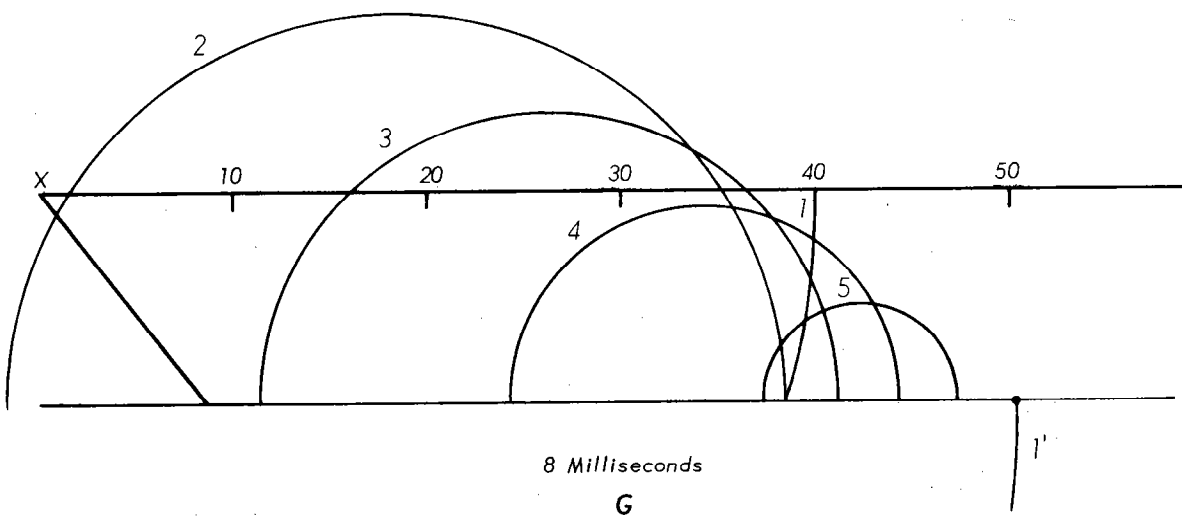

G

Figure 2–2. – Refracted Waves.
(Continued)

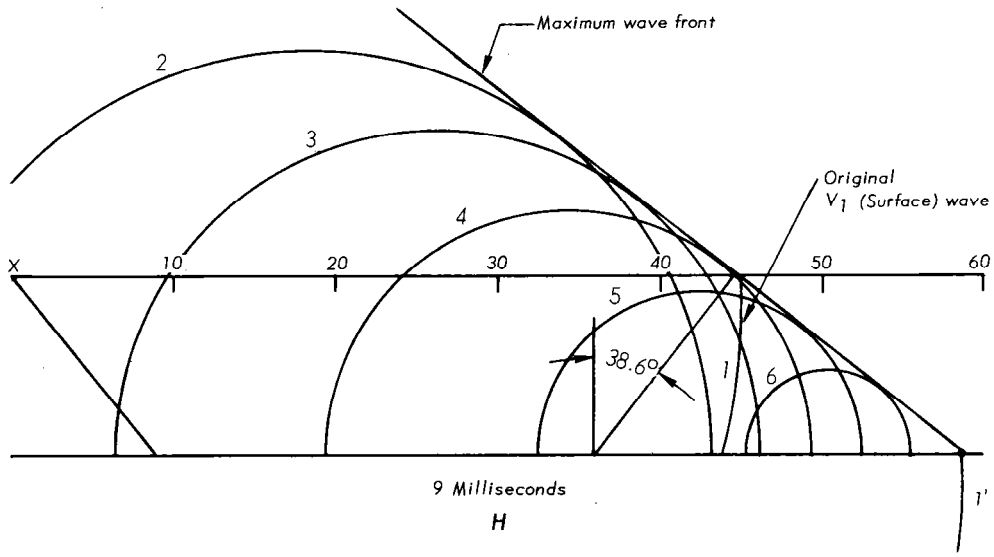

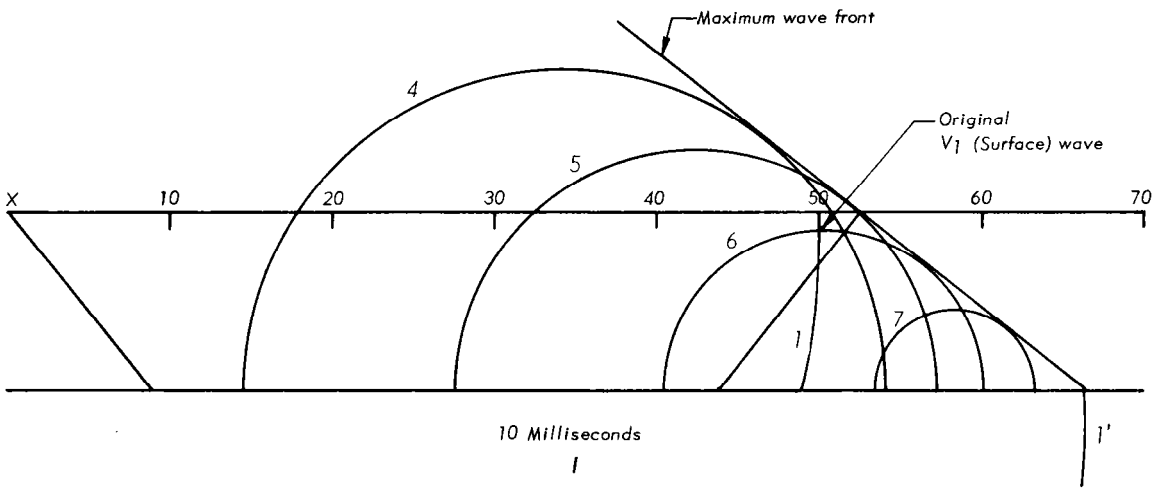

Figure 2–2. – Refracted Waves.
(Continued)

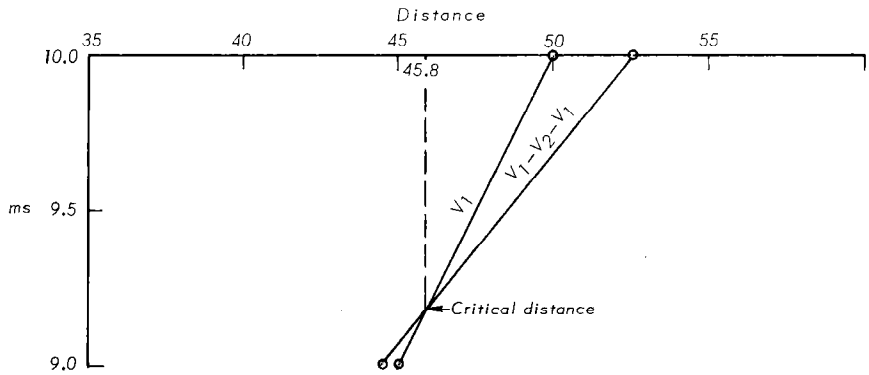

Figure 2–3. – Critical Distance Interpolation.

H_1 = 11 feet (This was assumed in creating the model and thus checks the accuracy of determining the critical distance)

The time of arrival of both waves at the critical distance is

$$\frac{45.8 \text{ ft}}{5000 \text{ ft/sec}} = 9.2 \text{ milliseconds}$$

Multiple layers can be plotted in the same manner as the two layer case above. However, the critical angle of incidence must be recomputed by Snell's law each time the ray of the wave front is refracted along the next lower interface. Using the velocities shown in Figure 2-4 the angles of incidence are computed as follows:

at the V_1 - V_2 interface the critical angle of incidence is

$$\frac{\sin i_1}{1} = \frac{V_1}{V_2} = \frac{1500}{5000} \quad \text{and } i_1 = 17.5°$$

and the angle of refraction is 90°.

When the angle of incidence is not the critical angle and the angle of refraction is not 90° the ray may be refracted so that it travels within medium V_2. If the angle of incidence is i_2 and the angle of refraction i_4 (See Figure 2-4) Snell's law states

$$\frac{\sin i_2}{\sin i_4} = \frac{V_1}{V_2}$$

If this ray then strikes the V_2 - V_3 interface at the critical angle and is refracted 90°, the critical angle is also defined by Snell's law as

$$\frac{\sin i_4}{1} = \frac{V_2}{V_3}$$

substituting this value in the previous equation

$$\frac{\sin i_2}{\frac{V_2}{V_3}} = \frac{V_1}{V_2} \qquad \text{so}$$

$$\sin i_2 = \frac{V_1}{V_2} \frac{V_2}{V_3} = \frac{V_1}{V_3}$$

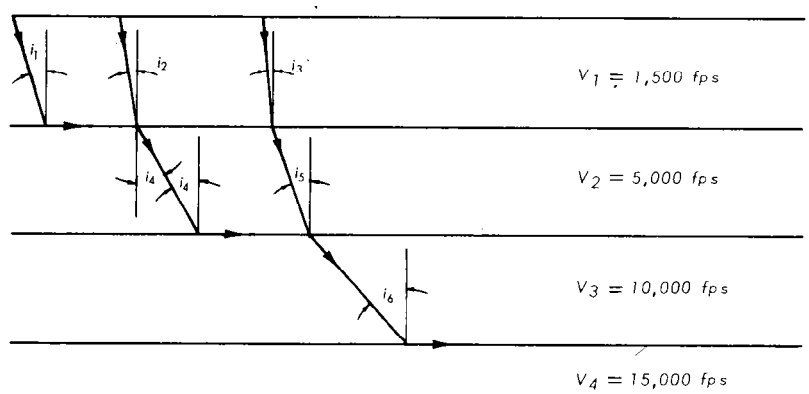

Figure 2–4. – Refracted Waves Multiple Layers.

The angles of incidence as shown in Figure 2-4 are computed as follows:

$$\sin i_1 = \frac{V_1}{V_2} \qquad \sin i_4 = \frac{V_2}{V_3}$$

$$\sin i_2 = \frac{V_1}{V_3} \qquad \sin i_5 = \frac{V_2}{V_4}$$

$$\sin i_3 = \frac{V_1}{V_4} \qquad \sin i_6 = \frac{V_3}{V_4}$$

and the angles of incidence are:

$$i_1 = 17.5^\circ \qquad i_4 = 30^\circ$$

$$i_2 = 8^\circ \qquad i_5 = 19.5^\circ$$

$$i_3 = 5.5^\circ \qquad i_6 = 42^\circ$$

In summary the angle of the path of a ray in any bed is determined by the velocity in that bed and the velocity of the fastest bed penetrated and is independent of the velocities in any intermediate beds.

Capabilities and Limitations

Seismic refraction analysis is based on the fact that for practical purposes the elastic wave velocities vary with structure, lithology, and depth of burial. Velocities are generally faster in denser, wet, more consolidated materials than in loose, dry, or weathered materials--the denser the material the higher the seismic velocity. Though the property of elasticity actually governs the rate of transmission of the energy (shock) wave, we generally can equate elasticity with density.

Thus, the statement that "velocity increases with density" is not totally correct, but rather, the higher the modulus of elasticity, the higher the rate of transmission of the elastic wave. It is generally true that the more dense soils and rock have a higher velocity than less dense soils and rock when determined by the refraction seismic method.

The refraction method is such that it will detect only horizons which increase in velocity with depth. If a firmly cemented hard pan exists along the survey spread it will mask any weaker (lower velocity) soil materials underneath. Low velocity sands or soft materials cannot be detected if they lie beneath denser high velocity soil materials. Similarly, a dense rock layer near the surface will mask weak or weathered rock underneath. Frozen ground will transmit waves at higher velocities than unfrozen and will not give reliable subsurface information.

The principle of operation is much the same for all refraction seismographs. A hammer blow, tamper, or light blast charge generates shock waves which travel through different horizons from the energy source to the detection device (geophone). The travel time is measured by the seismograph in milliseconds (1/1000 second) or microseconds in special types of seismographs. As the distance between energy source and the geophone increases the travel times increase. The times are plotted on a time-distance graph, and these points are connected by one or more straight lines.

The slope of these lines indicates the apparent velocity in each horizon of material. The intersection of one velocity line with the next is the critical distance and provides information by which the depth (interface) may be calculated to the denser material.

The geometry of refraction is such that the following rules of thumb can be used: Location of depth determinations are usually about 1/2 the length of the survey line (spread) to the critical distance, and generally each critical distance is 2 1/4 to 2 1/2 times the depth to

the interface. An exception is found where shallow soils overlie dense rock in a parallel arrangement.

Two to three horizons may be detected to depths of 30 to 100 feet depending upon the equipment used and the length of spread. The only requirement is that each soil horizon have a thickness that exceeds $(\frac{X}{2}(1-\frac{V_2}{V_3})$, where X is the first critical distance, and an appreciably higher velocity than the overlying horizon otherwise the layer will be undetected. A layer of solid rock as little as 6 inches thick will carry a shock wave which will mask less dense layers below it.

If the soil density and P(primary) and S(shear) wave velocities are known, the elastic constants for the material can be calculated using the formulas on page 2-4. These values are averages and are not as precise as laboratory tests because average velocities over relatively long distances (compared to laboratory specimens) are used.

Refined techniques in the investigation and interpretation of the character of waves enable the investigator to gain information on the engineering properties of soil and rock materials. On instruments using a cathode ray tube, by adjusting the gain, intensity, and delay, the shape of the wave can be interpreted in terms of approximate density, elasticity, and abnormalities in the soil and rock materials. The shape of the curve on the time-distance graph especially at the critical distances may indicate either a sharp break in density of materials at the interfaces or some abnormality in soil and rock conditions. Additional closer-spaced tests should be made at these positions if the break is not distinct.

The Portable Seismic Instrument

The seismograph is composed basically of two components; the detector(s) (geophones) and the amplifier-redorder.

The Geophone.

A geophone is essentially an extremely sensitive electromagnetic generator, with a coil and a permanent magnet. One is fixed to the case of the geophone and the other is suspended (floating) by a spring. The slightest vibration moves one in relation to the other, generating a minute electrical current. This current is transferred through the cable to the seismograph where it is amplified to start or stop the timing.

The conventional P-wave geophone is an extremely sensitive device, so sensitive that it will register raindrops falling near it, the vibrations of nearby voices, or weeds rustling in a breeze. It must be planted vertically because some are designed to register the oscillations in soil or rock only when the phone is aligned within 15 degrees of the vertical. Interferences should be avoided such as people walking or talking nearby, wind moving trees, and planes or vehicles which may create vibrations. Some nearby interferences may be reduced by placing the geophone in a shallow hole and covering it with a few inches of soil.

Several types of geophones are available with varying degrees of sensitivity and various frequencies, depending upon the information needed and the capabilities of the seismograph. Seismographs that use timing lights or digital counters use geophones with a frequency range of 5 to 500 cycles per second. The oscillators within the instrument register or step up this frequency from 4 to 100,000 cycles so that very accurate timing may be accomplished.

The S-wave geophone is one that contains two coils mounted horizontally opposite to the center spike. On top is a bubble for levelling the geophone. The alignment of the two coils must be perpendicular to the direction of the wave source. This arrangement enables the geophone to detect transverse or "shear" waves which travel at lower velocities than the compressional or P-waves. Both types of geophones are recommended if S-wave values are desired.

There is no limit to the distance that a geophone is effective. The only requirement is an elastic wave sufficient to vibrate the case and activate the contained coils. In average soil and rock conditions the geophones supplied with portable seismographs will detect hammer blows from distances of 100 to 400 feet and small explosive charges from 1,000 feet or more.

The Amplifier-Recorder.

The recording instrument is essentially an electronic amplifying and timing device. It amplifies the minute electrical current received from the geophone(s) and times the interval between shock generation (by hammer or explosives) and generation of the current in the geophone due to the arrival of the seismic wave. In most recorders the timing device is an electrically driven tuning fork that has a frequency of 1,000 cycles per second. Time intervals accurate to within 1/1,000 of a second (milli-second) can be measured. The method of recording the time interval varies with the instrument and ranges from a series of lights or digital readout indicating elapsed time to recording on paper or film.

Types of Instruments

For the purpose of this discussion, the term "single-channel seismograph" refers to those instruments that permit the determination of a time-distance relationship at only one given point for each seismic event.

The multiple-channel seismograph refers to those instruments that permit the determination of a time-distance relationship at two or more points for each seismic event.

Single-Channel Non-Recording Seismographs.

These models are generally referred to as refraction seismic timers for they are designed only to indicate the travel time of one or two types of seismic waves through different kinds of media.

The simplest ones use a series of lights to indicate milliseconds and are sensitive to interferences. They may require a great deal of sledge hammer pounding to get the desired results. Our experience has shown them useful for obtaining information on depth and average velocities of two or three horizons to depths of 30 or 35 feet.

The more improved models and those using cathode ray tubes give information at slightly greater depths and are better adapted for avoiding interferences. These models also have the capability of using an extra geophone to read a reverse spread from the same hammer positions. S-wave geophones also may be used with these instruments to measure shear wave velocities.

The use of firecrackers or small explosive charges will permit extending the spread to obtain information at greater depths.

Single-Channel Recording Seismographs.

One instrument (Huntec) uses one or two geophones and records a display of numerous short dashes for a period of perhaps two seconds from a single blast or hammer blow. It is reported to be capable of determining depths to 150 feet using the sledge hammer. Another instrument (Sprengnether) uses up to 200 feet of 70 mm photographic paper to record three traces from the three-component (orthagonal) sensor plus an optional fourth trace indicating the instant the shock is initiated. The sensor detects shear and compressional waves.

Multiple-Channel Recording Seismographs.

These instruments provide a permanent record on paper or film of the P-wave or S-wave arrivals from three to twelve geophones plus the trace marking zero time when the shock wave is initiated. This provides an immediate record for study and computations. The advantage of these instruments is that the geophones may be spaced at various intervals up to 30 or 50 feet and one blast charge or hammer blow will create shock waves that are recorded at all of these positions. Another shock at the opposite end of the spread will record the complete reverse spread shock waves. Under good soil and rock conditions

recordings can be obtained with the sledge hammer up to distances similar to the single-channel instruments.

Although these multiple-channel instruments are more complicated and somewhat more expensive, they usually give a great deal more information in much less time than the single-channel instruments.

Portable Commercial Refraction Seismographs

The following descriptions are taken mostly from the specifications and capabilities described by the manufacturers. Not all known models are listed--only those owned by the SCS and some which have been demonstrated as suitable for SCS needs. The prices listed are approximate 1968 retail prices.

Single-Channel Non-recording Models.

Thiokol Geochrone (formerly NEL Geochrone) is manufactured by Thiokol Chemical Corporation, Bristol Division, Bristol, Pennsylvania 19007. List price - $895. A single-channel seismic timer using two geophones--one placed near the instrument where the steel plate beside it is struck with a sledge hammer and the other set at distances. It can be operated by one man, but two are more efficient. Readings are indicated in milliseconds on two decade counter tubes--one in tens and the other in units. A detonator is available ($210) for setting off explosive charges to obtain information at greater depths.

MD-1 - Engineering Seismograph is manufactured by Geophysical Specialties Division, Soiltest, Inc., 2205 Lee Street, Evanston, Illinois 60202. List price - $1,800. A single-channel seismic timer using one geophone at the instrument and a sledge hammer containing the starter switch. Two men are needed, but one could operate it with considerable inconvenience. Readings are indicated by 10 lights which give elapsed time from 1/4 to 255 milliseconds. An accessory blaster is available ($165) to obtain readings at greater depths with explosives.

The *MD-3 Engineering Seismograph* is an improvement over the MD-1. Instead of the timing lights, the MD-3 has a direct digital readout indicating milliseconds in tenths up to 99.9. It also has noise-reduction control, geophone polarity selector, and connection for an extra geophone to read reverse spread. List price is $2,250. A horizontal component shear-wave geophone may be used and an accessory blaster is available.

DynaMetric Seismic Timers, Models 117B and 117C--manufactured by DynaMetric, Inc., 330 West Holly Street, Pasadena, California 91103, and distributed by Soiltest, Inc. 2205 Lee Street, Evanston, Illinois 60202.

Price - $1,950. Single-channel seismic timers using one geophone at the instrument and a sledge hammer containing the starter switch. An extra geophone may be placed at the other end of the spread to take a reverse reading from each hammer position. One man could operate it with considerable inconvenience. Striking a large steel ball ($16.50) is reported to give better results than the steel plate. Readings up to 300 milliseconds are indicated by different combinations of the 24 lights, on the 117B and up to 99.9 or 999 by direct digital readout on the 117C. They indicate time also in 1/10 milliseconds for use in rock, concrete, etc. An exploder unit ($130) is available for longer spreads and greater depths.

A special S-wave geophone ($60) is available for recording transverse waves which arrive later than the first shock wave. A visual timer (Model 106) with oscilloscope, two geophones, and hammer is available for $2,450.

Bison Model 1501A is manufactured by Bison Instruments Inc., 3401 48th Avenue North, Minneapolis, Minn., 55429. List price $2300. A single-channel seismic timer with two geophone circuits to allow choice of operation. Forward and reverse readings can be taken at each hammer position, the timing can be started by one geophone and stopped by the second or the two geophones can be placed near the same position

to aid in signal attenuation. Readout is in two-inch by one-inch digits readable from a distance. Instrument has three timing ranges: 0.00-9.99; 00.0-99.9; and 000-999 milliseconds. Timing accuracy is ±0.1%. Can be operated by one man but two are more efficient.

Terra-Scout Model R-150 is manufactured by Soiltest, Inc., 2205 Lee Street, Evanston, Ill. 60202. List price - $2,490. (Accessory camera for photographing the flashes, $340.) Has self-contained rechargable battery and four removable legs. A single-channel timer using one geophone at the instrument and a tamper containing the starter switch. Two men are required to operate it. Direct digital readings are made by viewing the shock wave flash on a cathode ray tube (CRT) and adjusting the time delay to read milliseconds. Direct readout ranges from 0 to 250 milliseconds. Several accessories are available including blasting adapter, assembly for using two geophones, the Memory Scout and shearwave geophone.

By pressing the test button on the CRT seismographs with the geophone attached, a flash sweeps across the screen. This enables the operator to identify interferences or background noise. A plane overhead or trains or trucks within a mile will create sharp closely spaced waves on the sweep. If these waves are not too intense the survey may continue by ignoring these interferences.

The *Memory Scout Seismic Recorder Model R-172* List price $1180. A recording device for taking seismic data in the field without a seismograph. It records the verbal conditions as spoken by the operator including geology, hammer distances, and other pertinent information, and then records the tamper impact and the seismic wave arrivals. In the office it is attached to a Terra-Scout and the play-back will display the tamper impact, the timing marker, and the seismic wave arrival. Thus the field work can be done in less time, the computations and interpretations can be done inside, and the tapes may be stored for further study and rechecking.

A *Radio Link* is available from Soiltest and DynaMetric for use with their seismographs to eliminate the use of cables and exploder accessories. The transmitting unit is used at the striking plate or blast charge up to 1,000 feet distance to transmit the shock signal pulse. The receiver is placed on the seismograph to start the timing instantly. (Apparently useful only with single-channel refraction seismic timers.) List price - $465.

Single-Channel Recording Models.

Huntec Model FS-3 Seismograph is manufactured by Huntec, Ltd., 1450 O'Connor Drive, Toronto 16, Ontario, Canada. List price - $4,144. A portable facsimile seismograph which records the entire seismic event at each hammer location in a series of short dashes on paper. Recorder range is 3-340 milliseconds with an accuracy of ±1 millisecond. Power is supplied by dry cells or rechargeable battery. A shear wave geophone may be used. The manufacturer claims it can measure depth readings of 150 feet with hammer blows. It also may be used as a reflection seismograph.

Sprengnether Engineering Seismograph Vs-1100 is manufactured by W.F. Sprengnether Instrument Company, 4567 Swan Avenue, St. Louis, Missouri 63110. List price is $3,500. A single unit containing a three-component sensor receives data for recording on 200 feet of 70 mm photographic paper for determining velocities of compressional and shear waves. A fourth trace marker is available for recording the instant the shock wave is initiated. A built-in calibration pulse allows an immediate check on the system. Used with a hammer or light blast charges and has self-contained 12 V battery.

Multiple-Channel Recording Models.

GSC Model GT-2, Portable Refraction System is manufactured by Geo Space Corporation, 5803 Glenmont Drive, Houston, Texas 77036. List price - $4,800. A recording multiple-channel refraction system which automatically photographs the seismogram on polaroid film.

Three to 12 geophones may be used. A built-in blaster with safety switch sets off the blast charge. A special hammer may be used for short spreads. It can be operated by one man, but two are more efficient. Timing accuracy is ±0.5 millisecond.

GSC Model GT-2B with some improvements has become available recently. It features an external rechargeable power supply.

Electro-Tech ER-75, Porta-Seis is manufactured by Electro-Technical Labs., 6909 Southwest Freeway, P. O. Box 36306, Houston, Texas 77036. Three-channel model is $1572; 12-channel model is $4,010. Recording refraction seismographs which record 1 to 3 or 1 to 12 traces on 4 x 5 inch polaroid film, with an accuracy of ±1/2 millisecond up to the capacity of 200 milliseconds. Explosives or firecrackers are recommended, but a hammer may be used for short spreads. It can be operated by one man and has a self-contained rechargeable battery.

Dresser RS-4 Recording System is manufactured by Dresser Systems, Inc., P. O. Box 2928, Houston, Texas 77001. List Price is $5,135. A multiple-channel (up to 12) photo recording system, it permits continuous display of traces for monitoring. Built-in rechargeable battery timing accuracy is ±0.05%; has built-in blaster.

Micro-Seismic Timers.

For ultrasonic testing of rock, concrete, or other high velocity materials, more sensitive instruments are needed which register micro-seconds (1/1,000,000 sec.). One such timer is the *DynaMetric 217* which is available from Soiltest and DynaMetric for $2,500. Another is the *S.B.E.L. Seismic Timer Model VT-1007*, manufactured by Structural Behavior Engineering Laboratories, Inc., P. O. Box 9727, Phoenix, Arizona 85020. List price is $1,550. This timer is designed to test cores or small specimens of rock, concrete, etc.

Operation Techniques

Good operating techniques and correlation are essential in seismic surveying if adequate field data are to be collected or interpretation.

General Rules

A few basic rules may seem elementary, but adherence to them may be the difference between success and failure or wasted time.

1. Before going to the field, check thoroughly to see that batteries are charged and the equipment is complete and in good condition, including hammer and switch (plus a spare switch), wire-splicing tools, pliers, screwdriver, spade, measuring tape, instructions, charts, nomographs, and notebooks.

2. Select a location to make the survey which will give the most useful subsurface information. Run a correlation test near a logged drill hole, or the edge of a quarry or a deep cut.

3. Avoid interferences such as power lines, nearby railroads or highways. Avoid running a survey line on compacted surface soils, frozen ground, a field road, or near a wire fence or water-filled channel. Avoid a wire or steel tape lying near the survey line. Frozen ground may give abnormally high velocities. Ice has a P-wave velocity of over 10,000 feet per second. The water in a channel near a spread may pick up the shock wave and give a higher velocity than the alluvium several yards away.

4. Insure that there is adequate distance and direction to run a survey line and the reverse, and to run other nearby spreads. If the rock formations are dipping, or if abnormal readings or time-distance graphs are found, run the survey lines on the strike of the formation, and on the contour of the ground surface. If the strike is unknown, two reversed spreads run perpendicular to each other will give a better indication of the direction of strike and increase the chance of making an accurate interpretation.

5. Set up and operate the equipment according to the manufacturer's instructions. Be sure that the manual has a chapter on trouble-shooting to aid in field checking any operating troubles.

6. Use a uniform technique in striking with the sledge hammer or tamper. Always strike vertically downward. A glancing blow or a blow struck at an angle either away from or toward the stop geophone may produce different intensities and travel times for the shock waves.

7. Do not mix hammer blows and explosives in running a spread. The waves from these sources have different characteristics and intensity and will give misleading results. Likewise, striking different size boulders instead of the steel plate will be misleading.

8. If higher density materials are expected at shallow depths (5 feet or less) the first hammer positions or geophone spacings should be at 5 foot or possible 2 or 3 foot intervals up to distances of 20 or 25 feet.

9. Always run reverse spreads to be certain that the tests are accurate. The reverse curve on the time-distance graph will be the reciprocal of the curve from the forward spread if the interfaces and ground are parallel and there are no facies change along the phone spread. Phone lines should always be run in a straight line. Fan spreads from a central point can be used to determine direction and slope of dipping hard layers. This applies to single or multiple-channel equipment with or without the use of explosives.

10. The geophones must be planted firmly and in a vertical position, regardless of the slope of the ground. In loose or spongy soil, use a long spike (10-12 inches) on the geophone or bury the phone firmly in a shallow hole.

11. Tests may be made with the spreads extending up or down steep slopes, but the results require a more thorough knowledge for proper interpretation. Also the possibility of buried rock ledges or cliffs may cause difficulty in interpretation.

12. A short-cut method may be used if, for example, you want to learn whether rock occurs at or above the designated bottom of a proposed channel. For designed depth of 12 to 20 feet, hammer positions at 10 and 20 feet and at 40 and 70 feet may give the two

velocities to determine whether rock occurs within the design depths. If these hammer positions plot on a straight line indicating a low or moderate velocity, it is obvious that hard rock is deeper than 20 feet. For lesser or greater depths, the hammer positions must be decreased or increased depending upon the depth determinations needed.

13. Velocity calibration surveys should always be made prior to investigation shooting whether using mechanical or explosive energy sources. These are normally made by laying out a short line on outcrops of the rock types expected in the profile. These lines normally need not exceed 30 feet in length if the exposure is good. Record velocities parallel to and perpendicular to the strike. A second useful survey is an uphole velocity survey where an auger hole or drill hole is available. In this survey, charges are detonated at different levels in the drill hold to obtain values of vertical velocity. These soil and rock values are necessary for the successful interpretation of subsequent information. Also, when logged drill holes are available, seismic lines should be placed over these holes for further correlation purposes. These surveys will provide profile velocities with which interface depths may be extended away from the drill holes or determined at other locations.

Geophone Layout

Reverse seismic profiles are required in order to obtain a factual picture of subsurface conditions. As will be shown later, subsurface interfaces which are not parallel to the ground surface will create apparent V_2 and subsequent velocities which are either greater than or less than the true velocity of the material.

The reverse profile permits detection of this condition. It is also necessary, when running reversed profiles, that no new earth section be incorporated in the profile. In other words, the reversed profile should encompass the exact same subsurface section as the forward profile. The geophone (or hammer) layouts in Figure 2-5 are designed to encompass the exact same subsurface interval in the forward and reverse spreads.

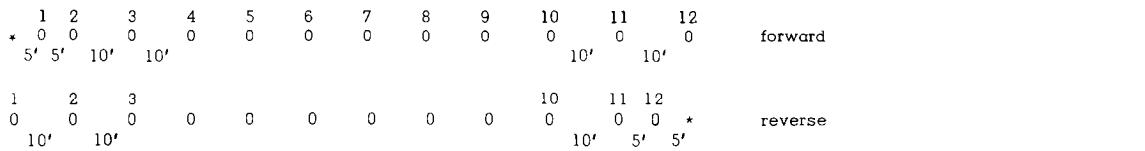

5–5–10–10 spacing 110 ft. spread

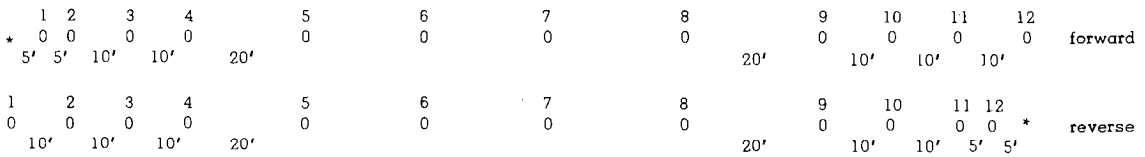

5–5–10–10–20–20 spacing 160 ft. spread

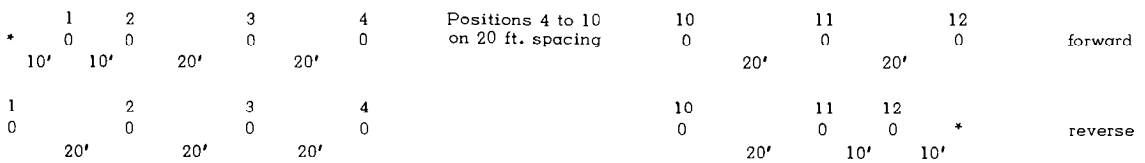

10–10–20–20 spacing 220 ft. spread

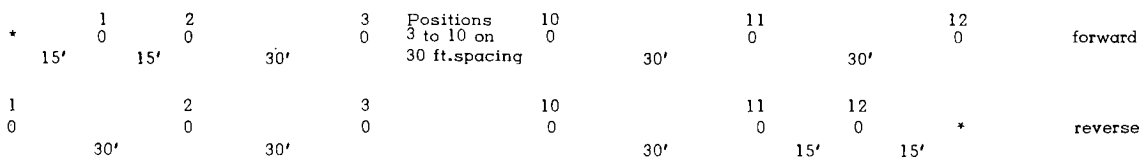

15–15–30–30 spacing 360 ft. spread

The numbered positions can either be geophone locations for multiple-channel system or hammer positions for single-channel systems. The * positions are shock points for multiple-channel systems or receiver positions for single-channel systems. The various layouts give either more or less definition near the surface as required. Note the changes of the end positions for forward and reverse spreads. The number and spacing of positions can be modified as required.

Figure 2–5. – Geophone Locations.

Energy Sources

Energy sources used in seismic survey can be either mechanical or explosive.

Mechanical Energy.

Mechanical energy sources most commonly used include 8 to 10 pound sledge hammers striking a steel plate or thumper devices which strike directly upon the ground surface. These devices generate approximately 2,000 foot-pounds of energy. These sources work well for shallow investigations and where the ambient noise level is low to moderate. In the cases of deeper investigations these methods sometimes do not provide the necessary amount of seismic energy because of high noise levels, unconsolidated alluvial materials or mucks and peats.

For those instruments using starting switches on the hammer or tamper, the switch should be very sensitive for close-up hammer positions. Stiff switches may require such heavy pounding that distances of 10 feet or less may vibrate the ground too much to get reliable timing.

Under good conditions and experience with the single-channel timers usually 3 or 4 blows with the sledge hammer or tamper are sufficient at each position. Experience with the instruments equipped with cathode ray tube will enable the operator to predict the required adjustments at each increasing tamper position, and sometimes only 2 or 3 blows may be required.

Complex geologic conditions and interferences are so common that more blows are usually required, and where anomalies occur at the critical distances some in-between hammer positions may be required.

Explosive Energy.

The safe and prudent use of explosive energy can effectively increase the reliability and amount of information gained through seismic investigations. They do not preclude the use of mechanical energy devices where applicable to the site conditions. In many areas, however, they provide the means for seismic evaluation where site conditions are such that mechanical means will not suffice.

Explosive energy sources can be used to excellent advantage where noise levels and signal attenuation require more energy than mechanical devices can produce. In contrast to an energy level of approximately 2,000 foot-pounds for most mechanical sources, 1/4 pound of 50 percent dynamite (1/2 stick) will produce approximately 200,000 foot-pounds of energy. This is an advantage of about 100 times and will provide penetration of the most unconsolidated materials and permit the use of low gain receiver settings to eliminate noise. Single large blasting caps or firecrackers can be used under some conditions.

If personnel do not have a blasters' license or the local conditions do not permit the use of explosives, fircrackers have been found to be a useful alternate. They produce good shock waves at distances two or three times greater than sledge hammers. Their use will be described following the discussion on the use of dynamite.

Use of Dynamite. - Numerous types and grades of explosives are available (see DuPont Blasters' Handbook) which cover a wide range of site conditions. For the average type of seismic investigation where shallow holes are used, a very satisfactory explosive is DuPont 50% "High Velocity" gelatin. This explosive imparts a quick, sharp blast desirable in seismic work and yet is not sensitive to shock or friction. It is also easy to split where 1/2 or 1/4 sticks are desired. This explosive is manufactured in sticks of 1/2 pound, 1 1/8 inches in diameter and eight inches long. Under most site conditions, 1/2 stick provides excellent results. Also available are 1 inch by 4 inch sticks of 40 percent gelatin. These are whole sticks and are easily handled and used without having to split larger sticks. These are ideal

for the "usual" spreads and depths associated with SCS work. This explosive can be bought by the individual stick (25 to 30 cents); however, a 50 pound case contains about 200 sticks and costs about $18.

Seismic charges are detonated by electric blasting caps. Only instantaneous caps should be used with multiple-channel instruments because these caps provide the instantaneous detonation required when dealing in time intervals of thousandths of seconds in seismic work.

Costs of explosives will vary with type and area. Generally, they will average 30 cents per stick of explosive and 30 cents per electric blasting cap. Bulk purchase will reduce this price. As described under Storage and Transportation, it has often been found more convenient to purchase only that amount required for a single day's operation. However, if approved storage is convenient, bulk purchases may be stored and used as needed. All types of seismic equipment can be used with explosives. Most equipment can be readily adapted to the use of explosives by the addition of an electric blasting attachment which costs between $125 and $210. Most of the multiple-channel instruments have built in blasters. The single-channel instruments require multiple shot points, hence, more powder, caps, and layout time are required.

The suggested shooting methods for single and multiple-channel instruments are discussed below.

Using a single-channel instrument, all holes for the forward profile are loaded and shot in one direction; the holes for the reverse profile are then loaded and shot for the return line. Sympathetic detonation is not usually a problem if hole spacing is 5 feet or more. If sympathetic detonation is a problem, alternate holes can be shot.

Using this method, a 220 foot line (with shots spaced as shown in Figure 2-5) will require approximately two man hours, (assuming one Geologist and one Technician), plus the explosives and 24 blasting caps costing about $14.40.

Multiple-trace seismographs are the most effective units to use with explosive methods. These units with up to twelve-channel recorders require only two shot holes per line. This feature significantly reduces the cost per line although the initial investment is higher ($4,000-$5,000 as opposed to $1,000-$3,000 for single-trace models). The normal shooting layout is illustrated in Figure 2-5, page 2-25 Using this method a 220-foot shot line will require one man-hour plus the explosives, and two blasting caps costing about $1.20.

Shot holes for explosive use are best prepared with a 1 1/2 inch steel bar or hand auger. These holes should be 6 to 12 inches into the soil and well tamped (with wooden tamper) over the charge. Loaded holes should always be marked with red flagging. Precautions should be used if there is a chance that flying debris might cause damage or injury.

Safety Precautions.--It should always be recognized that whenever explosive agents are used there is risk involved in the safety of personnel, equipment, and property. For this reason, every crew involved in these operations should have a current set of safety regulations which are enforced at all times and supervised by men trained in the use of explosives.

Licensing.--All Federal personnel using or handling explosives must be licensed by a Federal examiner. These examinations are conducted at periodic intervals by the U. S. Forest Service and can be taken by personnel of all agencies.

The examination consists of a written phase and a practical demonstration of the use of different types of explosives. The examination usually includes from two to four days of classroom and practical instruction. These licenses must be reviewed and updated at periodic intervals.

Storage and Transportation.--Most states and the Federal government have published regulations covering the use, storage, and transportation

of explosives. Copies of these are available from the U. S. Forest Service and the applicable state agency (i.e., Fire Marshal, Industrial Accident Commission, etc.). These regulations list the types of storage facilities required, transport containers, vehicle markings, and general precautionary measures. Applicable Federal and state regulations must be followed in all cases. It has generally been found that for SCS seismic use it is best to procure only that amount of explosive required for each day's use. This eliminates the need for maintained powder bunker In areas of poor accessibility more than one day's supply may be stored at the site in temporary bunkers if state laws permit.

Equipment.--Specific equipment required by crews varies with the type of operations, but should always include the following:

(a) Safety helmets of the non-sparking type;
(b) static-free clothing;
(c) non-sparking tools, shovels, bars, etc.;
(d) foam rubber or wood lined metal containers for explosives and blasting caps (separate container for each);
(e) safety warning signs indicating the use of explosives in the area;
(f) red flags to mark buried explosives.

Electro-Magnetic Radiation.--Extreme care should be exercised in using electric blasting caps near high voltage power lines and in the vicinity of high frequency radio or TV transmitting stations. It is possible with certain lead wire arrays to receive this energy and prematurely detonate the electric blasting caps. Cap wires should never be unravelled and the shunt removed until the charge is buried and the blaster wires are ready to be connected. Additional handling information is available from handbooks published by explosive manufacturers.

Use of Firecrackers.- Another source of explosive energy for seismic refraction studies employs the use of firecrackers. Where state law law permits, firecrackers may be used without a Federal Blasters license. An M-80 salute (a type of firecracker containing one gram

of black powder) is used to produce the shock. This method was developed during the course of a seismic survey by Criner (1966) in the Trace Creek Basin, Humphreys County, Tennessee.

The preparation of an M-80 requires punching a hole about 1/4 inch in diameter in the side and inserting a squib (or match assembly) which has electrical lead wires. Tape may be used to seal in the powder, to secure the squib in place, and to prevent absorption of moisture from the ground. The firecrackers are placed in holes punched in the ground with a crowbar or hand auger, and the holes are backfilled. Experiments show that a single M-80 salute may be sufficient for distances up to 700 feet from the geophone; when greater distances are involved, one or more salutes are taped to the one fitted with a squib.

An exploder unit is used with the seismograph to detonate the firecracker and start the timing simultaneously. The firecrackers also may be fired by a single flashlight battery where the start geophone is placed at the energy source.

The use of firecrackers for producing shock waves is safe and inexpensive. The M-80 salutes cost $2.50 to $3.00 per hundred and the squibs or match assemblies about $17.00 to $25.00 per hundred, making each detonation cost 20¢ to 28¢. One manufacturer has offered electric caps for $3.00 per hundred which are reported to serve the same purpose as the squib, and thereby reduce the cost to 6¢ per detonation.

Firecrackers also may be fired at individual positions by lighting the fuse, providing it is long enough to be safe. With this method a hole is punched two or three inches deep for the firecracker. If the seismograph is supplied with a thumper or tamper, it is placed over the firecracker as soon as the fuse is lit. With seismographs using a start geophone at the energy source, the geophone is placed eight to 12 inches from the hole. When the fuse is lit the hole is covered quickly by a steel plate or a slab of rock. This method is questionable from a safety viewpoint, unless double-length fuses are inserted and the

operator works fast. Seismographs using the cathode ray tube do not work well with explosives.

Computations

Several of the references listed and the manuals provided by manufacturers describe the procedures for computing many conditions in addition to depth, depending upon the type of seismograph and geophone used. These may include apparent density and hardness of horizons, Poisson's ratio, rigidity or shear modulus, elastic constants, and other physical characteristics of materials.

The following sketches illustrate the paths of refracted shock waves through earth and rock materials and the data plotted on time-distance graphs. The velocities and depths of the different horizons are computed from the velocity charts plotted on the graphs.

The first pair of sketches, Figure 2-6, illustrate the use of a single-channel seismograph with hammer positions (energy sources) plotted at 10-foot intervals. It is noted that the first arrivals from the 10 and 20-foot distances travel through the soil, the first arrivals from the 30 and 40 foot distances travel through soil and weathered rock, while the first arrivals from greater distances travel most of the distance through the high velocity hard rock.

The second pair of sketches (slightly exaggerated), Figure 2-7, illustrate a seismogram from a 12-channel seismograph and its projection above on a time-distance graph. In this case one shock wave (with its source at the left) is registered successively by the 12 geophones with the arrival time at each geophone recorded on the film. The paths travelled through soil and rock by the 12 first arrivals would be a composite of 12 paths in the sketch illustrated for the single-channel model (Figure 2-6) if it had been extended out to 12 hammer positions.

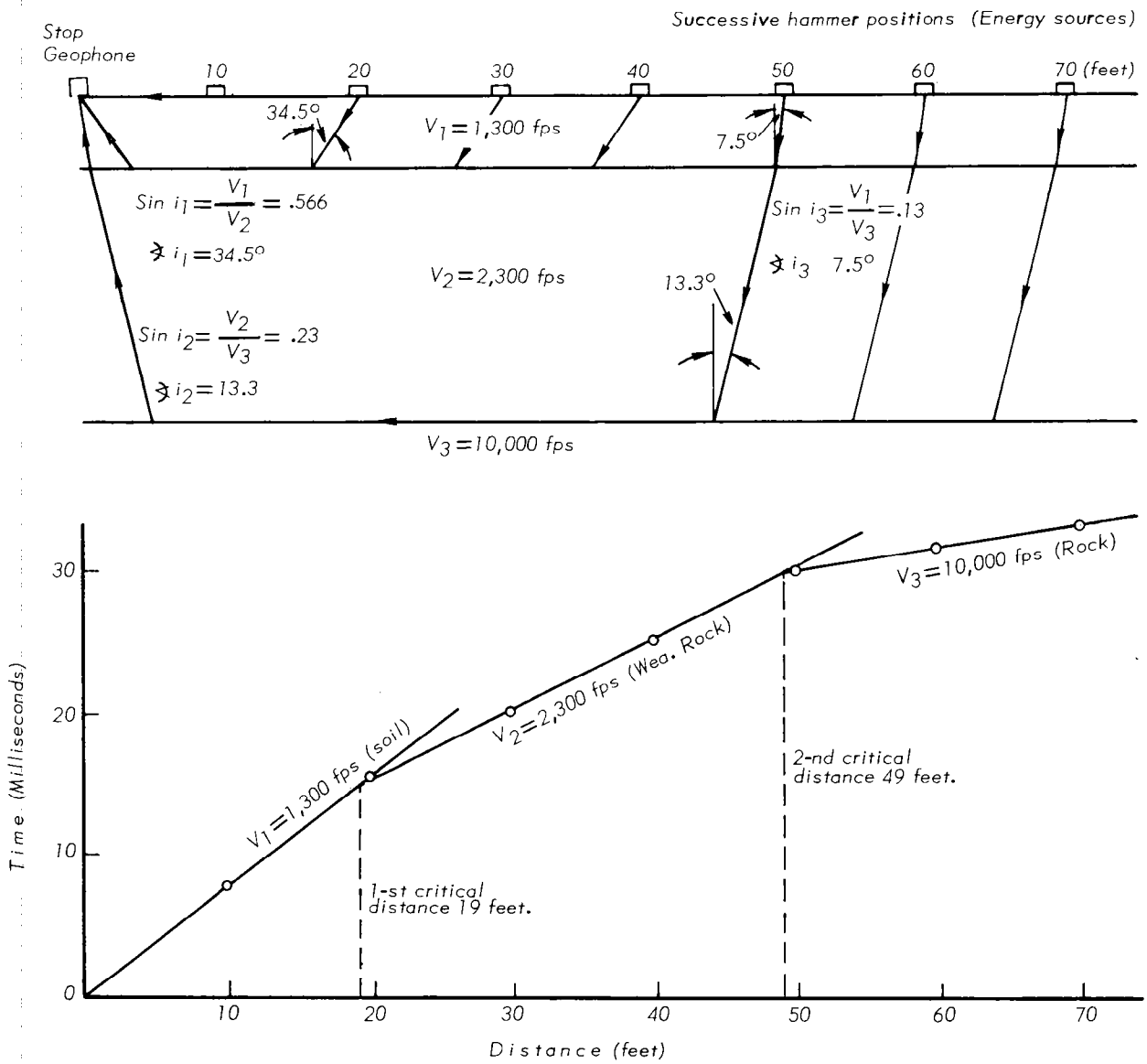

Upper: a 70 foot spread showing paths of first arrival waves.
Lower: The first arrivals plotted on a time-distance graph.

Figure 2–6. – Generalized Seismic Test and Velocity Curve for Single-Channel System.

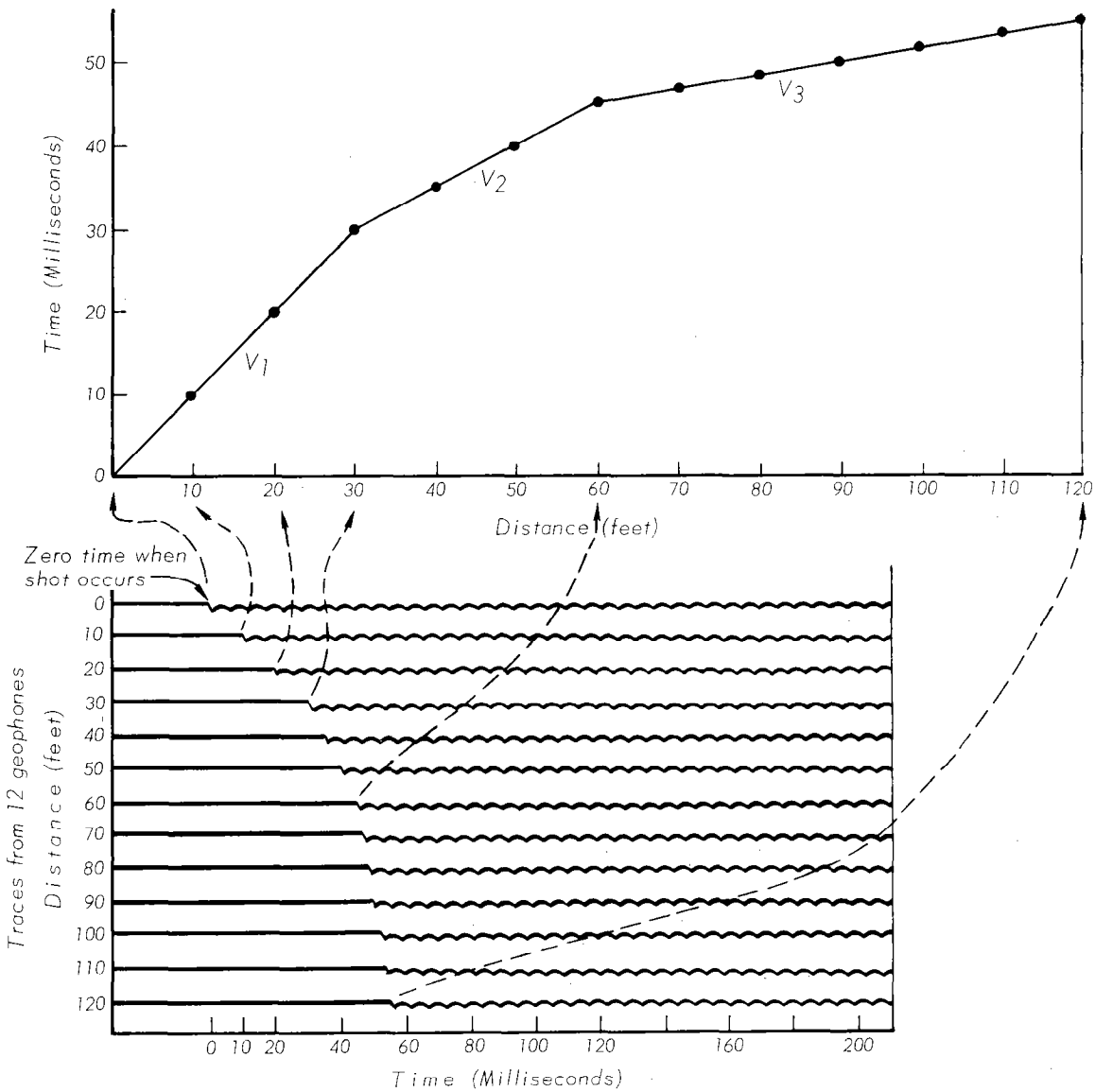

Upper: Velocity curve plotted from the 120' spread on the seismogram below.

Lower: Seismogram with traces from 12 geophones spaced 10' apart. The time break for each trace is measured on the vertical lines indicating 10 Ms intervals.

Figure 2–7. – Time–Distance Graph and Multiple–Channel Seismogram.

Time-Distance Graphs and Seismograms

For proper interpretations, the shock wave travel time must be plotted on a time-distance graph from each hammer or geophone position. Charts for this purpose are printed by some companies. Graph paper 8 x 10 inches or larger is convenient or Form SCS-315A may be used. Form EWP-45F, Seismograph Data and Velocity Chart, Figure 2-8, is useful. The series of points indicating milliseconds of time from each hammer or geophone position on the forward and reverse spreads may be connected by one or more straight lines. Where points are several milliseconds off these lines, these positions should be rechecked and perhaps tests made between these positions. It is not unusual that most points do not fall on one straight line, rather a line must be average through them. The slope of these lines indicates the seismic velocity in each horizon. It should be noted that the projected line for the first velocity usually begins at two or three milliseconds on the zero distance line. This results either from a time delay of two or three milliseconds built into the timing mechanism of some seismographs or from a very low velocity surface layer.

Quite often a quick field interpretation can be made from seismograms from multiple-channel recording instruments. Other features from the seismograms beyond the first arrival shock waves may be plotted or used for additional studies.

When plotting time-distance graphs for spreads up to 100 feet a scale of one inch = 10 feet and one inch = 10 milliseconds is recommended. For spreads greater than 100 feet a scale of one inch = 20 feet and one inch = 20 milliseconds is recommended.

Computations and Nomographs

The velocity indicated by any one of these velocity lines may be computed by taking any given horizontal distance on the line, dividing by the milliseconds time for this distance, and multiplying by 1,000 to get velocity in feet per second. Velocity chart templates (Figure 2-9) are

SEISMOGRAPH VELOCITY CHART

State _____ Watershed _____ Subwatershed _____ Site No. ___

Location of Test _____, Survey Direction: Forward _____, Reverse ____

Seismograph & Model _____, Explosives or hammer _____

Topog. of Ground Surface _____, Soil Materials _____

Type of Rock _____, Dip & Strike _____, Faults, caverns, other abnormalities_____

Depth to water _____, Depth to First Interface "H_1" _____ ft., Depth to Second Interface "H_2" _____ ft.

Investigated by _____ Computed by _____ Date _____

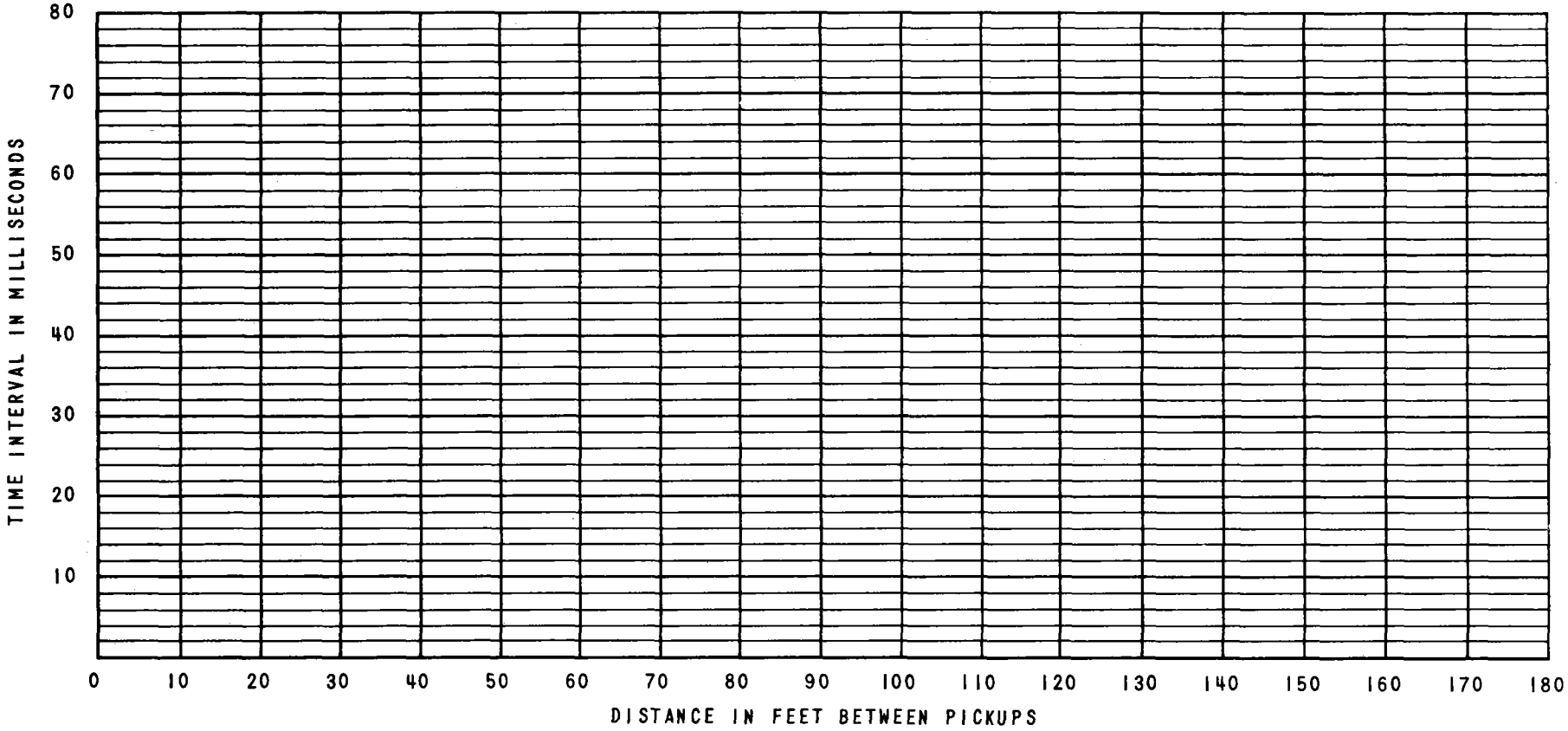

Figure 2–8. – Seismograph velocity chart

EWP-45F OVERLAY
ial
Fort Worth, Texas

U. S. DEPARTMENT OF AGRICULTURE
SOIL CONSERVATION SERVICE

OVERLAY - SEISMOGRAPH VELOCITY CHART

For determining velocities in feet per second on graphs
where 10 milliseconds vertical and 10 feet horizontal are equal

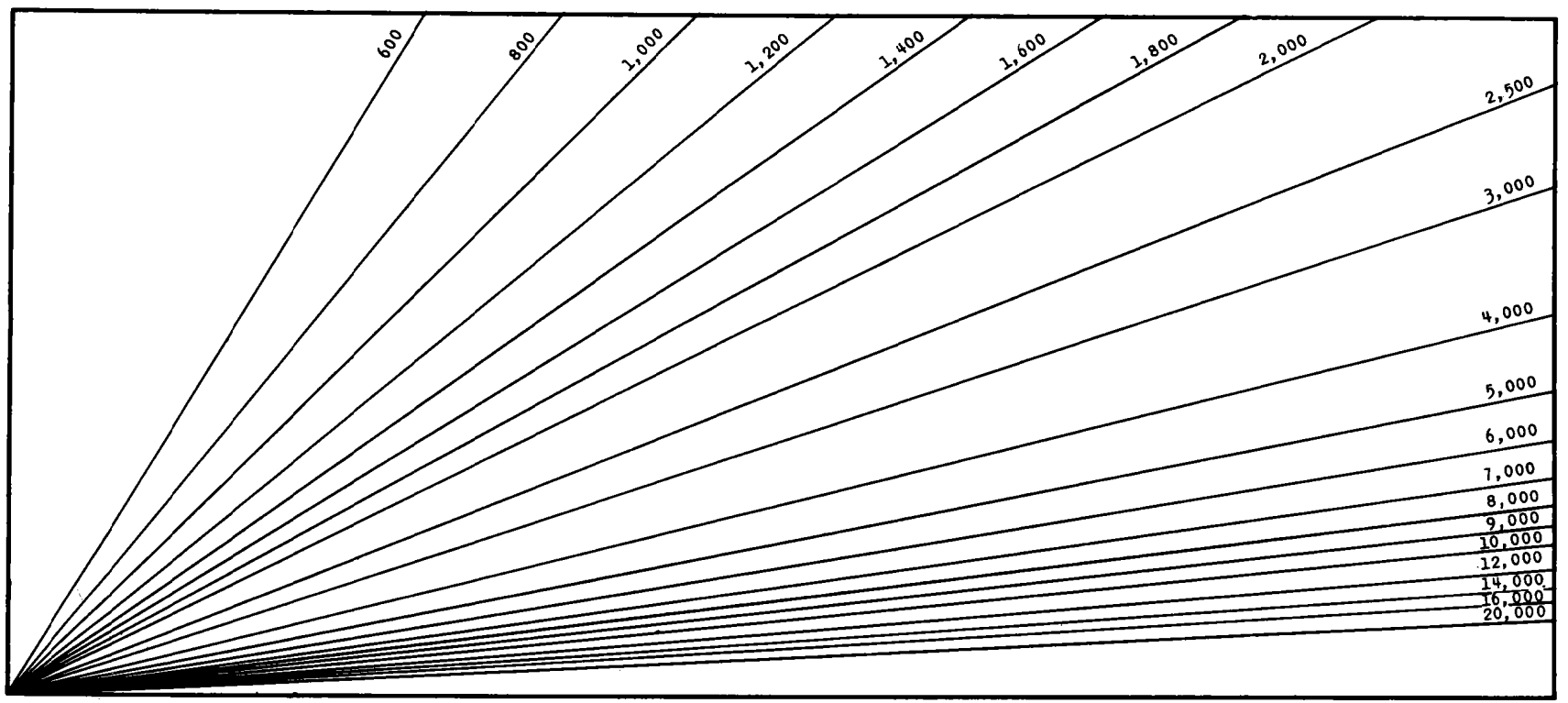

Figure 2–9. – Velocity overlay

available to place over the time-distance graph and read the velocity directly. The velocity chart must be made for the scale used on the time-distance graph. That is, 1 inch = 10 milliseconds and 1 inch = 10 feet requires a different velocity chart from the graph using one inch = 10 milliseconds and one inch = 20 feet. Overlay EWP-45F, "Overlay-Seismograph Velocity Chart" (Figure 2-9), may be used with Form EWP-45F (Figure 2-8) or 10 x 10 or 20 x 20 time-distance graphs.

Each break in the velocity lines on the time-distance graph is a critical distance indicating that a material of different elasticity (interface) refracted the shock waves. The two velocity lines on each side of this critical distance are used in the following formulas to determine the depth to the interface.

To compute the depth to the first interface (H_1) the following formula is used: (Critical distance method, see page 2-40 for derivation).

$$H_1 = \frac{X_1}{2}\sqrt{\frac{V_2 - V_1}{V_2 + V_1}}$$ (for interfaces parallel to the ground surface)

where X_1 is the distance in feet to the first critical distance shown on the following time-distance graph (Figure 2-10)

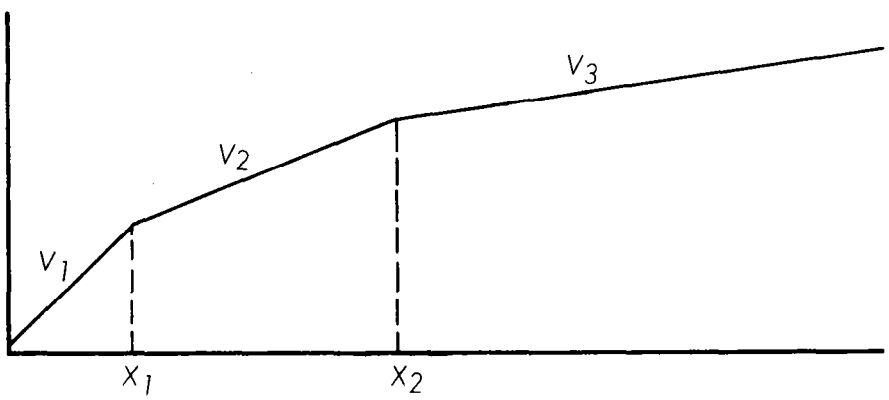

Figure 2–10. – Critical Distances.

To compute the depth to a second interface the following simplified formula can be used:

$$H_2 = H_1 + \frac{X_2}{2}\sqrt{\frac{V_3 - V_2}{V_3 + V_2}} - H_1R$$ (for interface parallel to the ground surface.)

The V_2 and V_3 values used in the equations should be the average values for these materials obtained from the forward and reverse spreads (see formula on page 2-51). H_1 and H_2 are the depths in feet to the first and second interfaces. X_2 is the distance in feet to the second critical distance. V_1, V_2, and V_3 are the first, second, and third velocities obtained, in feet per second. R is a factor for which values are given in Table 2-1.

TABLE 2-1. R Values

Ratio of $\frac{V_2}{V_1}$

ratio of $\frac{V_3}{V_2}$	1.1	1.5	2	3	5	10
1.1	0.39	0.17	0.12	0.06	0.03	0.02
1.5	0.56	0.31	0.21	0.12	0.07	0.03
2	0.60	0.34	0.24	0.15	0.08	0.04
3	0.63	0.36	0.26	0.16	0.09	0.04
5	0.64	0.37	0.26	0.16	0.09	0.05
10	0.64	0.38	0.27	0.17	0.11	0.05

The Table 2-2 gives the square roots of decimal numbers and will assist in computations of depths to interfaces.

TABLE 2-2. Square roots of Decimal Numbers

	0.0	0.01	0.02	0.03	0.04	0.05	0.06	0.07	0.08	0.09
0.0		0.10	0.14	0.17	0.20	0.22	0.25	0.27	0.28	0.30
0.1	0.32	0.33	0.35	0.36	0.38	0.39	0.40	0.41	0.43	0.44
0.2	0.45	0.46	0.47	0.48	0.49	0.50	0.51	0.52	0.53	0.54
0.3	0.55	0.56	0.57	0.58	0.58	0.59	0.60	0.61	0.62	0.63
0.4	0.63	0.64	0.65	0.66	0.66	0.67	0.68	0.69	0.69	0.70
0.5	0.71	0.71	0.72	0.73	0.74	0.74	0.75	0.76	0.76	0.77
0.6	0.78	0.78	0.79	0.79	0.80	0.81	0.81	0.82	0.83	0.83
0.7	0.84	0.84	0.85	0.85	0.86	0.87	0.87	0.88	0.88	0.89
0.8	0.89	0.90	0.91	0.92	0.92	0.92	0.93	0.93	0.94	0.94
0.9	0.95	0.95	0.96	0.96	0.97	0.98	0.98	0.99	0.99	0.99

Derivation of two Layer Formula

Figure 2-11 illustrates the two layer case for which the formula $H_1 = \frac{X}{2}\sqrt{\frac{V_2 - V_1}{V_2 + V_1}}$ is derived.

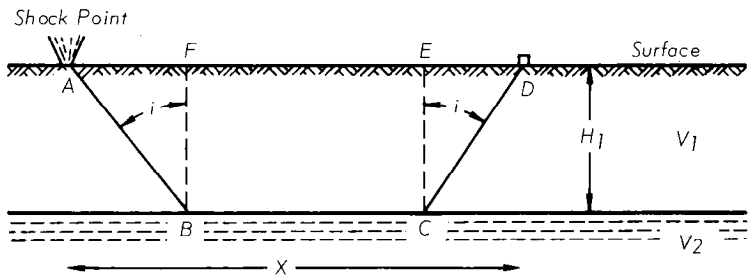

Figure 2–11. – Two Layer Case.

Two basic relationships are utilized:

Snell's Law which states $\frac{\sin i}{\sin r} = \frac{V_1}{V_2}$

Rate X Time = Distance

From Snells law we know that AB-BC-CD is the minimum time travel path for the refracted wave because r = 90°

T = Total time required for refracted wave to travel from shock point to the critical distance, X.

A,B,C,D,E,F, = Points on Figure 2-11.

X = critical distance (in this case = AD)

T_1, T_2, T_3 = Time of wave travel from A to B, B to C, and C to D respectively.

H_1 = Distance from ground to interface

$$T = T_1 + T_2 + T_3 \qquad (1)$$

but, $T_1 = \frac{AB}{V_1}$, $T_2 = \frac{BC}{V_2}$, $T_3 = T_1 = \frac{AB}{V_1}$

substituting, $T = \frac{AB}{V_1} + \frac{BC}{V_2} + \frac{AB}{V_1} = \frac{2AB}{V_1} + \frac{BC}{V_2}$ (2)

in (1)

$$\cos i = \frac{H_1}{AB}, \quad AB = \frac{H_1}{\cos i} \qquad (3)$$

$$BC = X - AF - ED \text{ or } BC = X - 2\,AF \qquad (4)$$

$$\tan i = \frac{AF}{H_1}, \quad AF = H_1 \tan i \qquad (5)$$

$$BC = X - 2\,H_1 \tan i \qquad (6)$$

Substituting in (2)

$$T = \frac{2\,H_1}{V_1 \cos i} + \frac{X - 2\,H_1 \tan i}{V_2}$$

$$T = \frac{2\,H_1}{V_1 \cos i} + \frac{X}{V_2} - \frac{2\,H_1 \sin i}{V_2 \cos i}$$

$$T = \frac{X}{V_2} + \frac{2\,H_1}{V_1 \cos i} - \frac{2\,H_1 \sin^2 i}{V_2 \cos i \sin i} \qquad (7)$$

bus, $\sin i = \frac{V_1}{V_2}$ when r = 90°

Substituting in (7)

$$T = \frac{X}{V_2} + \frac{2\,H_1}{V_1 \cos i} - \frac{2\,H_1 \sin i}{V_1 \cos i}$$

$$T = \frac{X}{V_2} + \frac{2\,H_1}{V_1 \cos i}(1 - \sin^2 i) \qquad (8)$$

but, $\sin^2 i + \cos^2 i = 1$, $\cos^2 i = 1 - \sin^2 i$

so $$T = \frac{X}{V_2} + \frac{2 H_1 \cos i}{V_1}$$

at the critical distance, $T = \frac{X}{V_1}$

Substitute in (8) $$\frac{X}{V_1} = \frac{X}{V_2} + \frac{2 H_1 \sqrt{1 - \sin^2 i}}{V_1}$$

$$\frac{X}{V_1} = \frac{X}{V_2} + \frac{2 H_1 \sqrt{1 - \frac{V_1^2}{V_2^2}}}{V_1}$$

$$\frac{X}{V_1} = \frac{X}{V_2} + \frac{2 H_1 \sqrt{\frac{V_2^2 - V_1^2}{V_2^2}}}{V_1}$$

$$\frac{X}{V_1} = \frac{X}{V_2} + \frac{2 H_1 \sqrt{V_2^2 - V_1^2}}{V_2 V_1}$$

Solve for H_1

$$\frac{2 H_1 \sqrt{V_2^2 - V_1^2}}{V_2 V_1} = \frac{X}{V_1} - \frac{X}{V_2}$$

$$2 H_1 \sqrt{V_2^2 - V_1^2} = X V_2 - X V_1$$

$$H_1 = \frac{X (V_2 - V_1)}{2\sqrt{V_2^2 - V_1^2}}$$

$$H_1^2 = \frac{X^2}{4} \frac{(V_2 - V_1)(V_2 - V_1)}{V_2^2 - V_1^2}$$

$$H_1^2 = \frac{X^2}{4} \frac{(V_2 - V_1)(V_2 - V_1)}{(V_2 - V_1)(V_2 + V_1)}$$

$$H_1^2 = \frac{X^2}{4} \frac{V_2 - V_1}{V_2 + V_1}$$

$$H_1 = \frac{X}{2} \sqrt{\frac{V_2 - V_1}{V_2 + V_1}}$$

Another formula which can be used to compute the thickness of a second layer (V_2) is the following:

$$H_2 = \left[t_3 - \frac{2 H_1 \sqrt{V_3^2 - V_1^2}}{V_1 V_3} \right] \frac{V_2 V_3}{2\sqrt{V_3^2 - V_2^2}}$$

where t_3 is the time intercept when the V_3 line is projected to the time axis (See Figure 2-12).

To determine the thickness of a third layer (V_3) the following formula may be used:

$$H_3 = \left[t_4 - \frac{2 H_1 \sqrt{V_4^2 - V_1^2}}{V_1 V_4} - \frac{2 H_2 \sqrt{V_4^2 - V_2^2}}{V_2 V_4} \right] \frac{V_3 V_4}{2\sqrt{V_4^2 - V_3^2}}$$

where t_4 is the time intercept when the V_4 line is projected to the time axis. The values of H_1, H_2, H_3, etc. are the thicknesses of the layers, and must be added in order to determine the depths to the interfaces.

To simplify the depth determinations, several manufacturers have prepared nomographs on which the data are plotted from the time-distance graph. (Figure 2-13). The projection of the lines connecting these points on the nomographs will give the depths to the first two interfaces.

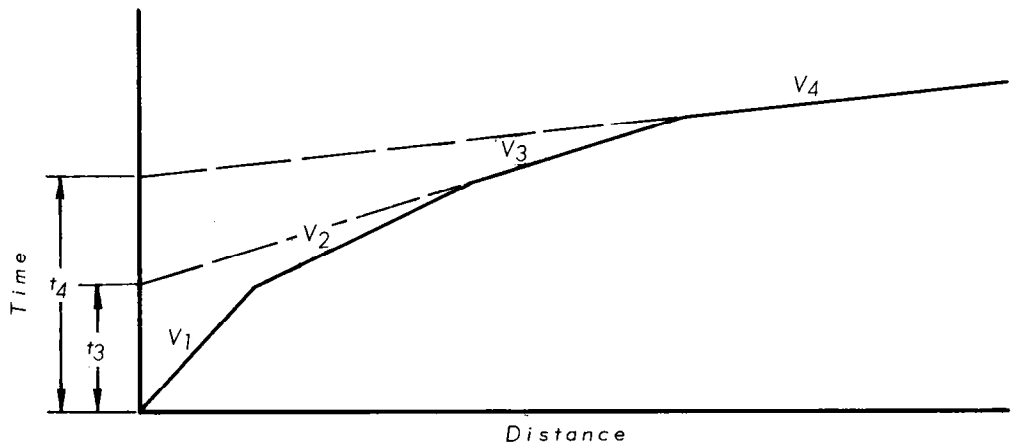

Figure 2–12. – Time Intercepts.

Determination of the Location of Depth Measurements

When seismic readings are made, the depths that are computed do not lie beneath any particular point along the spread. In fact, under field conditions, the depth is not measured at any particular point but rather is an average between two points. The location of these two points varies as the velocities of the materials vary. The following procedure will outline the method of determining these points:

1. From the time-distance graph the velocities of the materials must be determined, V_1, V_2, V_3.

2. From Snell's Law determine the angle i for the V_1V_2 materials, ($\sin i_1 = V_1/V_2$) Plot the complement ($90° - i_1$) of the angle i_1 from the point of origin and from the critical distance on a seismic profile as shown in Figure 2-14.

3. Compute H_1 from the standard formulas.

4. Plot a line parallel to the ground surface at depth H_1 on the seismic profile.

5. The surface projection of depth H_1 should be taken as midway between points A and B. If the interface was not parallel to the surface, the determination of the H_1 depth by this method would introduce the minimum possible error when the standard formulas are utilized. The formulas discussed on pages 2-38 and 2-41 were derived

NOMOGRAPH FOR DEPTH TO FIRST 2 INTERFACES

for any system of units (Feet, Meters, etc.) as used in Seismic Graph

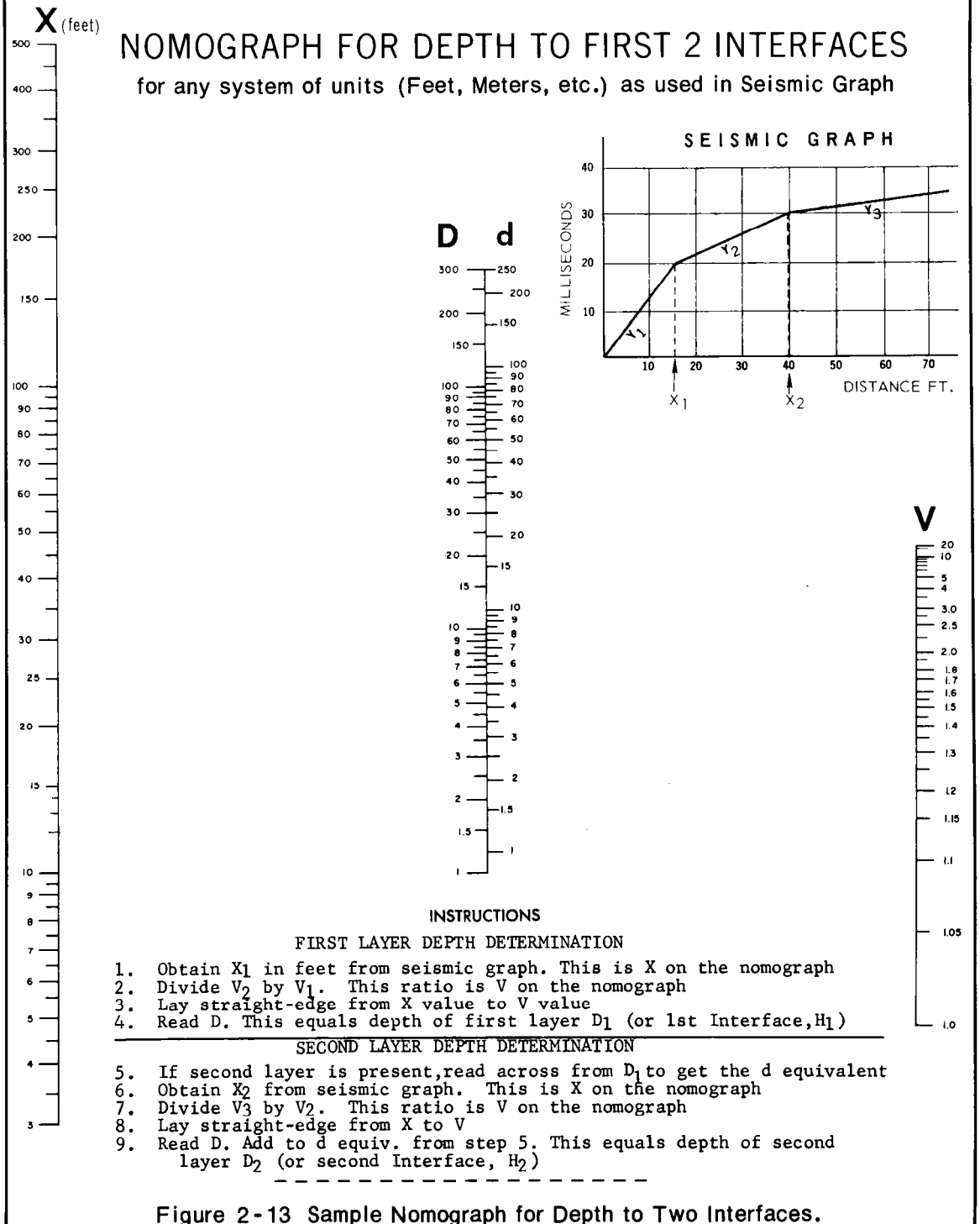

INSTRUCTIONS

FIRST LAYER DEPTH DETERMINATION

1. Obtain X_1 in feet from seismic graph. This is X on the nomograph
2. Divide V_2 by V_1. This ratio is V on the nomograph
3. Lay straight-edge from X value to V value
4. Read D. This equals depth of first layer D_1 (or 1st Interface, H_1)

SECOND LAYER DEPTH DETERMINATION

5. If second layer is present, read across from D_1 to get the d equivalent
6. Obtain X_2 from seismic graph. This is X on the nomograph
7. Divide V_3 by V_2. This ratio is V on the nomograph
8. Lay straight-edge from X to V
9. Read D. Add to d equiv. from step 5. This equals depth of second layer D_2 (or second Interface, H_2)

Figure 2-13 Sample Nomograph for Depth to Two Interfaces.

(Adapted from depth computer prepared by Geophysical Specialties Division of Soiltest, Evanston, Ill., used by permission of Soiltest.)

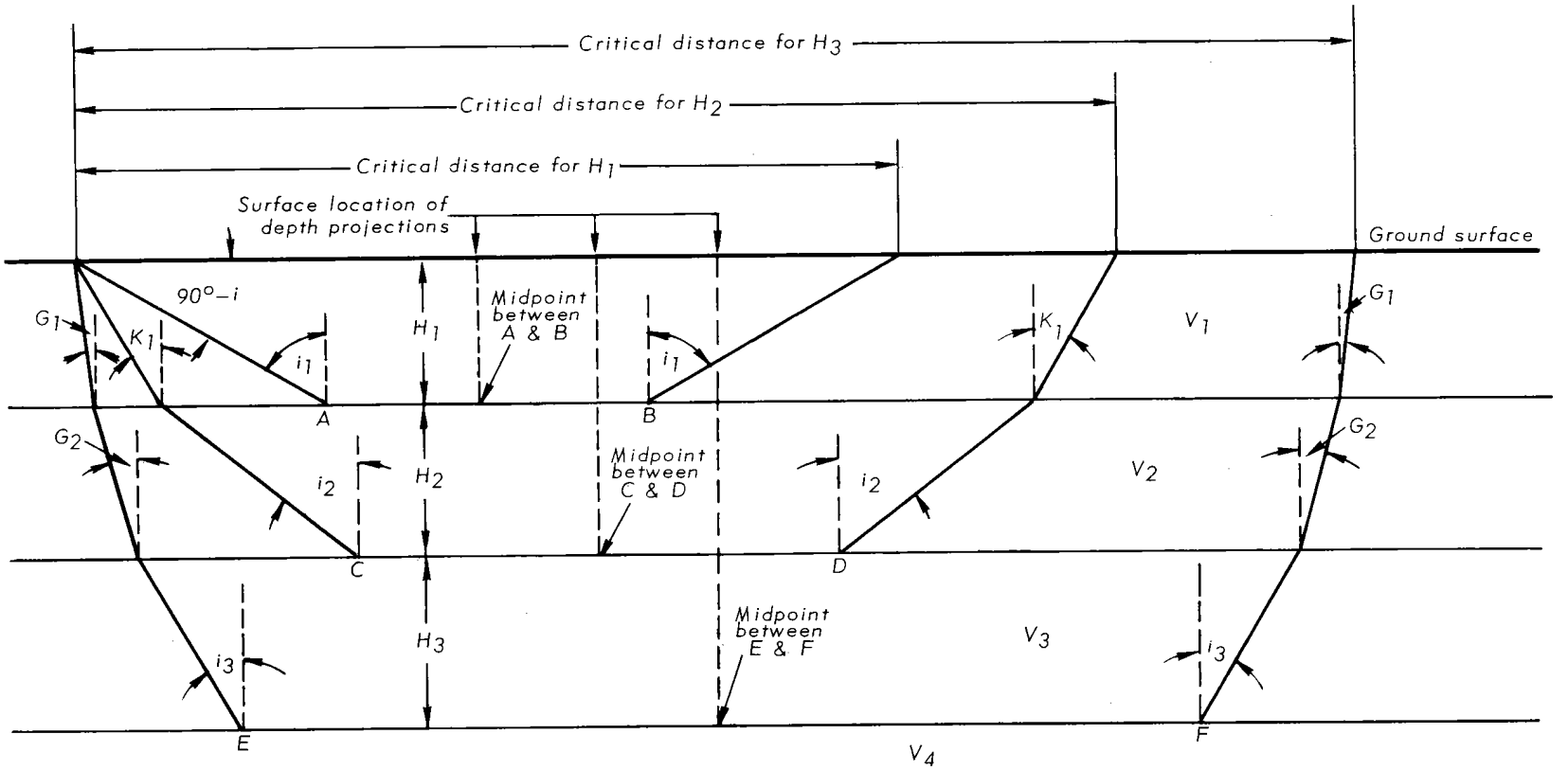

$$\text{Sin } i_1 = \frac{V_1}{V_2} \qquad \text{Sin } K_1 = \frac{V_1}{V_3}$$

$$\text{Sin } i_2 = \frac{V_2}{V_3} \qquad \text{Sin } G_1 = \frac{V_1}{V_4}$$

$$\text{Sin } i_3 = \frac{V_3}{V_4} \qquad \text{Sin } G_2 = \frac{V_2}{V_4}$$

Figure 2–14. – Location of Depth Measurements.

for parallel interface conditions so sloping interfaces will create errors in the depth determinations. For a sloping interface condition both the forward and the reverse profile depths must be plotted by this method to minimize the error. Thus the two points would provide an indication of the behavior of the interface. If this information is studied in relation to the position and variation of the time-distance points on the seismogram, then an interpreted "picture" of the interface can be drawn on the profile.

6. When more than one interface is involved this same procedure is utilized; however, the angles of incidence for the refracted ray must be recalculated each time it is refracted along a deeper interface (See Figure 2-14).

7. For practical purposes (as seen in Figure 2-14) the depth measurements for each interface are located at one-half the critical distance.

Determination of angle of slope of a dipping interface

If a seismic line is run parallel to the direction of maximum dip of an interface, it is possible to determine the angle of dip (α). The following equation gives the relationship between the angle of dip (α) and other known parameters.

V_1, V_2 : Velocities of materials (true), (feet per millisecond).

D : Distance on the ground surface between the points for measuring the time difference (feet).

T_2, T_1 : The difference in total elapsed travel time for the seismic wave between two points measured down dip from the V_2 line. (milliseconds)

The time difference must be measured from the velocity line down dip. The equation is simplified by substituting known values and then solving for a quadratic equation. (See Figure 2-15).

$$V_1\sqrt{V_2^2 - V_1^2}\sqrt{1 - \sin^2\alpha} + (V_2^2 - V_1^2)\sin\alpha - \frac{V_1V_2\sqrt{V_2^2 - V_1^2}\ (T_2 - T_1)}{D} = 0$$

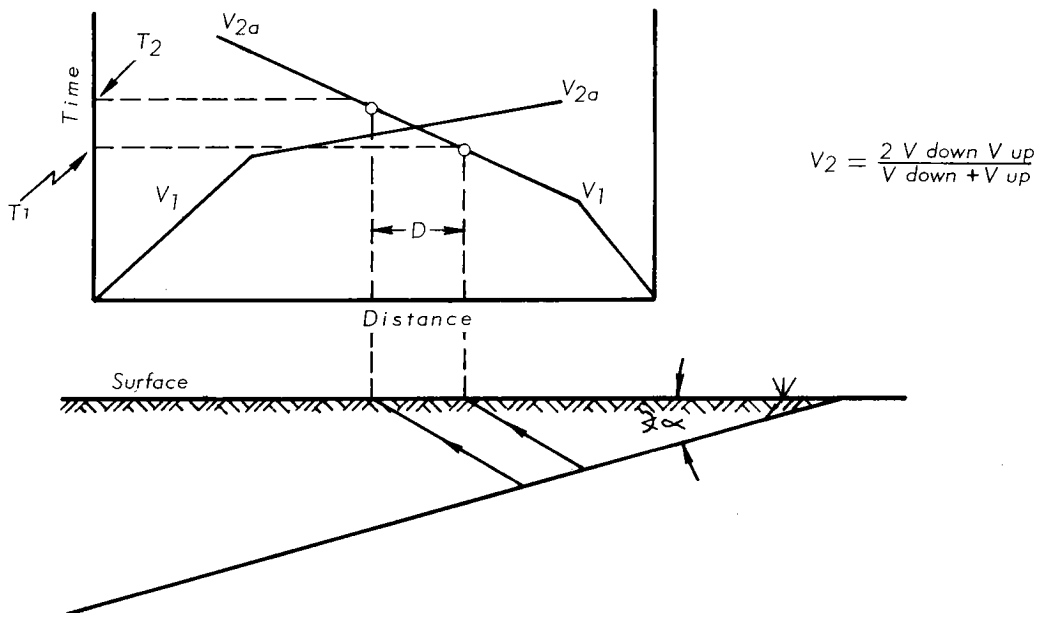

Figure 2–15. – Determination of Angle of Slope of Interface.

Determination of Elastic Properties by Shear Wave Analysis

Refraction seismic equipment can be used to measure the shear wave as well as the compressional wave. The only portion of the standard equipment that may require modification or replacement is the geophone. Shear wave geophones are available from some manufacturers.

Under some circumstances that compressional wave geophone can be used as a shear wave phone. In fact, the compressional geophone will detect vertically polarized shear waves. For example, the Hall-Sears X-25 geophone has the long axis of the moving mass in a vertical position, the normal position for compressional wave studies. By placing the long axis of the moving mass in a horizontal position (laying the phone flat, long axis transverse to the seismic line) the phone can be used to detect horizontally polarized shear waves.

Shear wave analysis techniques are not well developed. The application of current methods should be limited to relatively simple subsurface conditions. The presence of dipping interfaces, thin or

discontinuous strata, or irregular topography could present too complex a problem for analysis.

Once a shear wave time-distance graph is made for a given earth profile, depth computations can be made in a manner as previously described.

Shear wave velocity values can then be grouped with the compressional wave values for the same materials.

The formulas on page 2-4 establish the relationship between the velocities and the elastic properties such as:

Poisson's ratio: $\sigma = \dfrac{\frac{1}{2}(V_p/V_s)^2 - 1}{(V_p/V_s)^2 - 1}$ or $\dfrac{V_p}{V_s} = \sqrt{\dfrac{1-\sigma}{\frac{1}{2}-\sigma}}$

Young's modulus: $E = \rho V_s^2 \left[\dfrac{3V_p^2 - 4V_s^2}{V_p^2 - V_s^2} \right]$

Table 2-3 allows direct conversion of the V_p/V_s ratio to Poisson's ratio.

In addition to determining the numerical values of the moduli of elasticity, the shear wave velocities permit another phase of material interpretation. Moisture content has little if any effect on shear wave velocities, whereas it significantly affects the compressional wave velocities. This difference permits a good means of determining the location of the ground water table.

Contrasting shear and compressional wave velocities also permit interpretation in a manner similar to the complementary usage of seismic and resistivity data. Figure 2-16 illustrates the relationships.

Interpretations

Depth to parallel horizons with distinctly increasing densities are determined easily by plotting the data on time-distance graphs and

TABLE 2-3. CONVERSION FROM VP/VS VELOCITY RATIO TO POISSON'S RATIO

POISSON'S RATIO	VP/VS
0.05	1.453
0.06	1.462
0.07	1.471
0.08	1.480
0.09	1.490
0.10	1.500
0.11	1.511
0.12	1.522
0.13	1.533
0.14	1.546
0.15	1.558
0.16	1.572
0.17	1.586
0.18	1.601
0.19	1.616
0.20	1.633
0.21	1.650
0.22	1.669
0.23	1.689
0.24	1.710
0.25	1.732
0.26	1.756
0.27	1.782
0.28	1.809
0.29	1.839
0.30	1.871
0.31	1.906
0.32	1.944
0.33	1.985
0.34	2.031
0.35	2.082
0.36	2.138
0.37	2.201
0.38	2.273
0.39	2.355
0.40	2.449
0.41	2.560
0.42	2.693
0.43	2.854
0.44	3.055
0.45	3.317
0.46	3.674
0.47	4.203
0.48	5.099
0.49	7.141

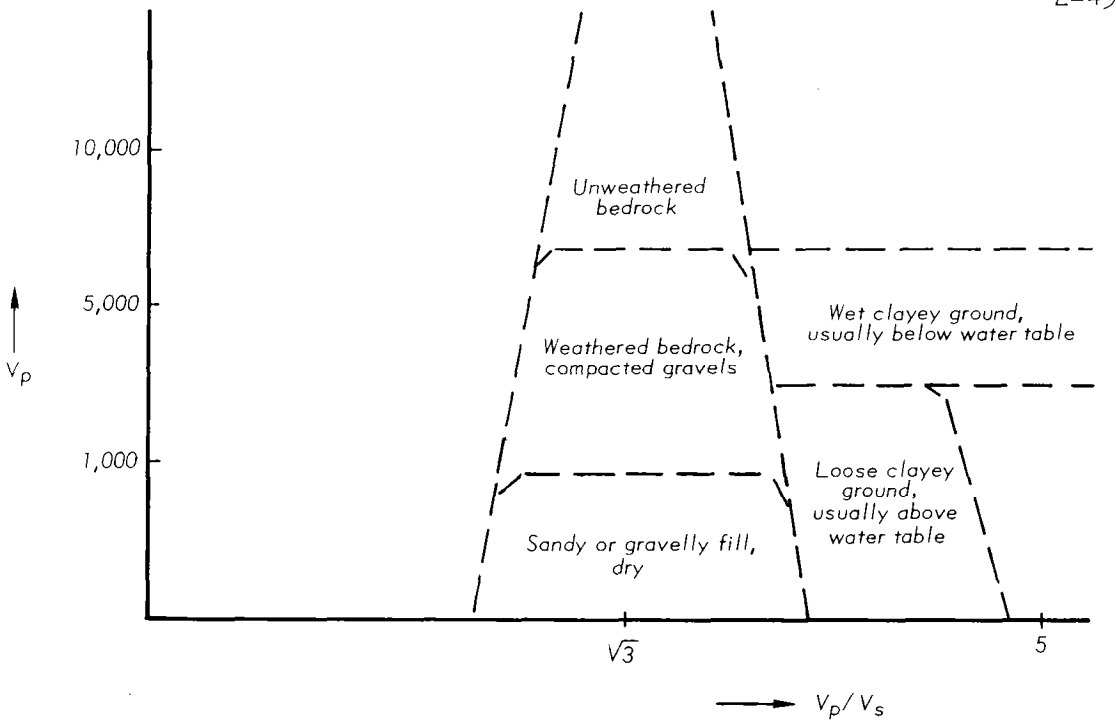

Figure 2–16. – Relationship Between V_p/V_s (or Poisson's ratio) and Characteristics of Earth Materials.

(From: Geophysical Methods in Highway Engineering, by N.R. Patterson and T. Meidav, 1968, HUNTEC LTD., Toronto, used by permission of HUNTEC a Division of Kenting Exploration Services Ltd., Toronto, Canada.)

making calculations as described in the preceding section on computations. However, subsurface conditions such as very irregular rock surfaces, rock ledges, sinkholes, channels, steeply dipping formations and many other concealed anomalies will require experienced and detailed interpretation. These conditions will show as irregularities on the reversed time-distance graph, the seismogram, or on the shape of the flash on the cathode ray tube.

Sometimes variable readings may be received at about the position of a critical distance. This could be due to a layer of disturbed material at the interface. Readings should be taken a few feet either side of this position along the survey line.

When using a seismograph which has a cathode ray tube (CRT) or photographic recording media, information can be gained from the shape of the flash or recorded wave. A second arrival refracted wave often can be seen as a smaller secondary wave on the upsweep or downsweep of

the first or second wave of the seismogram: 
The difference in travel time between the first and second arrivals can be determined if desired either by reading the time of the first arrival, adjusting the delay to read the second arrival, and substracting to get the milliseconds delay between the two, or by measuring the time directly on the recorded seismogram.

Sands, gravels, and sandstone bedrock usually give strong and distinct waves which retain good amplitude with distance. On the other hand, clays give fair shaped waves, some limestones and dolomites and also peat and muck give poor waves, and all of these decrease quickly in amplitude with distance.

Good discussions and sketches regarding interpretations may be found in the references listed and expecially in some of the manuals and reports published by manufacturers. Information from Soiltest and DynaMetric describe many details on the interpretation of the flashes on the CRT.

The following sketches of time-distance graphs and subsurface conditions illustrate some normal and some problem conditions which we may expect to find. In the sketches "T" indicates the total elapsed travel time for first arrival (P) waves over a specific distance. "T" is always approximately equal for the forward and reverse spread.

Parallel Layers

On a typical graph with forward and reverse spreads over uniformly parallel layers, the velocity curves will be mirror images of each other as in Figure 2-17.

Dipping Interface

A dipping interface will give different critical distances, and V_2 velocities on the forward and reverse curves, as shown in Figure 2-18.

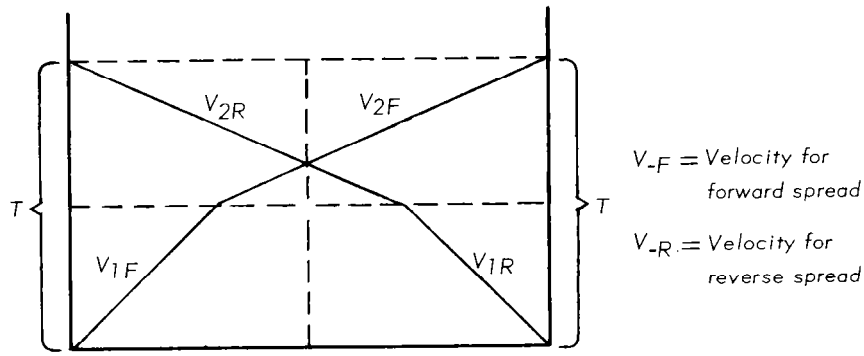

Figure 2–17. – Parallel Layer.

The velocities of the surface material are nearly the same on the forward and reverse graphs. The apparent velocities of the second horizon are quite different. The best approximation of true velocity of this horizon is determined from the equation.

$$V_t = \frac{2\ V_d\ V_u}{V_d + V_u}$$

where V_u is run updip and V_d is run downdip.

The average depth to the rock can be determined by averaging the two critical distances and using this value in solving the formula for depth if the dip of the rock interface is less than 10 percent. A more exact method is explained on page 2-42 . The approximate dip of the rock interface can be determined by using more complex formulas (see page 2-45). The total elapsed time for each spread (forward and reversed) must always be approximately equal.

High or Low Rock Points

Abnormally high or low points in the buried rock surface may plot below the average velocity line where there is a rise in the rock profile, or above the velocity line where a large depression exists (Figure 2-19). Also, points will plot above or below the line where an uneven ground surface lies over a smooth rock surface. All "second arrival" readings will plot above the line.

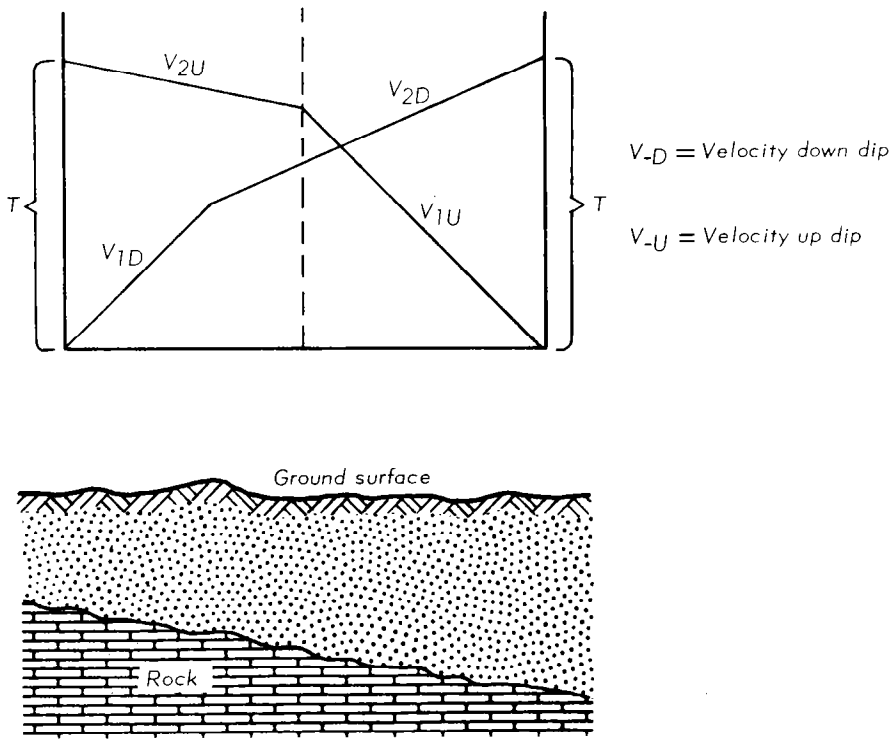

Figure 2–18. – Dipping Interface.

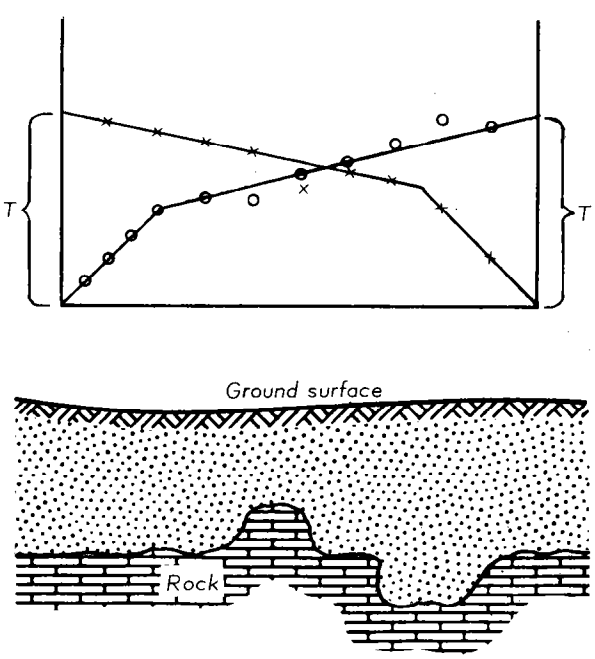

Figure 2–19. – High or Low Rock Points.

Buried Rock Ledge

Upon passing the end of a buried rock ledge the velocity curve turns upward, (Figure 2-20) indicating that low velocity materials exist beyond the end of the ledge.

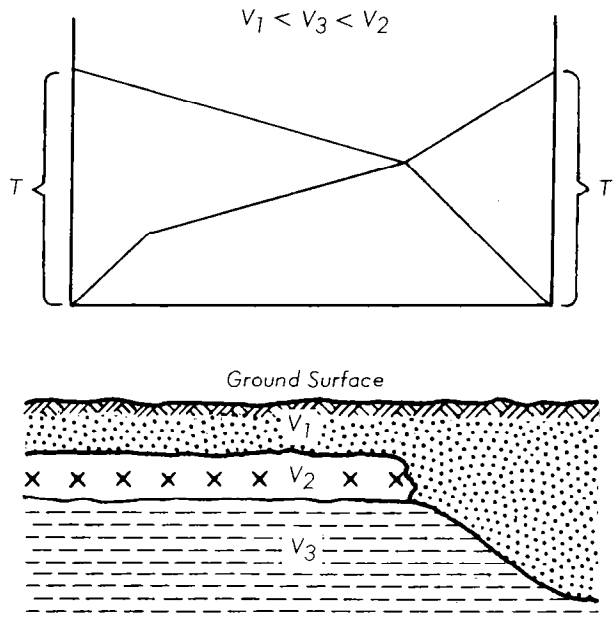

Figure 2–20. – Buried Rock Ledge.

Subsurface Stream Channel

A subsurface deeply incised stream channel or cliff will give unusual velocity curves. Note the difference in the curves for the forward and the reverse spreads in Figure 2-21.

Subsurface Cliff

Somewhat similar to Figure 2-21, however, the slope of the break of the rock surface is very steep, and the velocity lines show a definite up-or-down step in Figure 2-22.

Offset Velocity Curve

An offset in the velocity curve as shown on Figure 2-23 may be caused by any one of several conditions: (1) starting to pick up and plot

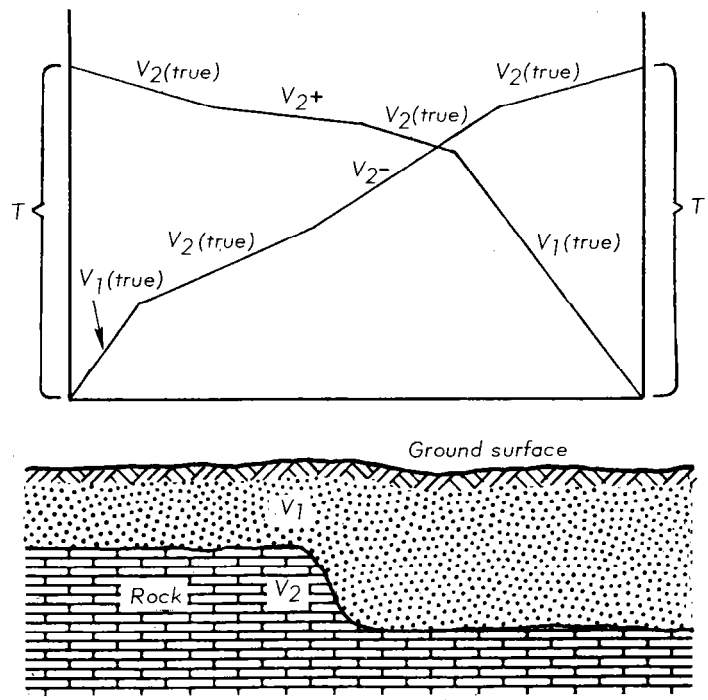

Figure 2–21. – Subsurface Stream Channel.

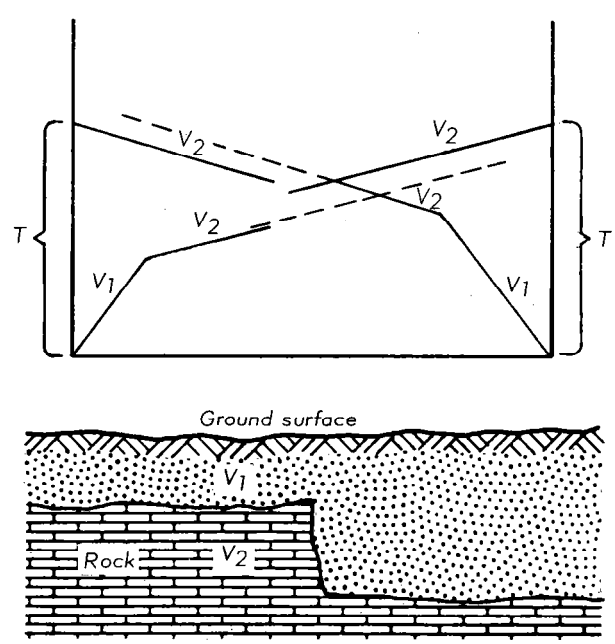

Figure 2–22. – Subsurface Cliff.

"second arrivals"; (2) passing a vertical offset downward in the rock profile; or (3) as shown by the dashed V_2 line, passing a narrow fractured fault zone, a vertical mud seam, or a large open cavern or sinkhole.

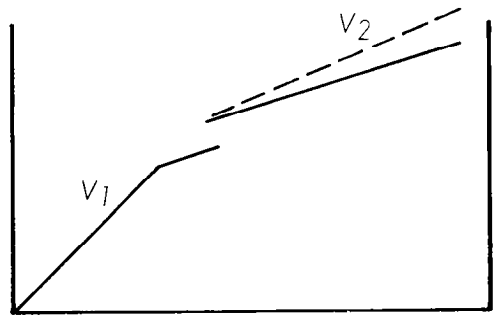

Figure 2–23. – Offset Velocity Curve.

Parabolic Velocity Curves

In an area of very deep soils or alluvium which gradually increase in density with depth, no interface can be plotted, but instead the velocity curves will be parabolic as shown in Figure 2-24.

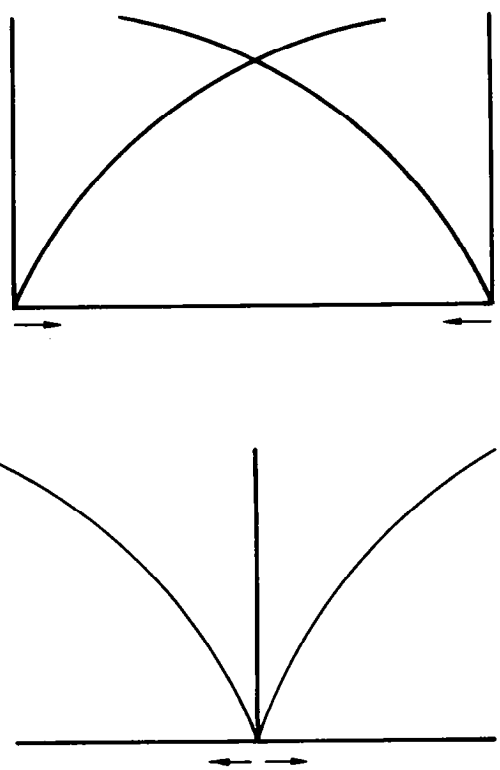

Figure 2–24. – Parabolic Velocity Curve.

Abnormal Velocity Curves

Abnormal curves like the following Figure 2-25 in which V_2a (V_2 apparent) is less than true V_2 velocity may be found when: there is a change in dip downward on the surface of the second horizon, or the survey line starts up a grade, as shown by the reverse profile; or when there is a change in dip upward on the surface of the second horizon, or the survey line goes over a hill.

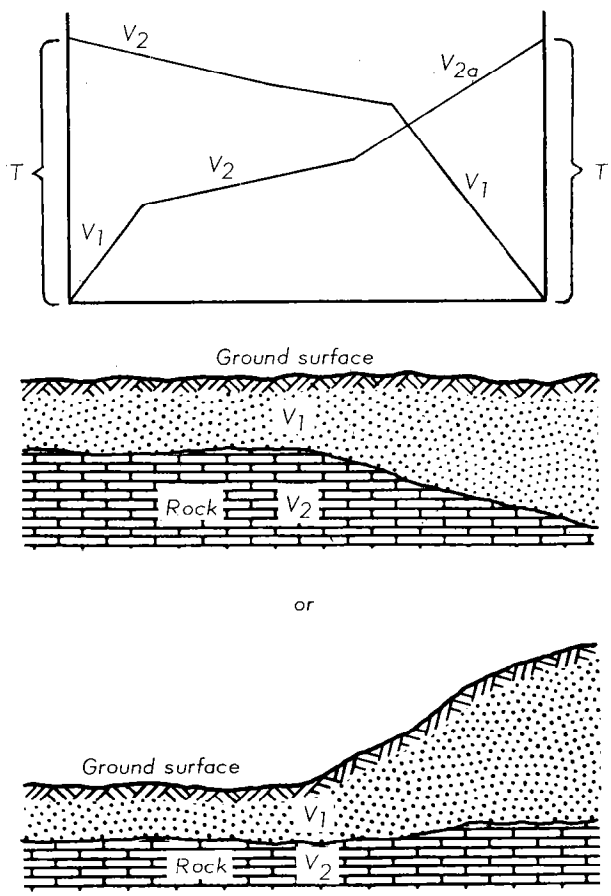

Figure 2–25. – Abnormal Velocity Curves.

Subsurface Fault

A forward and reverse spread across steeply dipping or faulted massive bedrock overlain by alluvium would give time distance curves similar

to Figure 2-26. The V_1, V_2, and V_3 and velocities are true velocities.

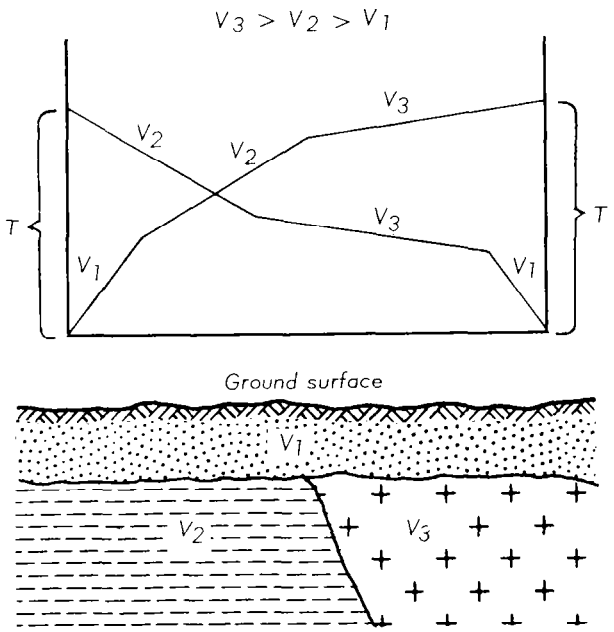

Figure. 2–26. – Subsurface Fault.

Buried Ridge

A vertical or steeply-dipping buried ridge of hard rock aligned at an angle to the direction of the survey line may give a curve similar to that shown in Figure 2-27. Unless an outcrop is found which will provide an indication of thickness and direction of strike, several survey lines may be required to make these determinations.

Critical Thickness

In the three layer case with velocities V_1, V_2, and V_3, it is possible for the V_2 layer to be obscure. The U. S. Corps of Engineers (1948) has discussed this problem and their data is used in the example.

On the time-distance graph (Figure 2-28) the V_1, V_2, and V_3 layers have velocities of 1500 fps, 4000 fps, and 15000 fps respectively. The thickness (H_1) of the top (V_1) layer is 8.1 feet computed from the formula on page 2-38.

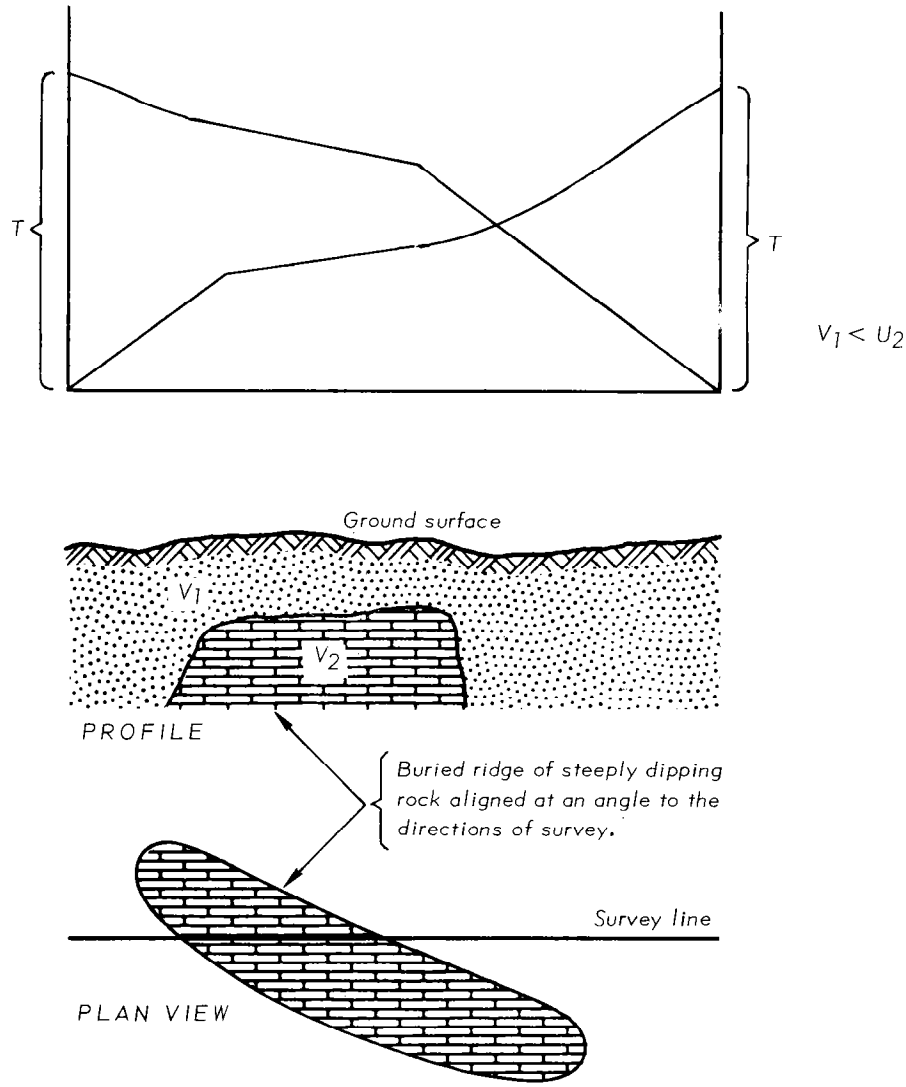

Figure 2–27. – Buried Ridge.

If the second critical distance is 110 feet (velocity line I) the thickness of the V_2 layer is 40.2 feet and the depth to the V_3 layer is 48.3 feet as computed from formula on page 2-41. If the V_2 layer is this thick (40.2 feet) sufficient first arrivals will be obtained to plot the V_2 velocity curve. If the thickness of the V_2 layer is 19.7 feet (velocity line II) the distance between the first (24 feet) and second (56 feet) critical distances is small enough that only one first arrival from the V_2 layer may be detected. This is especially true if the 10-10-20-20 or 15-15-30-30 geophone layout is used (see page 2-25).

If the thickness of the V_2 layer is 7.5 feet (velocity line III) the first and second critical distances coincide and the V_2 layer is

totally masked. Thicknesses between 19.7 feet and 7.5 feet will be difficult to detect.

Also, if the true critical distances coincide, (V_2 layer 7.5 feet thick) calculations for H_1 would give the depth to the V_3-15,000 fps layer as 10.9 feet completely ignoring the V_2 layer and would result in considerable error.

The following formula will determine the critical thickness of a layer of material. If the actual thickness is less than the computed value, the material will be undetected on the seismogram.

X_0 - first critical distance

H_2 - critical thickness

V_2 - an assumed velocity value for the layer in question.

V_3 - The velocity of the material underlying the material in question.

$$H_2 = \frac{X_0}{2} \left(1 - \frac{V_2}{V_3}\right)$$

Masked Layer

If a high velocity layer overlies a lower velocity layer, the lower velocity layer will be completely masked. In this diagram (Figure 2-29) the V_2 velocity is higher than V_3 but less than V_4. The time distance graph does not show any indication of the V_3 velocity (or layer). The depth calculation, based on this time-distance graph, of the V_4 layer would be in error because the V_3 velocity is not used. The amount of error would depend on the velocity difference between V_2 and V_3 and the actual thickness of the V_3 layer.

A different type masking problem occurs quite often. In the three (or more) layer case there may be a question if there is an intermediate layer present. If a recording multiple-channel seismograph is used the film record can be examined for strong secondary arrivals. An example of strong secondary arrivals is plotted in Figure 2-30. These secondary arrivals may suggest the presence of an intermediate layer, but

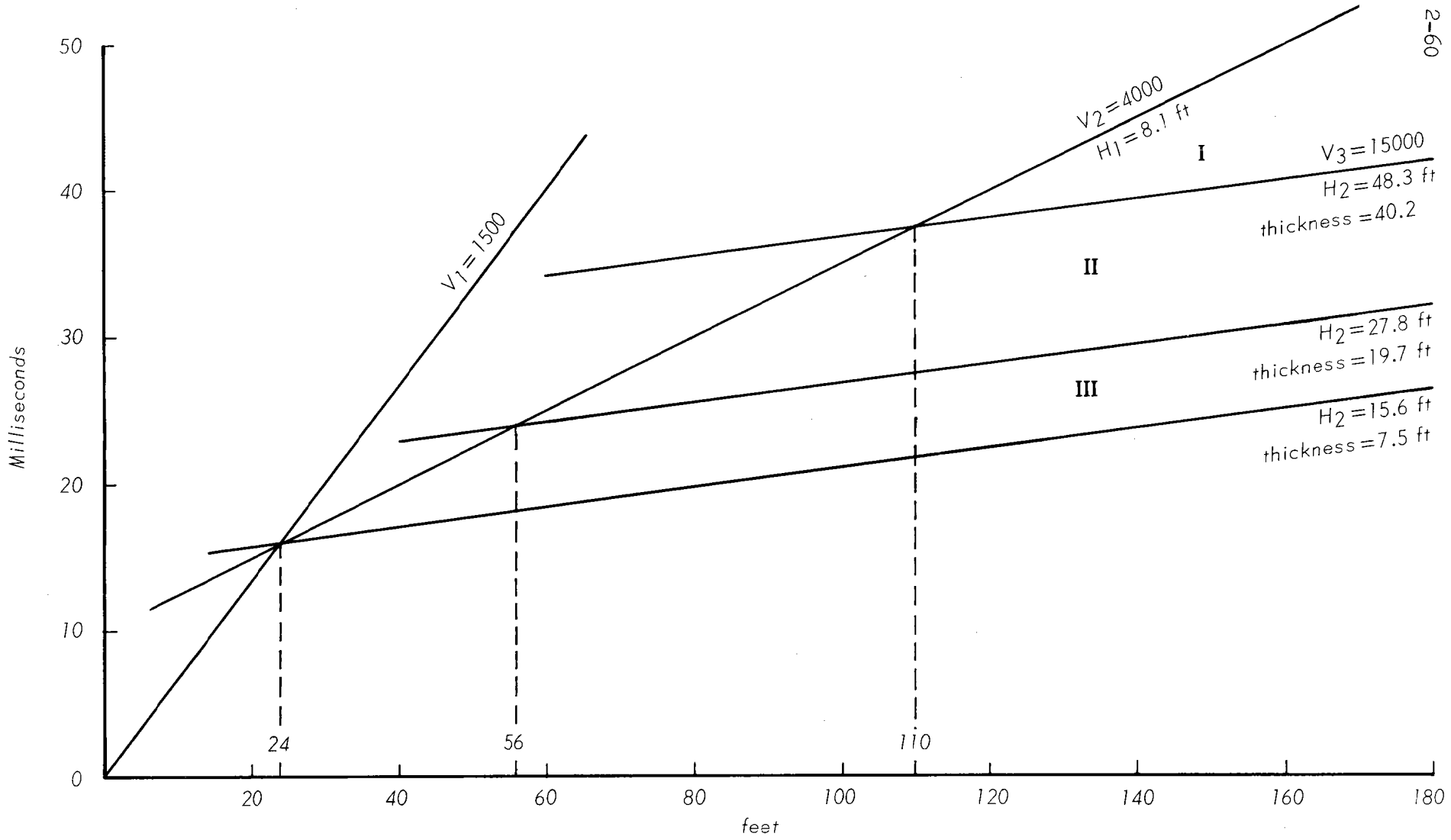

Figure 2–28. – Critical Thickness.

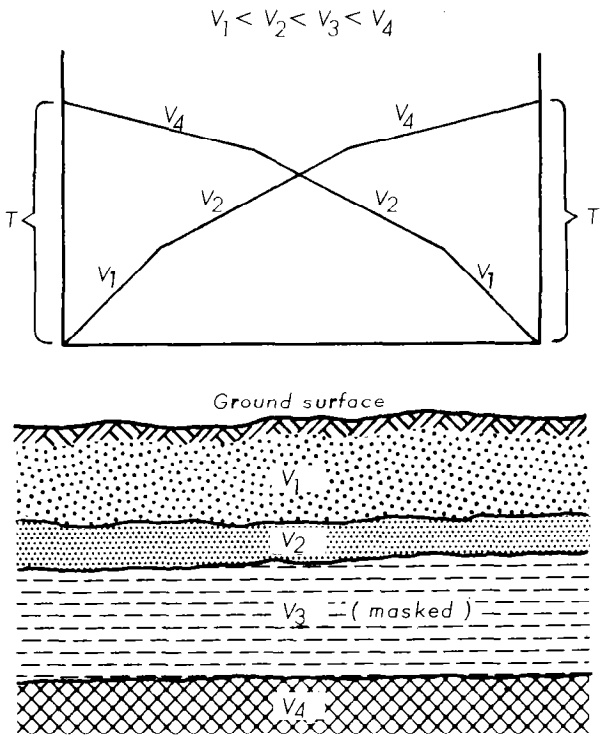

Figure 2–29. – Masked Layer.

the arrangement of the points suggests a material of increasing velocity with depth and not one velocity. Six theoretical velocity lines are shown in their proper location for the theoretical section in the right corner. First arrivals could be detected from the upper three (V_1, V_2, and V_3) layers and the V_6 rock layer. First arrivals from the V_3 layer would be very close to the critical distance for V_1 –V_2 and V_2-V_6 and probably not be detected. First arrivals from layers between V_3 and V_6 would be completely masked.

The U. S. Army Corps of Engineers (1948) analyzed this problem and computed the depth to rock using two different methods of calculation and seven combinations of velocities. They concluded that the best method considering time involved and accuracy required is o use two average intermediate velocities and the velocity of the rock in the depth calculations. Depths calculated in this manner were within ±1 foot of true depth.

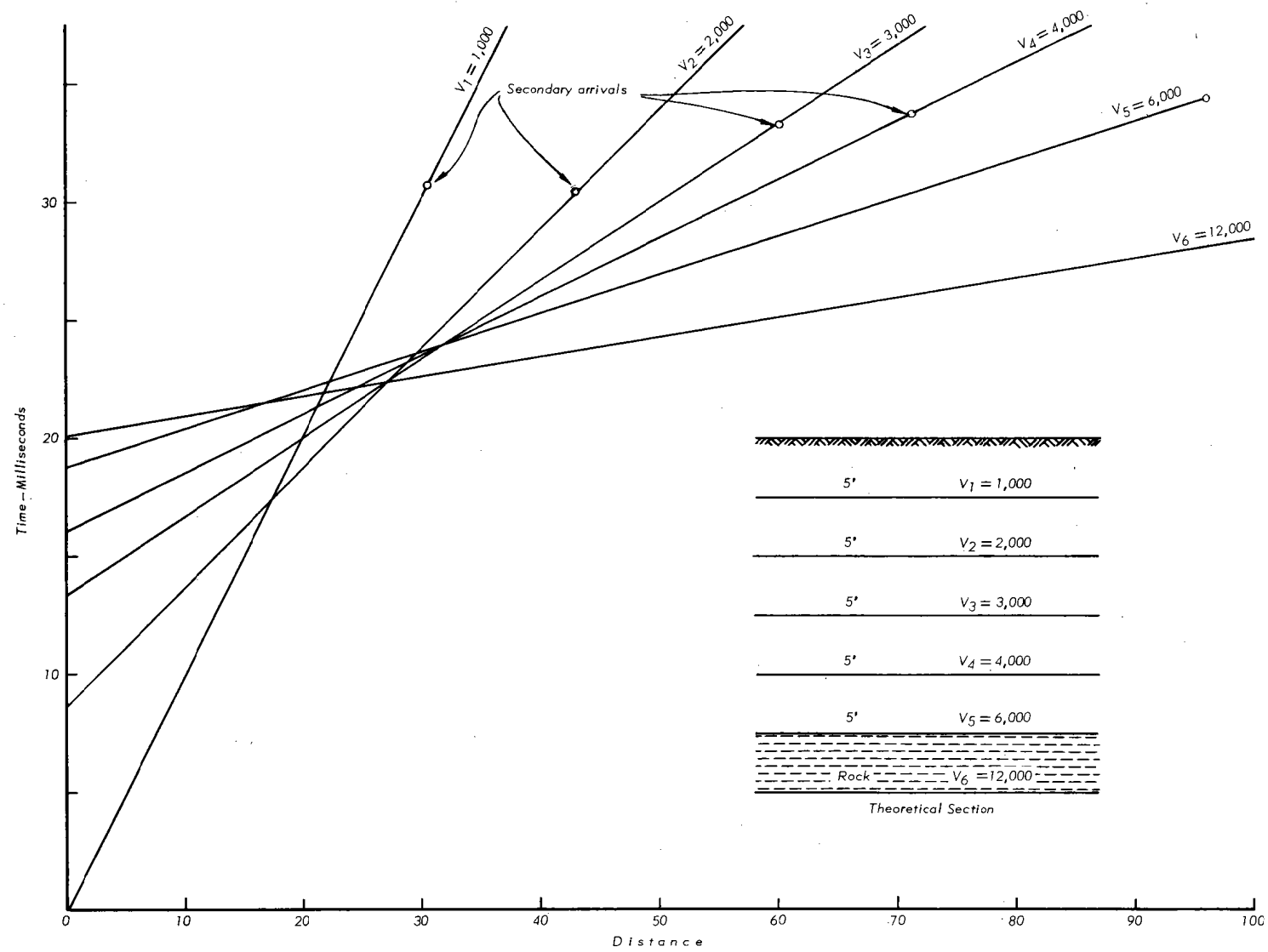

Figure 2–30. – Masked Layer Problem.

Discontinuous Layer

A discontinuous layer can be difficult or impossible to detect by refraction seismic methods. The followin example was encountered by Maine SCS Geologist Erinakes.

The time-distance graph plotted from the seismogram of a twelve channel recording seismograph using 10-10-20-20 geophone spacing is shown in Figure 2-31. The interpretation of this time-distance graph provides the following results:

Forward Profile	Reversed Profile
V_1 = 4,500 fps	V_1 = 4,500 fps
V_2 = 10,100 fps	V_2 = 16,500 fps
V_3 = 16,800 fps	X_1 = 88.5 ft
X_1 = 64 ft	
X_2 = 152 ft	

$$V_2(\text{average}) = \frac{2\ V_u V_d}{V_u + V_d} = 12{,}500 \text{ fps}$$

$$H_1(\text{forward}) = \frac{64}{2}\ (.472)^{1/2} = 22 \text{ ft}$$

$$H_1(\text{reversed}) = \frac{88.5}{2}\ (.472)^{1/2} = 30.5 \text{ ft}$$

$$\sin i = \frac{4490}{12{,}500} \quad \text{and angle } i = 21^\circ$$

The H_1 (forward) depth would be plotted 32 feet from the forward shot point. The H_1 (reversed) depth would be plotted 44 feet from the reversed shot point. The V_3 forward velocity of 16,800 fps might be interpreted as a slight rise in the rock surface at the outer end of the spread.

Subsequently correlation test holes revealed the presence of an intermediate velocity discontinuous layer at both ends of the seismic spread. As indicated above, the presence of this layer was not suspected from the time-distance graph.

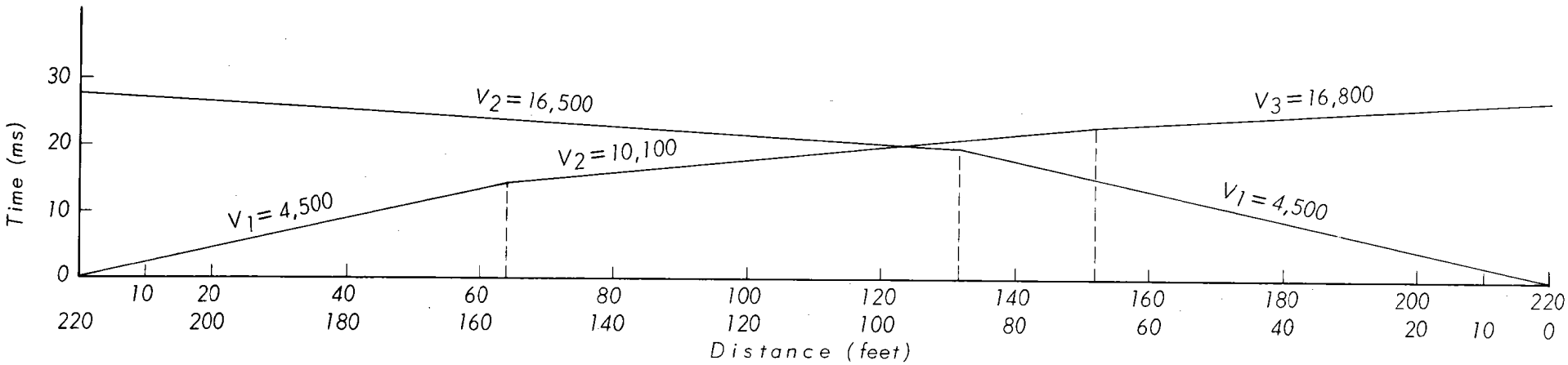

Figure 2–31. – Time – Distance Graph.

The forward and reversed profiles in Figure 2-32 show the actual subsurface condition. The paths of direct and refracted waves and their time of arrival at selected points are shown.

The time-distance graph (Figure 2-32) was constructed using the computed time of first arrivals at selected points. The points were selected to give the best definition to the time-distance graph and are not necessarily the actual geophone locations.

By studying the paths of the refracted and surface waves and their times of arrival at various points it becomes obvious why the discontinuous layers were missed in the first interpretation.

This again emphasizes the necessity for correlation of geophysical interpretations with test holes etc.

Remember the time-distance relationship is a representation of a physical situation and is repeatable. It is the interpretation of its meaning that creates variability.

Subsurface Drop-off

If a subsurface ledge of rock or a steep drop-off is located, its true depth may be determined by running the survey line above and parallel to its edge. If the depth of the soil material is needed below the face of the buried escarpment, a survey line may be run perpendicular out from the ledge or parallel to its edge, but further away than the maximum depth to rock. See Figure 2-33.

To determine the depth to the top of the rock escarpment a forward and reverse seismic line is run between points 1 and 2 (Figure 2-33). To determine the location of the escarpment a forward and reverse seismic line is run between points 2 and 3. To determine the depth to rock below the escarpment forward and reverse seismic profiles are fun between points 3 and 4. This seismic line between points 3 and 4 must

be located so that distance D_1 always is greater than distance D_2. If D_1 is not greater than D_2 the shortest time path for the seismic waves at distances greater than the critical distance would be through the rock in the escarpment instead of the rock below the escarpment.

This placement also applies to the distance away from a buried pipeline.

Drill Hole Correlation

In order to correlate seismic results with drill hole information it is necessary to make the seismic measurements as near as possible to the bore hole.

As was previously demonstrated, the location of the depth measurements made by the seismic method is a function of the relative velocities of the materials involved and varies with a change in velocities.

The following procedure is suggested in order to perform correlation seismic measurements.

1. Lay out and run seismic spread (forward and reversed) over the drill hole (center over hole).
2. Determine the velocities of the materials involved.
3. Locate the depth measurements using the method described on page 2-42.
4. With the information of where the depth measurements were made along the seismic spread, lay out and run a new seismic line so that the H_1 depth location is centered on the drill hole. In order to check the H_2, H_3 etc. measurements, a new seismic layout will be required with each location centerd on the drill hole.
5. Compare the depth measurements made under step 4 with the drill hole information. Compute the percentage of error and use it as a guide to the accuracy of other seismic measurements.

Continuous Profiles

Whenever possible, seismic lines should be laid out end to end in order

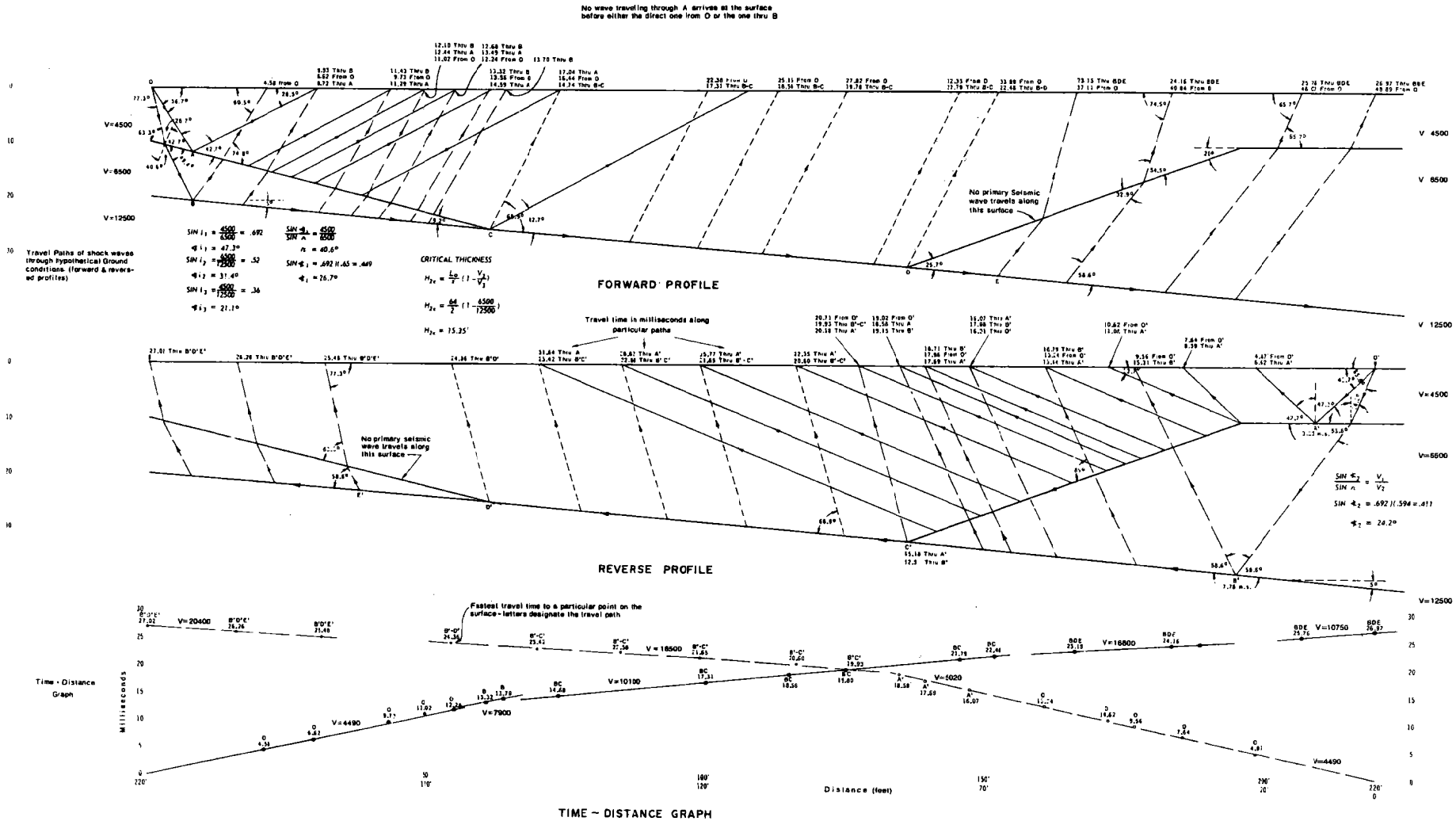

Figure 2–32. – Computed Seismogram.

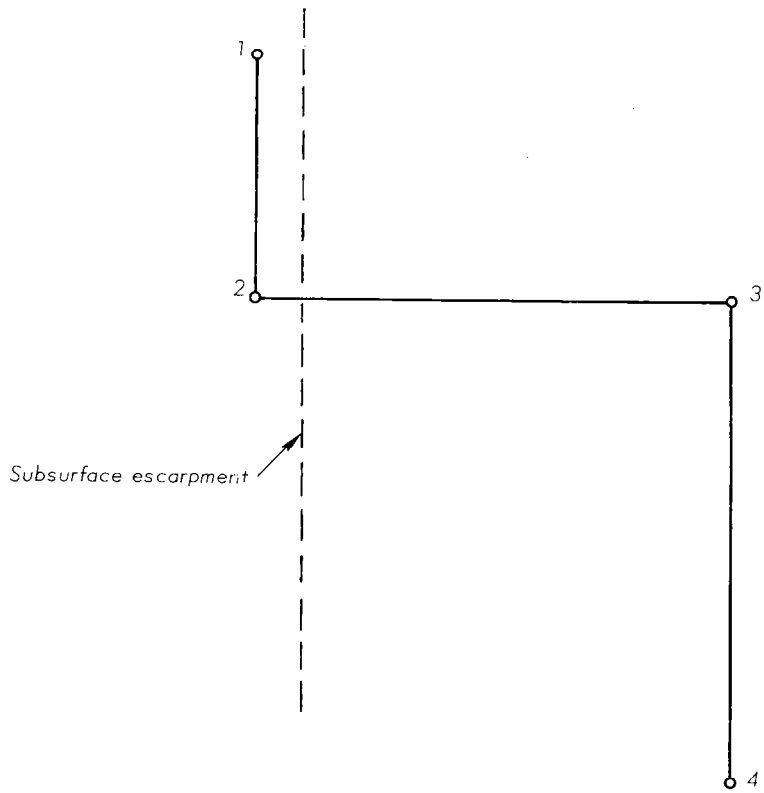

Plan View

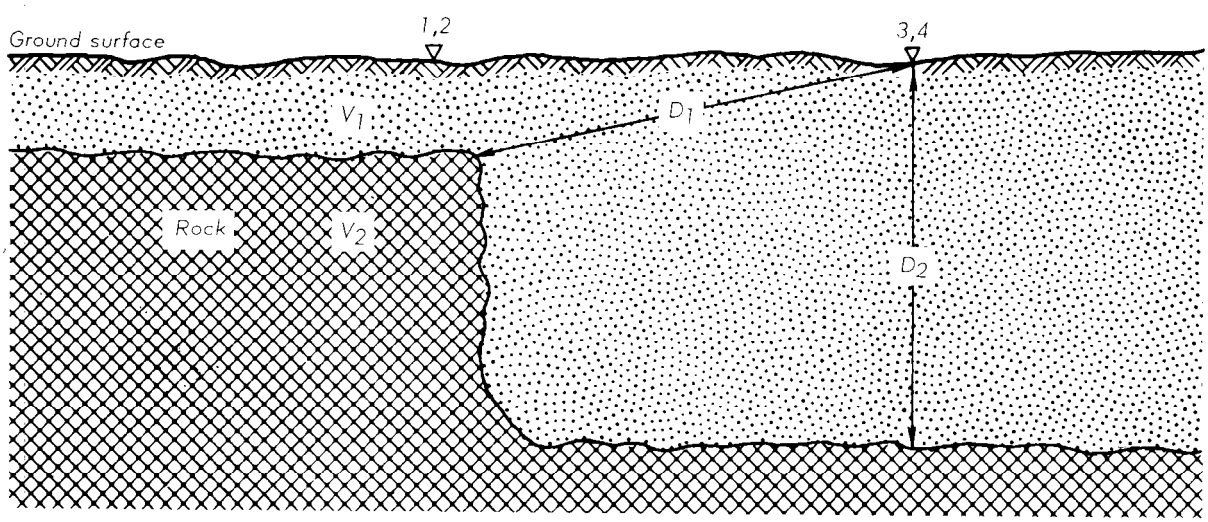

Section

$V_2 > V_1$

Figure 2–33. – Seismic Line Layout for Subsurface Escarpment.

to establish "tie-in" points. Seismic lines that are run end to end as continuous spreads provide a means of checking the continuity of subsurface conditions and allow each profile to be checked against other profiles.

Figure 2-34 illustrates the method of establishing tie-in points. It is important to note the use of common shot holes or end points. Only by this means are the continuous profiles valid.

Velocities of Various Soil and Rock Materials

The principal factors influencing velocities in soil materials are density, elastic constants, degrees of wetness, and in cobbly or bouldery materials whether the individual cobbles and boulders are in contact or are separated by soil. In rock formations velocities are influenced by elastic constants, degree of weathering, density, cementation, and amount of fracturing, jointing, or faulting.

Water has a seismic velocity of about 4800 feet per second. A soil material having velocity of about 1200 feet per second when dry, may have a velocity of about 5000 feet per second when saturated. Likewise, dry fractured rock would have slightly lower velocity than the same rock material when saturated. Shales and sandstones may vary from 3,000 to 10,000 feet per second depending upon whether they are soft, weak and poorly cemented or whether they are hard and well-cemented.

It is possible that velocities of 3,000 to 7,000 feet per second could indicate either soil materials or rock. This emphasizes the importance of the geologist being familiar with the geology of the area and correlating and calibrating instrument data with proven data from logged drill holes or deeply exposed profiles of the soil and rock. Table 2-4 lists the relative seismic velocities of some typical materials.

Rippability and Rock Excavation

Since the middle 1950's seismic analysis has been used by some

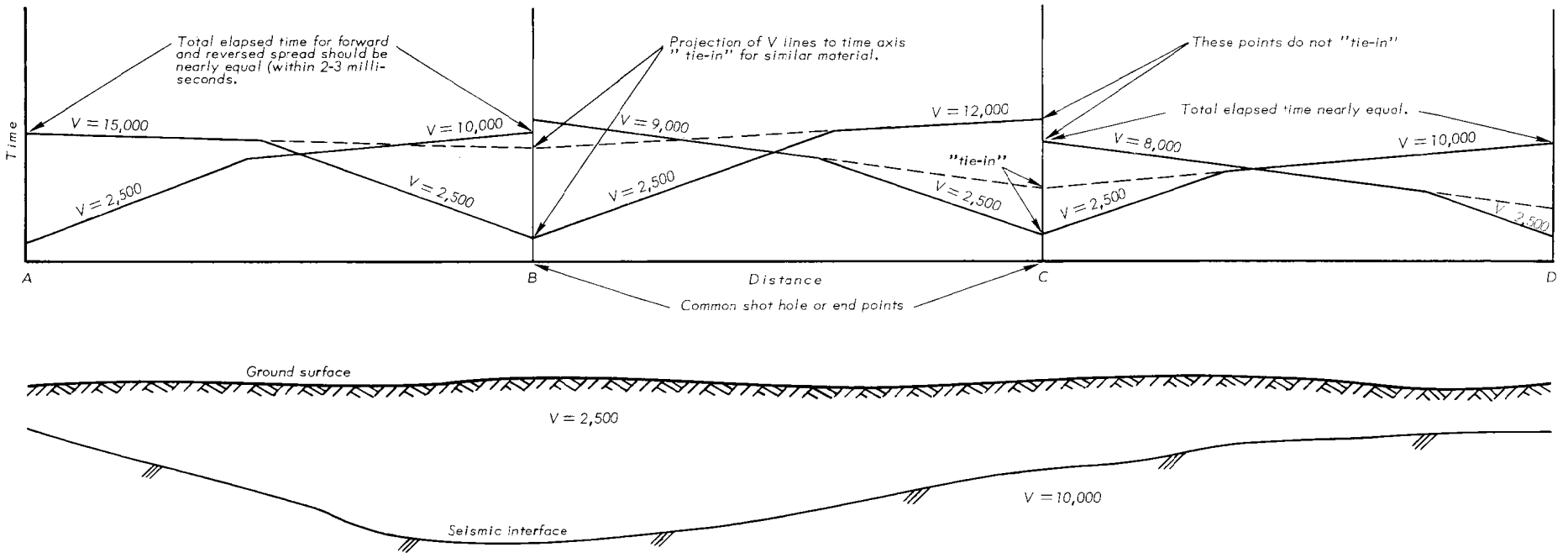

Figure 2–34. – Tie-in Points on Continuous Profiles.

Table 2-4. Relative Seismic Velocities (P-Waves).

Feet Per Second	
600 - 1,200	Dry, loose topsoils and silts
1,000 - 1,600	Dry sands, loams, and slightly sandy or gravelly soft clays
1,500 - 3,000	Dry gravels; moist sandy and gravelly soils; dry heavy silts and clays; moist silty and clayey soils
3,000 - 4,800	Dry, heavy gravelly clay; moist heavy clays; cobbly materials with considerable sands and fines; soft shales; soft or weak sandstones
4,800 - 5,000	Water; saturated silts or clays; wet gravels
4,800 - 6,000	Compacted moist clays; saturated sands and gravels; soils below the water table; dry medium shales, moderately soft sandstones, weathered moist shales & schists
5,500 - 8,000	Hardpan; cemented gravels; hard clay; boulder till; compact cobbly and bouldery materials; medium to moderately hard shales and sandstones; partially decomposed granites; jointed and fractured hard rocks.
8,000 - 12,000	Hard shales and sandstones; interbedded shales and sandstones; slightly fractured limestones and crystalline rocks
12,000 - 20,000	Unweathered limestones, granites, gneiss, and other dense rocks

(Note: the velocity of sound in air at sea level and 32 degrees F., is 1087 feet per second.)

consultants as a basis for estimating the rippability of rock and hard soil materials. Some contracts have been accepted for rock excavation based on seismic velocity and an analysis of the type and characteristics of the rock.

For the purpose of rock excavation by the SCS, the following is quoted from Construction Specification 21, Section 20, National Engineering Handbook:

"Common Excavation shall be defined as the excavation of all materials that can be excavated, transported, and unloaded by the use of heavy ripping equipment and wheel tractor-scrapers with pusher tractors or that can be excavated and dumped into place or loaded onto hauling equipment by means of excavators having a rated capacity of one cubic yard and equipped with attachments (such as shovel, bucket, backhoe, dragline or clam shell) appropriate to the character of the materials and the site conditions.

"Rock excavation shall be defined as the excavation of all hard, compacted or cemented materials the accomplishment of which requires blasting or the use of excavators larger than defined for common excavation. The excavation and removal of isolated boulders or rock fragments larger than one cubic yard in volume encountered in materials otherwise conforming to the definition of common excavation shall be classified as rock excavation.

For the purpose of this classification, the following definitions shall apply:

"Heavy ripping equipment shall be defined as a rear-mounted heavy duty, single-tooth, ripping attachment mounted on a tractor having a power rating of at least 200 net horsepower (at the flywheel).

"Wheel tractor-scraper shall be defined as a self-loading (not elevating) and unloading scraper having a struck bowl capacity of at least 12 yards.

"Pusher tractor shall be defined as a track type tractor having a power rating of at least 200 net horsepower (at the flywheel) equipped with appropriate attachments."

Test pits excavated with the equivalent of a D-7 or D-8 bulldozer are the most reliable means for determining rock excavation. Cores from test holes will provide identification of rock material but they may be misleading in estimating rippability.

Other than test pits, seismic analysis and a study of the rock formations by a competent geologist who is acquainted with excavating equipment may provide the quickest and most reliable method for determining rock excavation.

Manufacturers and contractors using crawler-type tractors have prepared tables on the rippability of rock based on seismic analysis. This method correlated with excavating experience in a given area may often be reliable. However, it may have serious and expensive pitfalls which can be recognized by a competent geologist.

For example, a thick bedded but poorly-cemented sandstone may be almost impossible to rip by the SCS specifications when dry because the ripper tooth cannot enter the material. However, if the sandstone is wet or saturated, the ripper tooth may penetrate and rip it with ease. This same sandstone may have a seismic velocity of 3,500 to 5,000 feet per second (fps) when dry, but may have a velocity of 5,000 to 8,500 fps when saturated. A thin-bedded hard sandstone or limestone with fractures or joints may have a seismic velocity of around 7,000 fps but may be ripped because the ripper tooth may enter at the joints.

Some compact or indurated massive clays, hardpans, claystones, chalks, and shales may have moderate velocities of 5,000 to 6,500 fps but may be almost impossible to rip by the SCS specifications. Important conditions affecting rippability include thickness of bedding, frequency of jointing, amount of weathering, direction and degree of dip, and in some cases wetness or dryness.

The following table is only a general guide and should not be taken literally. The conditions described in the preceding paragraph must be considered in relation to the seismic velocities.

TABLE 2-5. Relation of Seismic Velocities to Rippability

Type of Rock	Velocities in Marginal Conditions	Velocities Indicating Non-Rippability
	(Ft. Per Sec.)	(Ft. Per Sec.)
Clay	Indurated, thick bedded; or claystone 5,000-6,500	over 6,500
Glacial Till	Boulder Till, 4,500-6,000	over 6,000
Shale	Compact with hard laminae 5,500-7,000	over 7,000
Sandstone	Dry, poorly-cemented, thick-bedded 4,000-5,000	over 5,000
	Wet, poorly-cemented; thick-bedded 5,000-6,500	over 6,500
	Thin-bedded, jointed 5,500-7,000	over 7,000
	Thick-bedded, weathered 5,000-6,000	over 6,000
Limestone and Chalk	Thin-bedded or closely-jointed 5,000-7,000	over 7,000
	Medium to thick beds	over 6,000
Caliche	5,500-7,000	over 7,000
Schist or Slate	5,000-6,500	over 6,500
Gneiss or Quartzite	Frequent joints 4,500-5,500	over 5,500
Granite	Weathered & jointed 4,500-5,500	over 5,500
Basalt	4,500-6,000	over 6,000

The following steps should be considered in determining rippability and rock excavation:

1. Inquire from the experience of project construction engineers and contractors about the techniques and difficulty of excavating the

type of rock in question.

2. Make careful observations on the type of rock and its condition, especially apparent hardness, bedding thickness, jointing, inclusions of soft rock, interbedded soft layers, etc.

3. Make seismic analysis to determine depth to the rock surface, the areal extent of the rock, and its estimated rippability. Correlate with drill cores or exposures when possible.

4. Where a rock formation is exposed for 100 feet or more, its velocity may be measured directly with the seismograph. Likewise, if a rock layer extends through a ridge, and good exposures are found on each side of the ridge, the velocity of the formation may be measured by taking direct readings in the rock through the ridge.

Cost Data For Seismic Surveying

The cost of seismic surveys is composed of several parts. They are the instrument, travel, survey time, correlation test holes, and interpretations and preparation of a report.

The cost of the various types of refraction seismic instruments has been discussed in a previous section of this technical release. Travel expenses depend on location, distance from headquarters, etc., and have to be evaluated separately for each site.

Actual field survey time for a two man crew under average conditions will vary depending on equipment and method used and site conditions. As stated on page 2-24 using a single channel instrument and explosives a 200 foot line requires about 2 man-hours while a multiple channel instrument with explosives requires about 1 man-hour. Using a single channel instrument and a hammer or tamper, the usual maximum line length is about 100 feet. With a two man crew a 100 foot forward and reverse spread would require about 2 man-hours under good conditions. With bad conditions it may be impossible to receive the

seismic signals using the low energy hammer or tamper method while work could proceed uninterrupted using explosives.

Correlation test holes are required at every site to enable valid interpretations to be made. These test holes can be hand auger holes, test pits, power auger or core holes, or outcrops, depending on site conditions and equipment available. This time should be considered as part of the site investigation.

Interpretation of the field data and preparation of the report of investigation require about 1/2 the man days that the field investigation requires. If the geologist and one helper spend one week in the field gathering the data, it will require about one week of the geologist's time to make the computations, interpretations and prepare the report.

TECHNICAL RELEASE

NUMBER 44

SEISMIC AND RESISTIVITY METHODS OF GEOPHYSICAL EXPLORATION

CHAPTER 3. ELECTRICAL RESISTIVITY METHODS

Contents

Figures

Tables

CHAPTER 3. ELECTRICAL RESISTIVITY METHODS

Electrical resistivity investigations are based on the principle of applying electric current to the earth through two electrodes and measuring the potential difference between two or more other electrodes. The distance between the electrodes and the measured potential difference are the data used to make interpretations of subsurface conditions.

The theory of electrical resistivity surveying is more complicated than refraction seismology. The discussion on theory presented below is simplified but provides a basic understanding. If a more rigorous discussion is desired, the reader is directed to the references at the end of this guide, especially Van Nostrand and Cook (1966).

Theory

Various materials differ in their ability to conduct electricity. In some materials at least one of the electrons in each atom is loosely held and it requires only slight external influence to move or conduct some of the electrons from atom to atom through the material. In other materials there are very few free electrons and they conduct electricity poorly. This type of electrical conduction is called electronic conduction. Metals are excellent electronic conductors while rocks are poor to very poor electronic conductors. Another form of electrical conduction is electrolytic conduction, where the current is carried by ions, such as in mineralized ground water, resulting in actual movement of matter.

In electrical resistivity investigations both types of electric conductivity are involved; electronic conductivity through the soil particles and rock and electrolytic conducting in the ground water. The more mineralized (higher ion concentration) the ground water is, the higher its conductivity is.

Ohm's Law

In a given metallic circuit at a constant temperature a definite ratio exists between the current and the potential difference. This ratio is the resistance of the circuit. The equations for Ohm's Law are:

$$V = IR$$
$$I = V/R$$
$$R = V/I$$

where V is voltage or potential in volts, I is current in amperes, and R is resistance in ohms.

In electrical resistivity investigations, it is assumed that the earth acts as a linear conductor and Ohm's Law applies.

Whenever an electric current flows, an interchange of energy takes place. If the moving particles which constitute the current have work done on them by an external force, they gain energy; if they do work on something else, they lose energy. The gain or loss in energy when one coulomb of electricity (one coulomb per second equals one ampere) is moved from one point to another in an electric circuit is called the difference in potential and is measured in volts.

As can be seen from Ohm's Law, a ratio exists between the potential difference (V) and the current (I) which is equal to the resistance (R). Resistance is measured in ohms.

Another convenient electrical unit is conductance (G). Conductance is the reciprocal of resistance and is measured in mhos. The equation is:

$$G = \frac{1}{R} = I/V$$

The flow of electricity can be considered as analogous to the flow of water in an aquifer and Ohm's Law and Darcy's Law as similar.

It will be recalled that Darcy's Law states the volume of flow through a porous media is directly proportional to the hydraulic gradient and a constant depending on the character of the material. The equation is:

$$V = kI$$

Ohm's Law is:

$$I = V/R$$

and since

$$R = 1/G$$

restated, it is

$$I = GV$$

Darcy's V is volume of water and Ohm's I is amount of current. Darcy's k is coefficient of permeability which indicates the ease with which water flows through the media and Ohm's G is conductivity which indicates the ease with which electricity flows through a conductor. Darcy's I is hydraulic gradient of difference in head and Ohm's V is potential drop or difference in potential.

Resistivity

The resistivity of a material is a fundamental property of that material in the same sense that bulk density is a fundamental property.

The resistance of a conductor is proportional to its length and inversely proportional to its cross-sectional area. (See Figure 3-1) Expressed as an equation, this is:

$$R \propto \frac{\ell}{A}$$

where R = the resistance in ohms
ℓ = length
A = cross-sectional area

If a current I is applied to a block of material as indicated in Figure 3-1 and the potential drop of V volts is measured between the ends of the block, the resistance (R) of the block is:

$$R = V/I$$

If the block is ℓ centimeters long and the cross-sectional area is A square centimeters, the resistivity of the material in the block is:

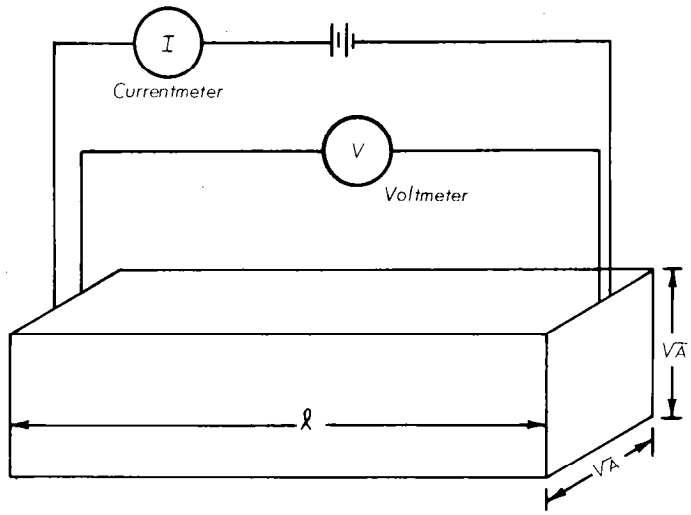

Figure 3-1. – Resistivity

$$R = \rho\frac{\ell}{A} \qquad \text{or}$$

$$\rho = R\frac{A}{\ell} \quad \text{ohm centimeters}$$

where ρ is a constant termed resistivity.

Resistivity is measured in various units depending on the units used for length and area. If length is measured in centimeters and area in square centimeters resistivity is in Ohm-centimeters. Likewise, it can be measured in Ohm-meters, Ohm-feet, etc.

In resistivity prospecting there must always be at least two current electrodes in contact with the earth--one as a source and the other as a sink. The total potential at any point can be computed by algebraic addition of the separate potentials due to each of the sources considered as though each were acting alone. Since a sink is no more than a negative source, the potential at a point may be computed for any combination of sinks and sources.

If current is applied to the earth through two current electrodes C_1 and C_2 (see Figure 3-2) spherical equipotential surfaces develop. Since the air is considered to have infinite resistivity the figure only shows the lower half of the sphere of equipotential surfaces that are developed in the earth. Perpendicular to these equipotential surfaces are current flow lines generated between the two electrodes.

This figure is similar to a ground-water flow net. The equipotential lines represent contours of equal head in ground water and equal potential (volts) in electricity. The flow lines represent amount of water flow in ground water and amount of current flow (amperes) in electricity.

A plan view of the same electrode arrangement and the equipotential and current flow lines is shown in Figure 3-3.

These figures are idealized and assume the earth has uniform resistivity. Any deviation from this uniform condition will cause displacement of the equipotential and current flow lines. As can be seen from the figure the volume of material through which the current passes is proportional to the distance between the current electrodes.

The potential at electrodes P_1 and P_2 (Figure 3-2) and the potential difference between these electrodes can be calculated using the equation of Ohm's Law ($V = IR$) and resistivity ($\rho = RA/\ell$) discussed above. This is done in the following manner:

The potential at point P_1 is the algebraic sum of the potential between points C_1 P_1 and P_1 C_2. Therefore:

$$V_{P1} = V_{C_1P_1} - V_{P_1C_2}$$

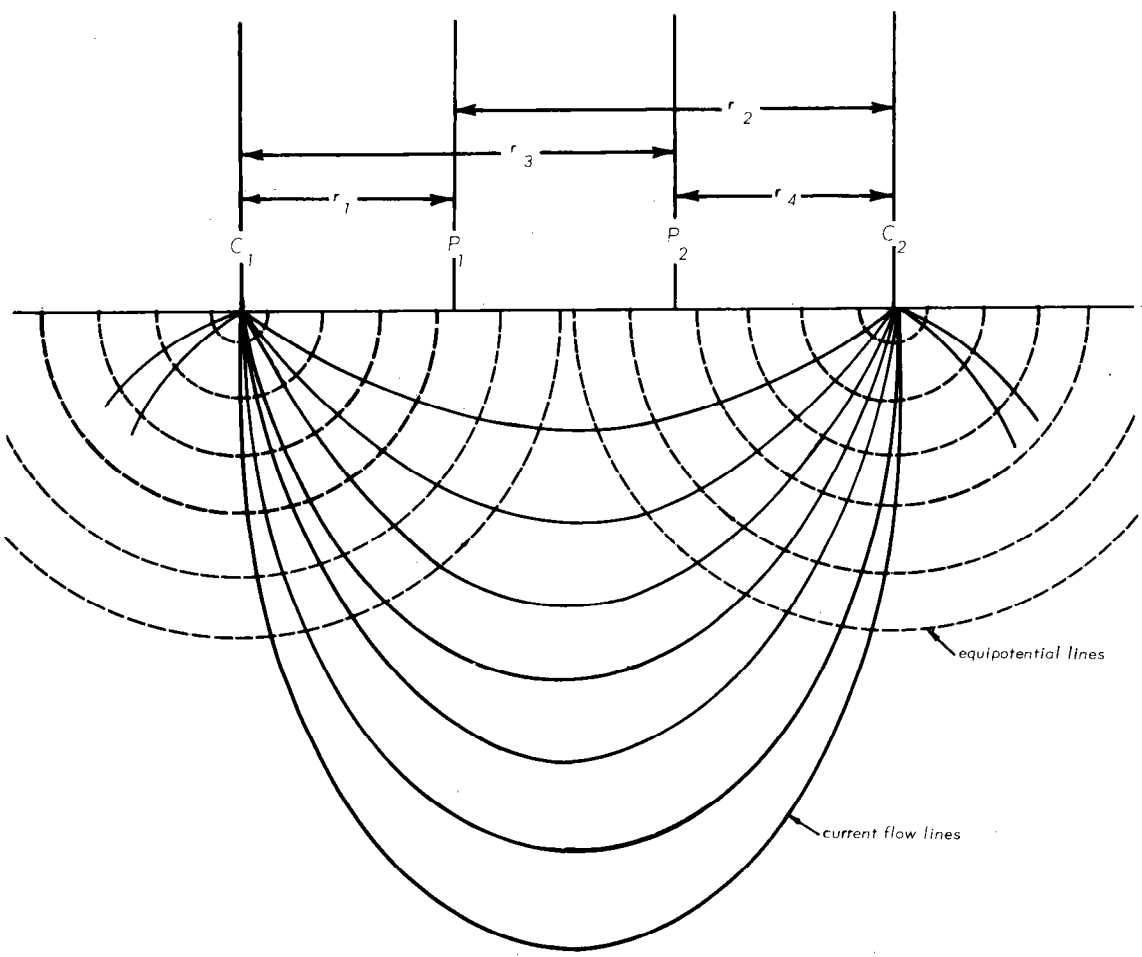

Figure 3-2. — Current flow lines and equipotential lines

The equation for resistivity is:

$$\rho = \frac{RA}{\ell}$$

from Ohm's Law:

$$R = V/I \quad \text{therefore:}$$

$$\rho = \frac{VA}{I\ell}$$

The area (A) of the conductor between P_1 and C_1 is that of a sphere of radius r_1. Since the air has infinite (theoretically) resistance, only one-half the sphere is the conductor and $A = 4\Pi r_1^2/2$.

Rearranging the resistivity equation to solve for V it becomes:

$$V_{C_1P_1} = \frac{\rho I \ell}{A}$$

Substituting $4\pi r_1^2/2$ for A and r_1 for ℓ it becomes:

$$V_{C_1P_1} = \frac{\rho I r_1}{\frac{4\pi r_1^2}{2}} = \frac{\rho I}{2\pi r_1}$$

In the same manner the potential at P_1 due to C_2 is:

$$V_{P_1C_2} = \frac{\rho I}{2\pi r_2} \quad \text{therefore:}$$

$$V_{P_1} = V_{C_1P_1} - V_{P_1C_2} = \frac{\rho I}{2\pi r_1} - \frac{\rho I}{2\pi r_2}$$

$$V_{P_1} = \frac{\rho I}{2\pi}\left(\frac{1}{r_1} - \frac{1}{r_2}\right)$$

The potential at P_2 is solved in the same way.

$$V_{P_2} = V_{C_1P_2} - V_{P_2C_2}$$

$$V_{C_1P_2} = \frac{\rho I}{2\pi r_3}$$

$$V_{P_2C_2} = \frac{\rho I}{2\pi r_4}$$

$$V_{P_2} = \frac{\rho I}{2\pi r_3} - \frac{\rho I}{2\pi r_4} = \frac{\rho I}{2\pi}\left(\frac{1}{r_3} - \frac{1}{r_4}\right)$$

The potential difference between P_1 and P_2 is:

$$V_{P_1P_2} = V_{P_1} - V_{P_2} = \frac{\rho I}{2\pi}\left(\frac{1}{r_1} - \frac{\rho 1}{r_2}\right) - \frac{1}{2\pi}\left(\frac{1}{r_3} - \frac{1}{r_4}\right)$$

$$V_{P_1P_2} = \frac{\rho I}{2\pi}\left(\frac{1}{r_1} - \frac{1}{r_2} - \frac{1}{r_3} - \frac{1}{r_4}\right)$$

Solving this equation for resistivity, it becomes:

$$\rho = \frac{V_{P_1P_2}\, 2\pi}{I} \cdot \frac{1}{\frac{1}{r_1} - \frac{1}{r_2} - \frac{1}{r_3} - \frac{1}{r_4}}$$

This is the basic equation for determining resistivity. However, since the earth is not homogeneous and of constant resistivity the term ρ is called apparent resistivity.

The method of resistivity investigation most commonly used and appropriate for SCS work is the Wenner electrode configuration used with the Barnes layer method of interpretation. This method will be explained more fully below under Operation Techniques. In the Wenner configuration the four electrodes are spaced equidistant. That is, the distance between each electrode is equal. If in Figure 3-2 above the distance between electrodes is "A", then:

$$r_1 = A$$

$$r_4 = A$$

$$r_2 = 2A$$

$$r_3 = 2A$$

Substituting these values in the equation for apparent resistivity, it becomes:

$$\rho = \frac{V}{I}\, 2\pi \cdot \frac{1}{(1/A - 1/2A) - (1/2A - 1/A)}$$

$$\rho = 2\pi\, A \frac{V}{I} = 2\pi\, A\, R$$

In a homogeneous material the apparent resistivity is equal to the true resistivity and, as long as the electrode spacing is constant, the location of the electrodes is not important. Even in heterogeneous earth material the apparent resistivity will be the same when the current and potential electrodes are interchanged.

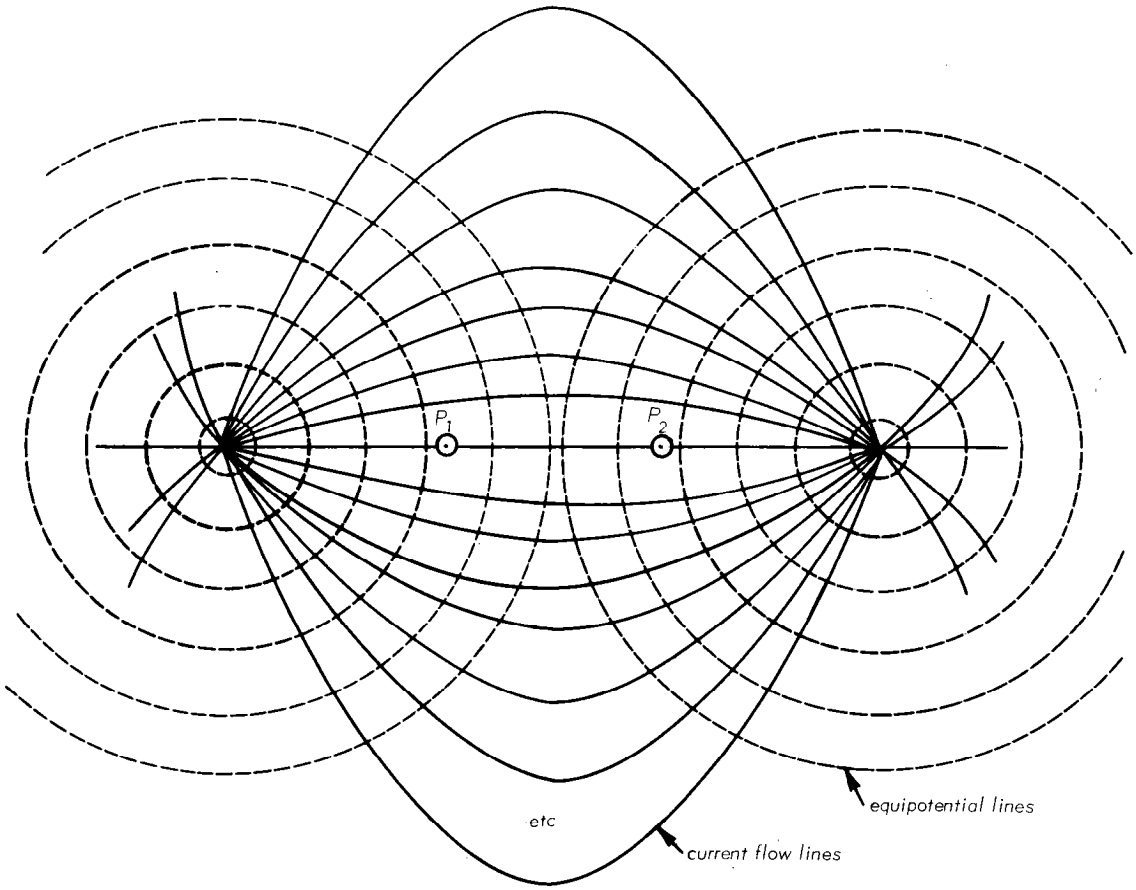

Figure 3-3. – Plan view

Current Density

The general theory as developed above has considered the earth homogeneous and of the same resistivity. The actual condition encountered in the field is a hetergeneous material vertically and often laterally as well. The actual measurements as made in the field only involve a small element of material between the potential electrodes (see Figure 3-4).

Resistivity theory states that the lines of current flow will be deflected toward a good conductor, that is, one with a lower resistance or higher conductance. This is similar to ground-water flow where the flow lines are more dense in the aquifer of higher permeability (equivalent to G here). The potential difference (V) between the potential electrodes is proportional to the current density and the true resistivity of the small near surface element of material between the potential electrode. Stated mathematically:

$$V \propto \rho_0 \, i$$

where V is voltage drop

ρ_0 is true resistivity

i is current density--the current passing through a unit cross-sectional area.

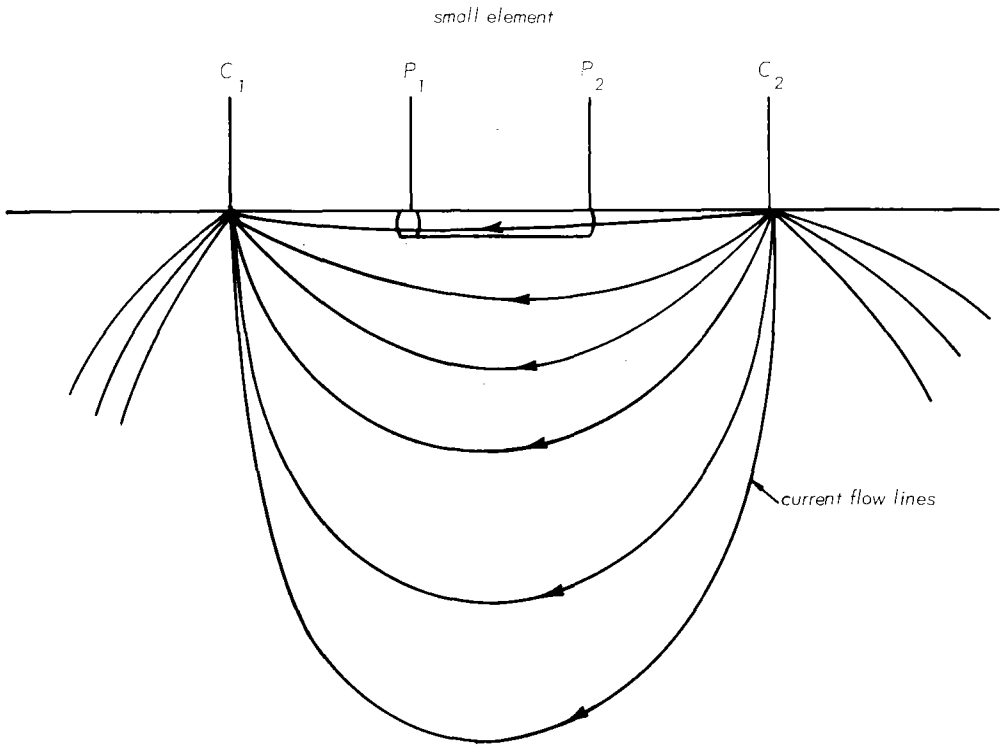

Figure 3-4. – Small element of material

If this equation is substituted into the equation:

$$\rho = 2\Pi A R$$

since $R = \frac{V}{I}$, then

$$\rho = 2\Pi \frac{V}{I} A$$

and since $2\Pi A$ is a constant.

$$\rho \propto (i/I)\, \rho_0$$

which states, the apparent resistivity, ρ, is proportional to the true resistivity multiplied by the ratio of the current density to the current.

The current density is directly proportional to the total current, therefore, the measured apparent resistivity is independent of the total current applied.

According to Soiltest (1968, p. 14) the equation:

$$\rho \propto (i/I)\ \rho_0$$

"Contains the key to the qualitative interpretation of resistivity effects. This key may also be stated in these words: Different subsurface conditions will produce different apparent resistivity readings. If a small volume element is imagined as extending along the earth surface between the two potential electrodes shown in Figure 3-4, then it will have a certain current density i, and a certain true resistivity, ρ_0. The measured apparent resistivity will be directly proportional to these two quantities."

Depth of Penetration

As stated before, the basic procedure in resistivity surveying is to measure the potential drop on the ground surface associated with a known current flow into the earth and then calculate the apparent resistivity from the equation. The resistivity determined by the equation applies to a volume of material that depends on the electrode spacing, and as the spacing is increased, the current penetrates deeper into the earth.

For a homogeneous material, consider a vertical plane at the midpoint between electrodes. One half the current flows through this plane at a depth equal to one half the electrode spacing and one half flows at a greater depth.

When the material is not homogeneous the resistivity calculated is apparent resistivity which depends on the resistivity of the various materials through which the current passes. As the electrode spacing is increased, the current flows through a greater volume of material both horizontally and vertically and the deeper materials will have an effect on the apparent resistivity. Thus, if the the deeper material is of higher resistance (lower conductance) the current flow lines will be deflected upward and the current density in the near surface volume element is increased. If the deeper material is of lower resistivity (higher conductance) the current flow lines will be deflected downward and the current density will be decreased. The increase or decrease in current density is measured by the resistivity apparatus. Interpretation of the apparent resistivity changes with change in electrode spacing will indicate changes in and types of material at certain depths.

Empirical observations have shown that for the Wenner electrode configuration changes in apparent resistivity are considered to occur at the depth equal to the spacing between adjacent electrodes.

Capabilities and Limitations

The resistivity technique if properly applied can furnish much useful information. Its capabilities and limitations will be discussed in this section.

Good conductors (low resistivity) are wet clay and silt soils, mineralized (especially saline) water, and metalliferous ores. On the other hand highly resistant materials are dry sands and gravels and dense massive bedrock free of metal ores.

Table 3-1 shows a range of resistivity values for several types of soils and rocks in ohms per cubic centimeter:

Table 3-1. Resistivity Values of Typical Materials.

Resistivity (ohms/cc)	Materials
Less than 1,500	- Brine
1,000 to 10,000	- Moist clay and saturated silts
10,000 to 20,000	- Dry silts; clayey, sandy, or gravelly till
15,000 to 50,000	- Sandy clays, saturated sands; well-fractured rocks filled with moist soils
30,000 to 100,000	- Moist sands, moist sand-silt-gravel mixtures; slightly-fractured bedrock (moist)
100,000 to 300,000	- Moist to saturated gravels; sandy gravel with some silt; slightly fractured bedrock with dry soil filling
300,000 plus	- Dry gravels and coarse sands; massive hard bedrock.

There is considerable overlap in the resistivity of various materials due to moisture content and expecially to the dissolved solids content of the water. The dissolved solids content of ground water can change due to drouth, excessive rainfall, etc. The possibility of this changed ground-water condition should be appraised if an interruption occurs during the resistivity investigation.

In New York, West Texas, and on Long Island, recent investigations have been made using resistivity equipment to investigate ground water pollution from septic tanks and oil field brine disposal pits (Warner, 1969). The contaminated water had higher concentration of dissolved solids than non-contaminated ground water. In some cases low apparent resistivity readings were interpreted as contaminated ground water.

In other cases the conditions of resistivity of unsaturated material overlying the aquifer, thickness and depth to the saturated aquifer, and resistivity of the material underlying the aquifer prevented identification of contaminated ground water.

The electrical resistivity method has an advantage over the seismic method in that there are no masked layers because of any density or resistivity changes. The layers near the surface have proportionally greater effect on the apparent resistivity than deeper layers. However, a thin layer of high (or low) resistance at depth may be indicated by a minor and unnoticed resistivity change at the critical electrode spacing. The apparent resistivity measured at the surface is a weighted average of all the resistivities within the zone of influence; therefore, deep, thin zones have proportionally less influence on the apparent resistivity than shallow or surface thin zones.

The resistivity method is unaffected by frozen ground but the electrodes should always be seated in moist ground. In dry conditions the area around each electrode should be moistened.

Extraneous electrical currents, either natural or artificial, may cause errors in apparent resistivity readings. Natural earth currents are such things as telluric currents, currents caused by oxidation of ore bodies or corrosion of buried pipelines. Artificial extraneous currents can be caused by the ground returns of electrical installations such as electric railroads. The commutated direct current used in modern instruments effectively eliminates this problem except in those cases where the extraneous earth currents have essentially the same frequency as the commutating rate used or if the capacity of the rocks is sufficiently

large so that the current transients do not cease before the potential electrodes are connected.

As with the seismic refraction method it is always desirable and in many instances essential that good geologic control be established for correlation--either drill holes or outcrops. The location of the point of depth determination for electrical resistivity is considered to be the center of the spread (much easier to determine than in refraction seismic). The depth determinations are generally not as accurate as in the seismic method but with good geologic control they can be quite good.

A quite serious limitation of electrical resistivity investigations is the requirement that the interfaces and the ground surface be parallel or very nearly so.

There are numerous configurations for the current and potential electrode for use in engineering investigation and prospecting. Three configurations are appropriate for SCS geologic investigations. They are the Wenner configuration, the Lee configuration, and the Schlumberger configuration. The Wenner configuration used with the Barnes layer method of interpretation is the technique that is probably most appropriate for SCS use but the other methods will also be discussed. A detailed discussion is given later under Electrode Configurations.

These electrode configurations are used in surveying techniques termed horizontal profiling and vertical profiling.

In horizontal profiling (also called traversing) the electrode spacing is maintained at a constant value and the whole configuration moved along a traverse with readings taken at regular intervals (stations). This technique has the advantage of covering a large area in a short period of time. However, since the effective depth of penetration is related to the electrode spacing, the depth of investigation is constant for all stations. This survey detects changes in apparent

resistivity (and thus changes in material) laterally above a specified depth.

In vertical profiling the center of the electrode configuration is fixed and the electrode spacing is increased (or decreased). Since the electrode spacing is increased, the depth of penetration is increased and indicates the vertical sequence of different resistivity zones (and materials).

Portable Resistivity Equipment

The portable resistivity instrument is composed basically of two components:-a current source and either a bridge type circuit for measuring the resistance or conductance, or separate circuits to measure the current and potential individually.

The following descriptions are taken mostly from the specifications and capabilities described by the manufacturers. Not all known models are listed--only those owned by the SCS and some which have been demonstrated as suitable for SCS needs. The prices listed are approximate 1968 retail prices.

R-50 *Stratameter*- manufactured by Soiltest, Inc. For deep electrical resistivity surveys. Electrode spacing to 500 feet or more, using either the Wenner or the Schlumberger electrode arrangements. The separate transmitter supplies up to 750 volts D. C. at a current capacity up to 150 milliamperes. Power receiver has a range of .002 to 10 volts on 3 scales. Weight of complete unit including probes, cables and reel is about 150 pounds. A generator is available for recharging the battery in the field.

Earth Resistivity Meter, Model ER-2- manufactured by Geophysical Specialties Division, Soiltest, Inc., 2205 Lee Street, Evanston, Illinois 60202. List price - $960. Uses 4 or 5 electrodes which measure electrical resistivity of soils, rocks, minerals, etc. A standard

resistivity guide is supplied with the instrument. The fifth electrode is used for the Lee configuration.

Michimho R-30 Earth Resistivity Meter - manufactured by Soiltest, Inc. R-30 meter - $575, test kit with electrodes and cables - $155, complete set - $715. Uses four electrodes which measure the conductance (mhos) of soil and rock materials. Mhos are converted to ohms resistance for interpretations. General applications same as listed for the ER-2, except there is no fifth electrode.

R-40 *Strata Scout Resistivity Meter* - manufactured by Soiltest, Inc. Set complete with electrodes and cable kit - $975. Uses four electrodes which measure directly in ohm resistance. Adaptable to a wide variety of resistivity techniques to depths of 100 feet. Current control regulator maintains constant current during readings. Instrument has built-in calibration circuit.

Earth Resistivity Meter Model 2310 - manufactured by Bison Instruments, Inc. 3401 48th Ave. North, Minneapolis, Minn. 55429. Set complete with electrodes and cable kit for electrode spacing to 50 feet - $945. Uses four electrodes. Direct digital readout of resistance with four multiplier scales (0.01-10.0) - value read is $2\pi R$. Has built-in test circuit. Voltage is 180 volts (peak to peak) and current is electronically limited at 25 milliamperes.

Earth Resistivity Meter Model 2350A - manufactured by Bison Instruments, Inc. 3401 48th Ave. North, Minneapolis, Minn. 55429. Set complete with electrodes and cable kit for electrode spacing to 300 feet- $1150. Can be used with four or five electrode arrays. Direct digital readout of resistance with five multiplier scales (0.001-10.0) - value read is $2\pi R$. Has built-in test circuit. Voltage is 540 volts (peak to peak) and current is automatically controlled at 50 milliamperes.

Resistivity Unit, Gish-Rooney Geohmeter "DC - Commutated" type - Model G-2697 . Available from Geophysical Instrument & Supply Co., 900 Broadway, Denver, Colo. 80203. Set complete with measuring instrument and commutator, dry-cell battery power supply unit, 2000 feet of cable, four

reels, five electrodes connecting cables, and instruction manual - $3025. Reads from 0.01 to 1000 ohms. Depth determination to generally 500 feet and under favorable geologic conditions to 1000 feet. Commutator can be rotated either manually by a hand crank or electrically by an electric motor contained in the unit connected to an external, 6 volt, automobile type battery.

Operation Techniques

As with seismic surveying, good operating techniques are essential in electrical resistivity surveying if adequate field data are to be collected for interpretation.

General Rules

Some of the same basic rules described under Operation Techniques in Seismic Surveying apply here also:

1. Before going to the field, check thoroughly to see that batteries are charged and the equipment is complete and in good condition, including electrodes, wire-splicing tools, pliers, screwdriver, water can, hammer, measuring tapes, instructions, and notebooks.

2. Select a location with adequate area to make the survey depending upon whether areal or depth survey is desired and which will give the most useful subsurface information. Run a correlation test near a logged drill hole if available.

3. Avoid interferences such as power lines, fences, buried piplines, or too close to the edge of a bluff, cliff, or quarry, Do not place a metal tape or extra wire near the survey line.

4. Set up and operate the equipment according to the manufacturer's instructions. Be sure that the manual has a chapter on trouble-shooting to aid in field checking any operating troubles.

5. If abnormal readings are found or suspected, run an additional spread perpendicular to the first or change from the Wenner to Lee electrode configuration.

6. Place the electrodes several inches into the ground, be sure the electrode is in contact with moist ground. Add water to area around electrode if necessary. Do not have the electrode in contact with a large rock or boulder.

7. Always run spread on the contour (horizontal) or nearly so.

Electrode Configurations

There are numerous configurations or arrangements for placing the current and potential electrodes for surveying. The three most appropriate for SCS geologic investigations are discussed.

Wenner Configuration

Figure 3-5, page 3-16 illustrates the Wenner Configuration or arrangement. This configuration uses four electrodes equally spaced along a line. The outer electrodes serve as the current electrodes and the inner ones as potential electrodes. Theoretically the current and potential electrodes can be interchanged without affecting the apparent resistivity values. With this configuration lateral resistivity variations can be misinterpreted as resistivity variations with depth. A second resistivity spread crossing at right angles at the midpoint to the first may aid in the proper interpretation of the subsurface condition. The Lee electrode configuration will also aid in proper interpretation of this condition.

A convenient way of determining the location of electrodes from the center of the spread is to remember that the potential electrodes are always at the distance A/2 (A is electrode spacing) on either side of the mid-point and the current electrodes are at the distance 3 A/2. In the Moore Cumulative Resistivity Method, equal increments of electrode spacing are required and they are desirable in the Barnes Layer Method.

A table of distances from the mid-point for various electrode spacing increments is handy. The following table shows 3-foot increments:

A short-cut method for rapid reconnaissance that minimizes the number measurements to be made is as follows. Make the first reading at the maximum electrode spacing (A_{max}). Subsequent readings are taken at $A_{max}/3$, $A_{max}/9$, etc. In this method for the second and subsequent readings the current electrodes will be at the location of the potential

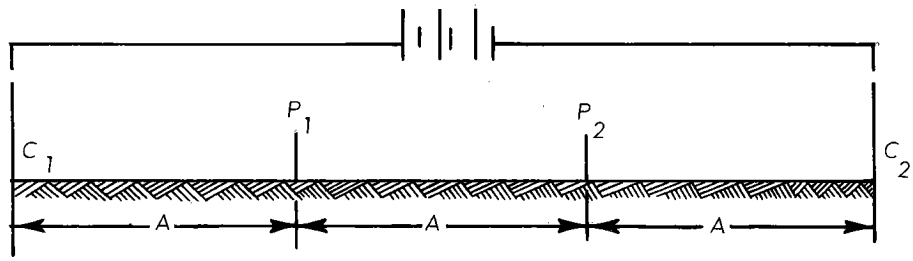

Wenner Configuration

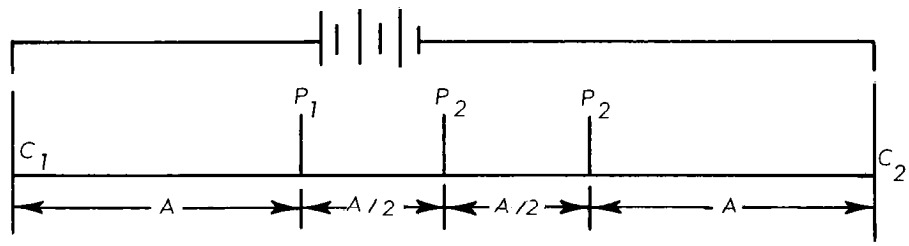

Lee Configuration

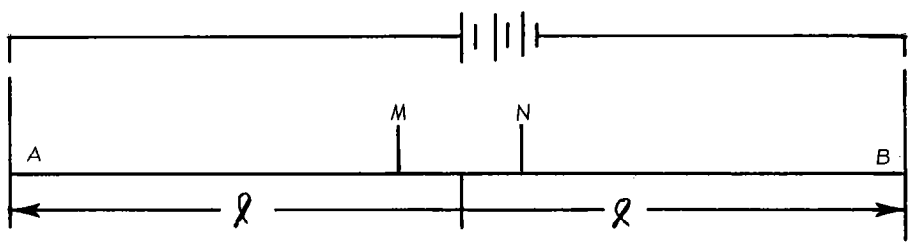

Schlumberger Configuration

Figure 3-5. — Electrode configuration

Table 3-2. Electrode distances from mid-point to the current (C) and potential (P) electrodes for Wenner Configuration at three-foot increments.

Electrode Spacing (A)	Distance to Each Potential Electrode (A/2)	Distance to Each Current Electrode (3 A/2)
3	1 1/2	4 1/2
6	3	9
9	4 1/2	13 1/2
12	6	18
15	7 1/2	22 1/2
18	9	27
21	10 1/2	31 1/2
24	12	36
27	13 1/2	40 1/2
30	15	45

electrodes for the previous reading. The only measurements required are for the location of the potential electrode. For example, if the maximum electrode spacing desired is 90 feet, the location of the electrodes is shown in the following table:

Table 3-3

A_{max} = 90 feet

Steps	Electrode Spacing (A)	Distance to each Potential Electrode (A/2)	Distance to each Current Electrode (3 A/2)
A_{max}	90	45	135
$A_{max}/3$	30	15	45
$A_{max}/9$	10	5	15
$A_{max}/27$	3 1/3	1 2/3	5

This method allows rapid comparison of vertical profiling curves at various locations. The points are widely spaced and additional readings are

usually necessary to provide good curve definitions.

Lee Configuration

Figure 3-5, page 3-16 , illustrates the position of the 5 electrodes in the Lee configuration. This configuration is a partition method where the apparent resistivities from P_1 to P_0 and P_0 to P_2 are measured. If they coincide (rare) or overlap, the resistivity changes are changes with depth. If they diverge, the resistivity changes probably are due to lateral variation in resistivity. The equation for apparent resistivity for P_1 P_0 and P_0 P_2 is $\rho = 4\Pi$ A R and is derived from the equation on page 3-5 in the same manner as for the Wenner configuration.

The field procedures for the Lee configuration are the same as with the Wenner configuration. The Lee can be used for both horizontal and vertical profiling.

Resistivity meters built to be used only for a four electrode array can be converted to the five electrode Lee configuration by using a fifth electrode and a double pole double throw switch plus necessary short lengths of cable. By using two double pole double throw switches, it can be converted to use the Lee and Wenner configuration interchangeable without disconnecting any wires. Figure 3-6 illustrates the conversion to Lee configuration and Figure 3-7 illustrates the Lee-Wenner interchangeable conversions. An alternate method would be to connect a separate wire to the P_0 electrode and then interchange this lead with the P_1 and P_2 terminals on the instrument. Readings are then made as previously described. The user will have to determine which conversion is most convenient to him. When using the Lee configuration for horizontal profiling the plotted locations for the apparent resistivity readings are not plotted at the mid-point of the spread (location of P_0). Due to the partitioning dimension in this method the apparent resistivities are plotted at distances A/4 to the left and right of the mid-point. In vertical profiling, the apparent resistivity is plotted against electrode separation and there are no special difficulties.

Schlumberger Configuration

Figure 3-5, page 3-16 , illustrates the Schlumberger configuration, a four electrode arrangement in which only the two outer (current) electrodes are moved. According to Van Nostrand and Cook (1966, p. 41) "The principle advantage in the Schlumberger technique is that the influence of local inhomogeneities close to the potential electrodes can be clearly located on the apparent-resistivity curves. These effects are shown by the differences between results obtained with the same $\overline{AB}$ and different $\overline{MN}$'s: On the other hand, these local heterogeneities do not appreciably alter the shape of those arcs of the resistivity curves which have been obtained with a given $\overline{MN}$; they only displace the arcs as whole units. This fact often allows one to make a correction and to trace the diagram which would have been obtained in a laterally homogeneous earth. The Schlumberger configuration apparently sacrifices accuracy, which comes from measuring potential differences between closely spaced potential electrodes."

Soiltest (1968) gives the equation for apparent resistivity as:

$$\rho = \Pi \overline{MN} \left[(L/\overline{MN})^2 - 1/4 \right] R$$

Van Nostrand and Cook (1968) simplify this equation to :

$$\rho_a = \Pi \ell^2 \frac{E}{I}$$

and state that provided $\overline{MN}$ does not exceed $2\ell/5$ the discrepancies do not usually exceed 2 or 3 percent.

Horizontal profiling has not been done using the Schlumberger configuration. The vertical profiling technique is an electrode expanding-type technique in which either the distance between current electrodes or potential electrodes is increased but only a single set of electrodes is increased between measurements. Usually $\overline{MN}$ is constant while successive readings are taken for increasing distances of ℓ. When the capability of the meter limits further readings, MN is increased and the distance ℓ is further increased. Two or three overlap readings of ℓ when $\overline{MN}$ is increased must be taken. $\overline{MN}$ must not be less than $2\ell/5$ for any readings.

Types of Surveys

There are basically two types of field procedures for electrical resistivity surveying. The first is horizontal profiling in which the electrode spacing remains constant and the whole array is moved along

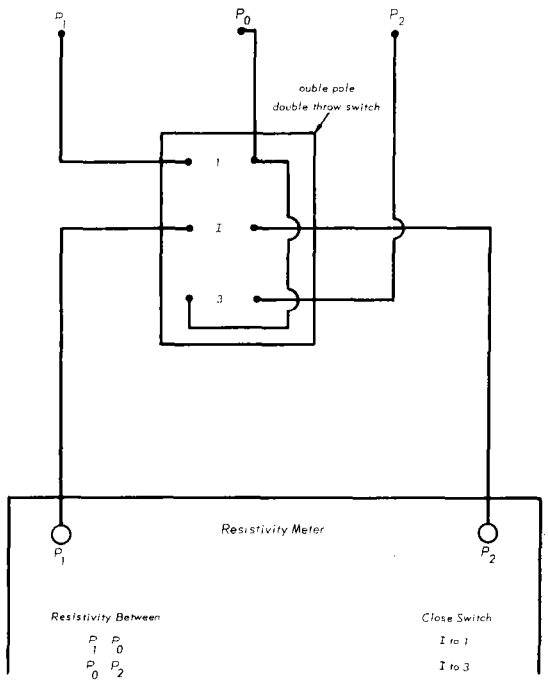

Figure 3-6. – Conversion for Lee Configuration

a traverse. The second is vertical profiling in which the center of the spread remains fixed and the electrode spacing is increased to determine apparent resistivities with increasing depth. A third method is a combination of the first two in which two or three different electrode spacings are used in the horizontal profiling technique.

Horizontal Profiling

This method is normally used for a rapid survey of an area. It usually is advisable to make a vertical profile first to determine the optimum electrode spacing for the horizontal profiling survey. This method is best suited for determining the location of faults or steeply dipping contacts between different types of material (e.g. rock and soil), locating sand and gravel deposits, and prospecting for ore bodies.

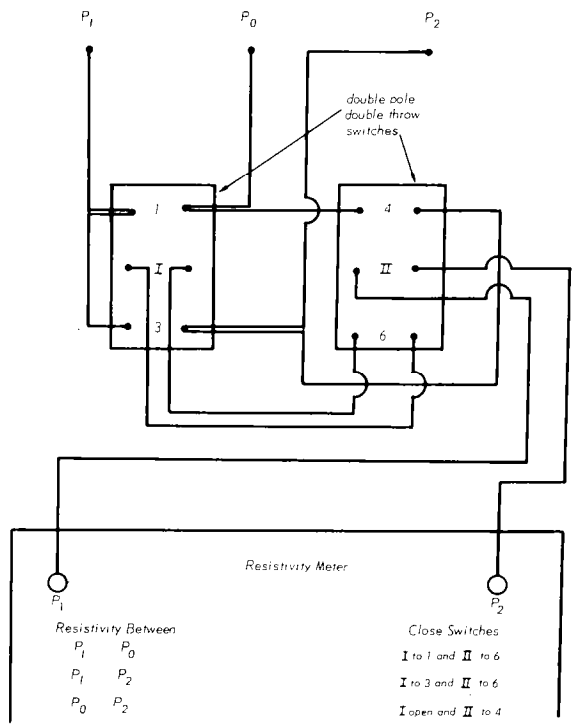

Figure 3-7. – Conversion for Combination Lee-Wenner Configuration

This method is particularly adapted to locating a high resistivity anomaly in low resistivity material or the reverse. An example would be an investigation of the alignment of a proposed channel to determine if the channel bottom would be in rock (high resistivity) underlying alluvial (low resistivity) material.

The apparent resistivities may be presented in two ways. First, for a single line the apparent resistivity versus station of the center of the spread is plotted on rectangular coordinate paper. Plottings of adjacent lines can be compared. Second, the apparent resistivity of the center point of each spread can be plotted on a map and equi-resistivity contours can be drawn. This equi-resistivity map has a failing according to Van Nostrand and Cook (1966, p. 42): "Although this map forms a very effective picture of the progress of the survey if it is kept current, it has one failing of which the inexperienced interpreter must be warned. The apparent resistivity varies according to the orientation of the line of electrode and thus the fact that the data were taken along a

series of parallel traverses tends to flavor the resulting map. Anomalies are abnormally elongated in the direction in which the traverses are run; and multiple anomalies occur even though their cause is one geologic feature only."

See Figure 3-8 for an example of an equi-resistivity map.

Vertical Profiling

Vertical profiling is a technique used to provide information on the variations in the resistivity of subsurface materials with depth. It is used to estimate the variation of resistivity with depth, showing the sequence of zones of different resistivity, and estimate the thickness and depth of various layers.

In this procedure the center of the electrode spread remains fixed while the electrode spacing is increased after each reading.

The effective depth of investigation increases as electrodes increase. Gish and Rooney (1925, p. 162) stated it thus: "The value of the resistivity thus found must, however, in general be considered an average in which the resistivity of the earth near the line of terminals is the more heavily weighted, while the weighting diminishes with distance from this line until at a depth, or lateral distance, equal to the distance between adjacent terminals the weights have become so small that all the earth beyond this range contributes comparatively little to the total result. Thus, the body of earth involved in a single determination has linear dimensions of the same order as the interval between terminals. By increasing this interval, greater depths of earth may be included so that from a series of such measurements a fairly satisfactory knowledge of the variation of resistivity with depth can be obtained provided the series are repeated at positions suitably distributed over the region."

The information from vertical profiling may be presented in graphical form on rectangular coordinate, semi-logrithmic, or log-log paper.

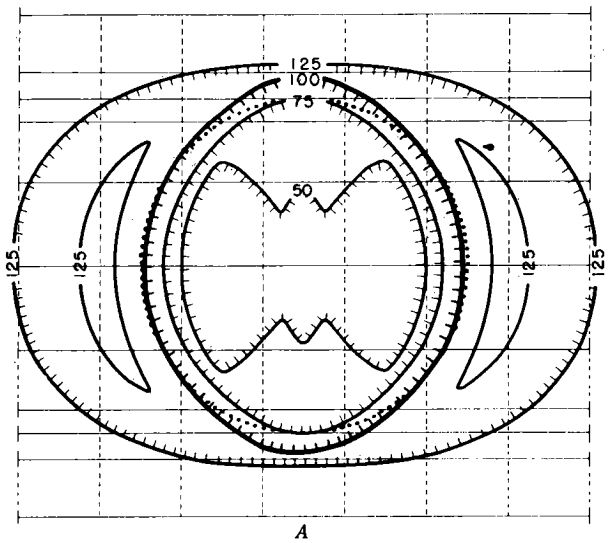

A

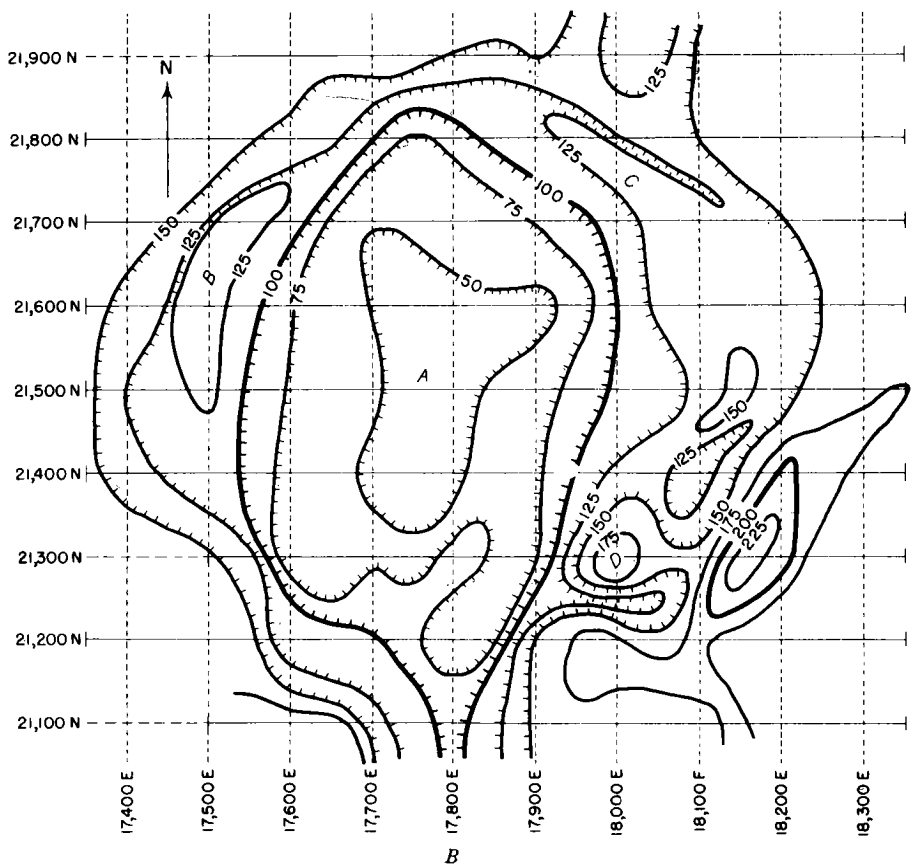

B

50 RESISTIVITY CONTOUR

21,500 N RESISTIVITY TRAVERSE - FIELD

RESISTIVITY TRAVERSE - THEORETICAL

BOUNDARY OF THEORETICAL SINK

0 100 200 300 400 FEET

CONTOUR INTERVAL 25 OHM-METERS

ELECTRODE SEPARATION a = 100 FEET

Comparison of (*A*) theoretical-resistivity map over hemispherical sink (shown in dotted outline) and (*B*) observed field resistivity map over filled sink, Tri-State lead-zinc mining district, Cherokee County, Kans., Wenner configuration. Resistivity field data by K. L. Cook, 1951–54.

Figure 3–8. — Equi–resistivity map

(From Van Nostrand and Cook, 1966)

The plots are apparent resistivity versus electrode spacing at a scale that will show the resistivity breaks. Figure 3-9 is an example of rectangular and log-log plotting of the same data.

The vertical profiling method requires more time for each station but provides more information at a particular point.

Combination Method

The combination method is as the name implies--a combination of horizontal and vertical profiling. It requires more time to run than a simple horizontal profiling but less than detailed vertical profile. The technique is to determine a depth range of particular interest and the two or three electrode spacings that will provide apparent resistivities of this depth range from an initial vertical profile. Then traverse the area of investigation using these two or three selected electrode spacings at each station.

The information can be plotted on rectangular coordinate graph paper or in a table in the Barnes layer method format for the Wenner configuration. Figure 3-10 is an example of the plot where the apparent resistivities are plotted at the location of the midpoint of the electrode spread for two electrode separations. Table 3-4 shows readings at two stations on a traverse. The readings are converted to 1/R (conductance) and the Barnes layer method of interpretation used in the table (Barnes layer method is explained more fully on page 3-31). Note that at station 1 a high conductivity (low resistance) material occurs between 30 and 35 feet. At station 2 this 30 to 35 foot interval contains high resistivity material similar to the 0 to 30 foot interval. The readings for a 30 foot interval at both stations are the same; this illustrates that the near surface materials exert greater influence on apparent resistivities than deeper material and occasionally mask the presence of lower lying material in a profiling survey.

The two or three electrode interval resistivity data may also be interpreted using the ohm-feet method explained on page 3-27.

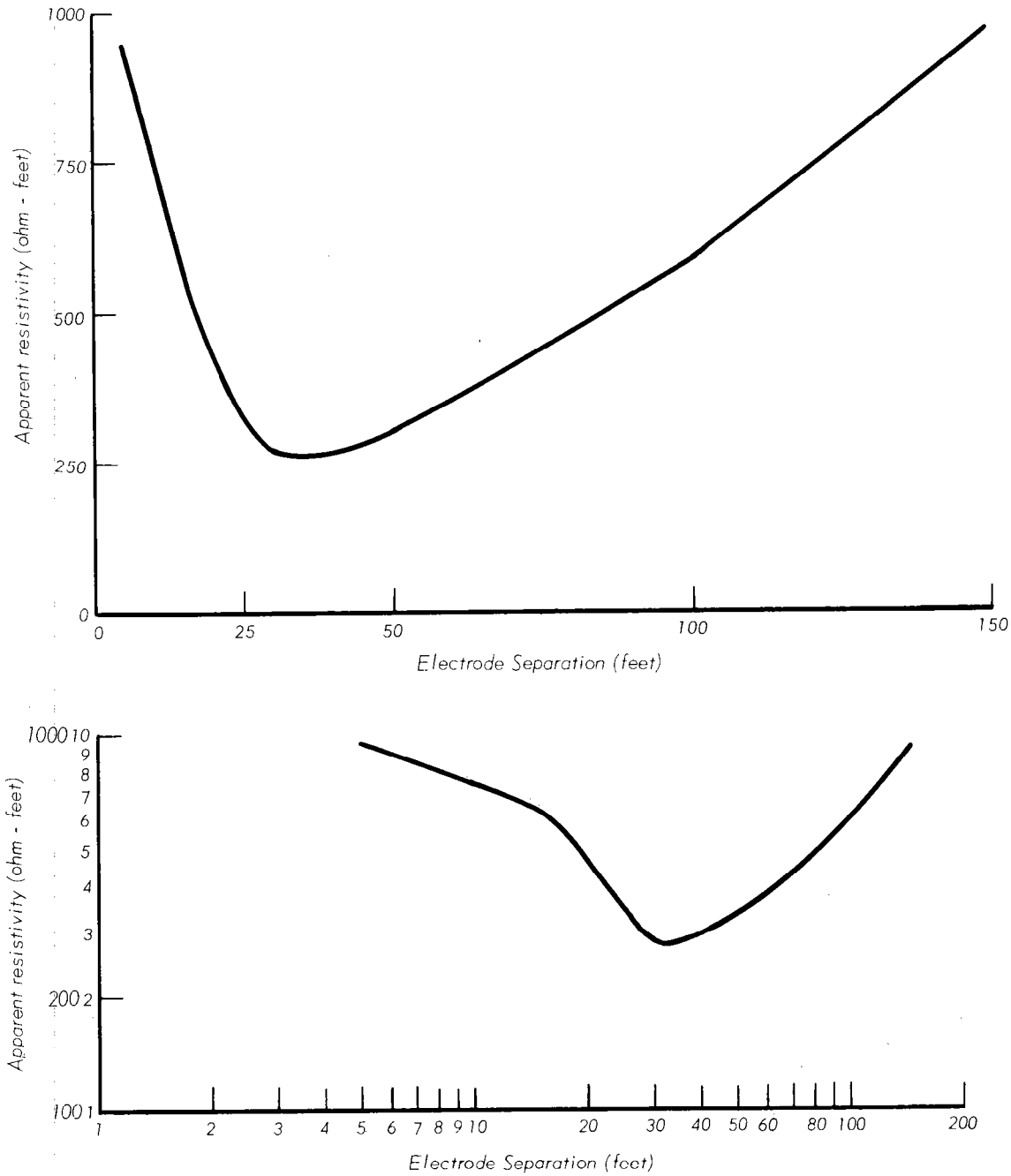

Figure 3-9. – Plots of vertical profiling data

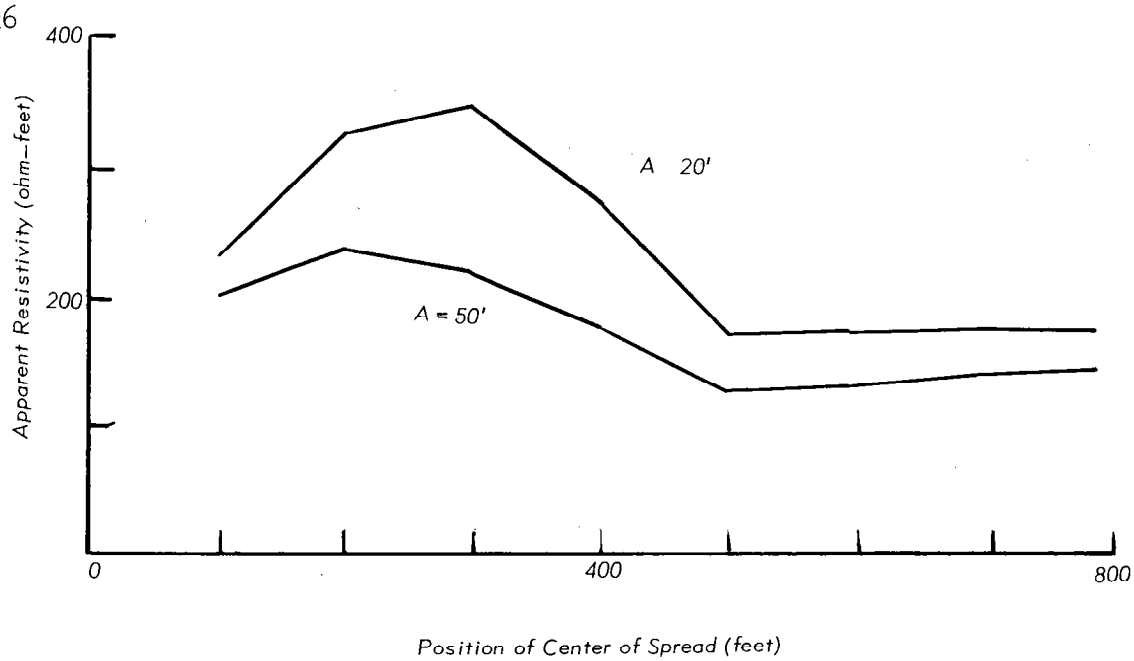

Figure 3-10. – Apparent resistivity versus center of spread (Adapted from Soiltest, 1968.)

Table 3-4. - Resistivity data.

Electrode Interval	2ΠAR	1/R	Layer mhos	ohm-cm (constant=957.5)
Station 1				
30 ft	2619	.072		
35 ft	683	.322	.250	3830
Station 2				
30 ft	2619	.072		
35 ft	2970	.074	.002	478,750

(From Earth Resistivity Manual, Soiltest, Evanston, Ill., 1968. Used by permission of Soiltest.)

Computations

Good geologic control is essential in making proper interpretations from resistivity data. Some techniques of computing depths from vertical profiling will be discussed below. The depths computed from these techniques are approximations and every use of geologic control and known depths for correlation should be made that are possible.

Ohm-Feet Method

The ohm-feet method was the first and simplest method of interpretation of vertical resistivity profiling. Apparent resistivities (in ohm-feet) are computed for each electrode interval (Wenner Configuration). The apparent resistivities are plotted versus depth (electrode separation). A curve is drawn through the plotted points and the interpretation made by noting the depths at which breaks occur in the shape of the curve. Either semi-logarithmic or rectangular coordinate paper can be used to plot the curve. The type and size of paper and scale used should be such that breaks in the curve are well defined. It is often necessary to plot the data on several types of paper and at several scales to determine which size and scale are best.

The curves plotted in Figure 3-11 illustrate the ohm-feet method of interpretation. The plots are on four different types of paper - rectangular-coordinate and single-cycle, two-cycle, and three-cycle semi-logarithmic. They are plotted as apparent resistivity versus depth (electrode spacing). The breaks, indicated by arrows, can be emphasized or subdued by plotting on different types of paper as shown in this figure.

Moore Cumulative Method

Moore (1945) devised an empirical method of interpreting vertical profiling data. His method is not based on theoretical consideration but is a manipulative technique that has had some success.

The Moore Cumulative method requires that resistivity readings be taken at equal increments of electrode separation. The computed apparent resistivity for each electrode spacing is plotted versus depth (electrode spacing) on rectangular coordinate paper (similar to the ohm-foot method). The cumulative resistivity at each electrode separation, obtained by adding successive apparent resistivity values to the previous cumulative value, is then replotted on the same paper but usually at a different scale. Then as many points as possible are connected by straight lines.

Table 3-5. Vertical Profiling Data

Electrode Spacing (feet) (1)	Resistance Readings (Ohms) (2)	Apparent Resistivity (Ohm-ft) (3)	Conductance (Mhos) (4)	Barnes Layer (Mhos) (5)	Layer Method Layer-Resistivity (Ohm-Cm) (6)	Boring Log (7)
A	R	$2\pi AR$	1/R	$1/R_L$	ρ_L	
3	15.1	284	.066	.066	8,700	Silty Sand Soil
6	15.5(13.3)[1]	584(501)	.065(.075)	(.009)	(63,800)	4± feet
9	11.5	650	.087	.012	47,800	Hard
12	9.60	723	.104	.017	33,800	Siliceous
15	7.99	753	.125	.021	27,300	Sandstone
18	6.61	747	.151	.026	22,100	16± feet
21	5.61	740	.178	.027	21,200	Soft
24	4.60	693	.217	.039	14,700	Sandstone
27	4.11	697	.243	.026	22,100	containing
30	3.41	642	.293	.050	11,400	clay and
33	2.90	601	.345	.052	11,000	ash layers

(Adapted from Soiltest, 1968)

[1]Figures in parenthesis are adjusted because of resistivity back-up.

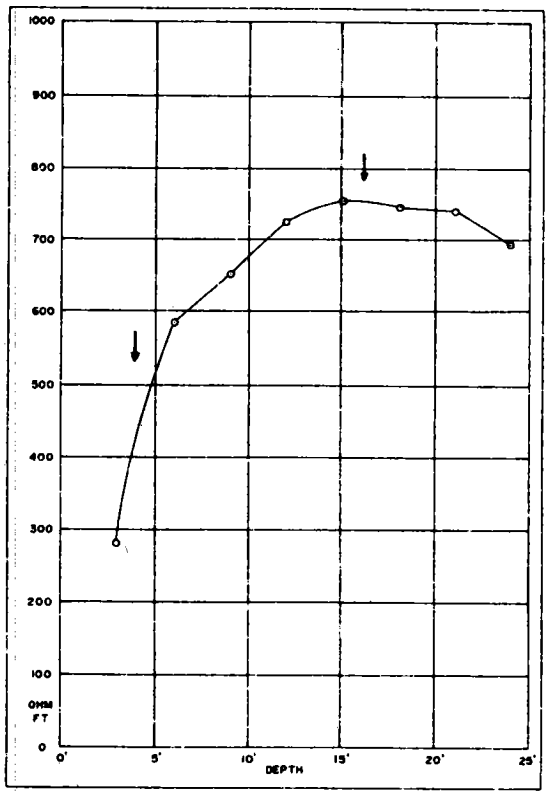

rectangular plot

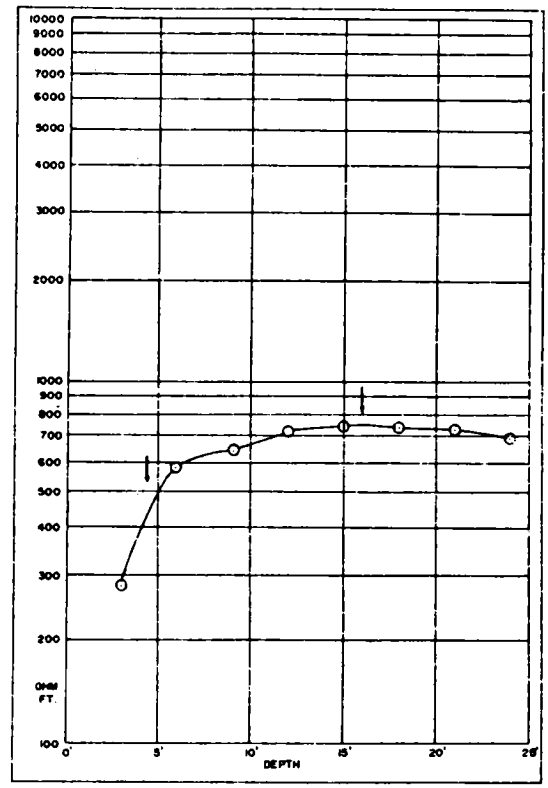

two cycle semi-log plot

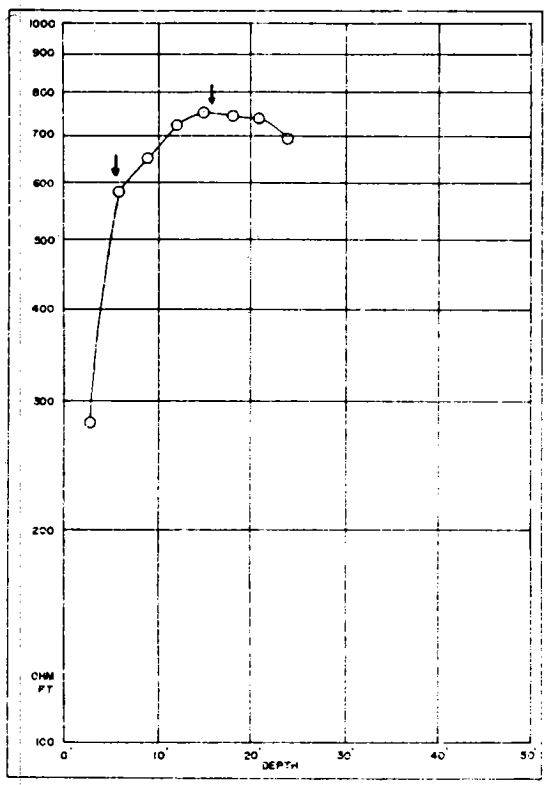

single cycle semi-log plot

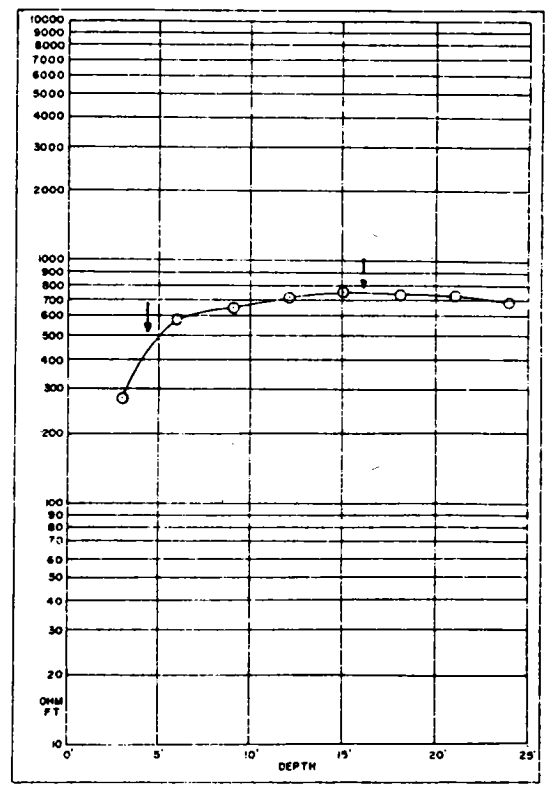

three cycle semi-log plot

Figure 3–11. – Resistivity versus depth

(From Earth Resistivity Manual, Soiltest, Evanston, Ill., 1968. Used by permission of Soiltest)

The electrode separation at which the straight lines intersect is considered to closely approximate the depth to a geologic boundary. A known depth at a control point and a knowledge of the local geology are used for guidance in drawing the straight lines.

The field data and resistivity computations in Table 3-6 are plotted in Figure 3-12 to illustrate this method.

Table 3-6. Vertical Profiling Data

Electrode Separation, A (feet) (1)	Resistance Readings, R (ohms) (2)	Apparent Resistivity (191.5 x AR) (ohm-cm) (3)	Adjusted Apparent Resistivity (ohm-cm) (4)	Cumulative Resistivity (ohm-cm) (5)
3	15.10	8,675	8,700	8,700
6	13.20	15,167	15,200	23,900
9	12.8	22,060	22,100	46,000
12	9.60	22,060	22,100	68,100
15	7.99	22,951	23,000	91,100
18	6.61	22,785	22,800	113,900
21	3.80	15,282	15,300	129,200
24	2.92	13,420	13,400	142,600
27	2.62	13,546	13,600	156,200
30	2.44	14,018	14,000	170,200

If when using the Moore Cumulative method a reading at an electrode interval is missed or a resistivity "back-up" (See page 3-53) occurs at a particular electrode interval, a straight line conecting two "good" readings on either side of the mixed reading will give an approximation of the value to be used in cumulative curve for that particular depth.

Soiltest (1968) states, "The Moore Cumulative Method seems to meet its greatest success in areas containing a sand and gravel deposit overlying clay with a shallow water table containing electrolytes. In general the Cumulative Method is better than other methods at ignoring changes in electrolytic content not caused by changes in texture

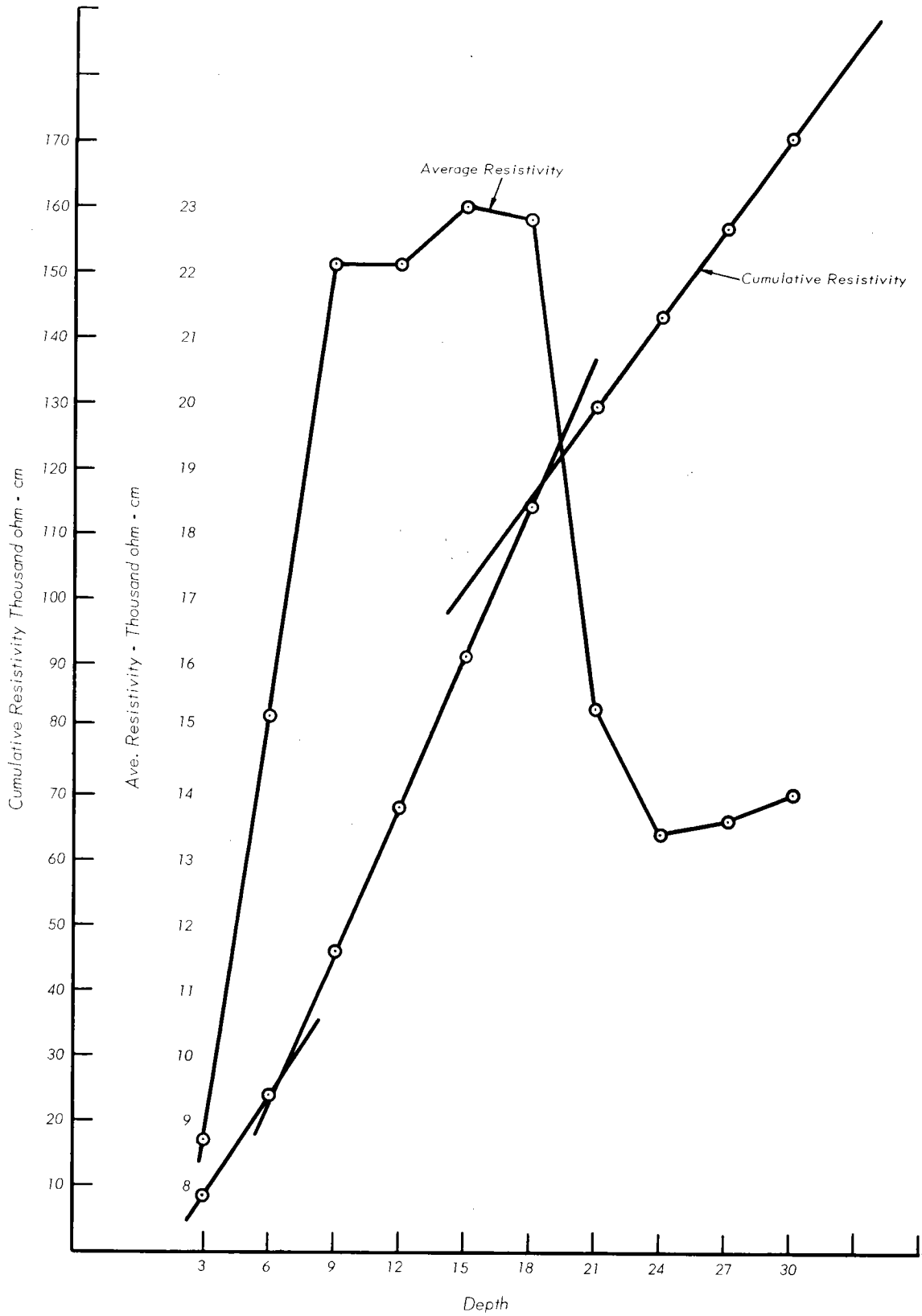

Figure 3-12. — Moore Cumulative Method

of the subsurface material. This is because the Moore Method employs approximations to the rate of change of the resistivity values independent of the actual resistivity value."

Moore (1961) gives several illustrations of his cumulative method successfully predicting depths to sound rock and weathered rock overlain by soil material.

Barnes Layer Method

Barnes (1954) devised a method of interpretation for vertical profiling which considers that each incremental electrode separation involves an additional incremental volume of material. Figure 3-13 is a vertical section through a Wenner electrode array illustrating how the incremental volume of material for each electrode separation increases at a lesser rate than the total volume of material being measured. In Figure 3-13A the resistivity is measured using a three foot electrode spacing, the volume of material being measured is V_1. Figure 3-13B is with an electrode spacing of six feet and the resistivity of volume V_2 being measured and Figure 3-13C with nine foot electrode spacing and volume V_3. The volume V_1 with three foot spacing is about 100 cubic feet and the volume V_3 with nine foot electrode spacing is about 2800 cubic feet. This again points out that a small near surface layer usually has a greater effect on resistivity readings than massive deposits at depths and that resistivity curves (depth versus ρ) are usually smooth, with no abrupt changes. By considering each increment of material (for each electrode spacing) separately the Barnes method attempts to partially overcome this masking effect of near surface layers.

In the Barnes method the thickness of each layer is assumed to equal the incremental electrode spacing. An equal electrode increment is not necessary with this method but it is usually more convenient to use since the field data can then also be used with the Moore Cumulative Method.

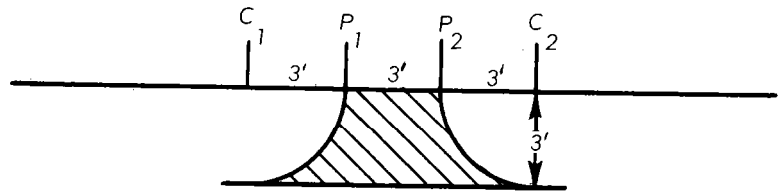

A

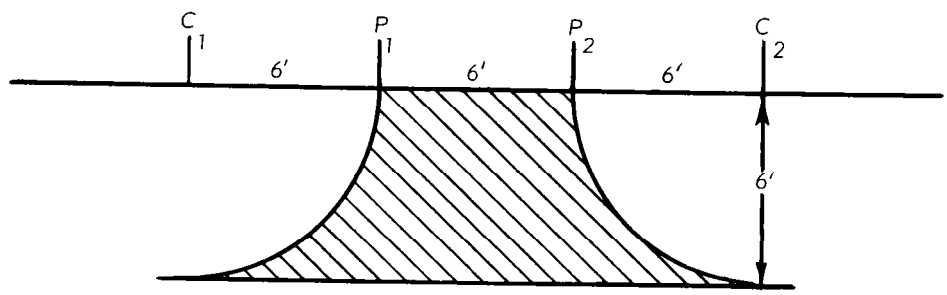

B

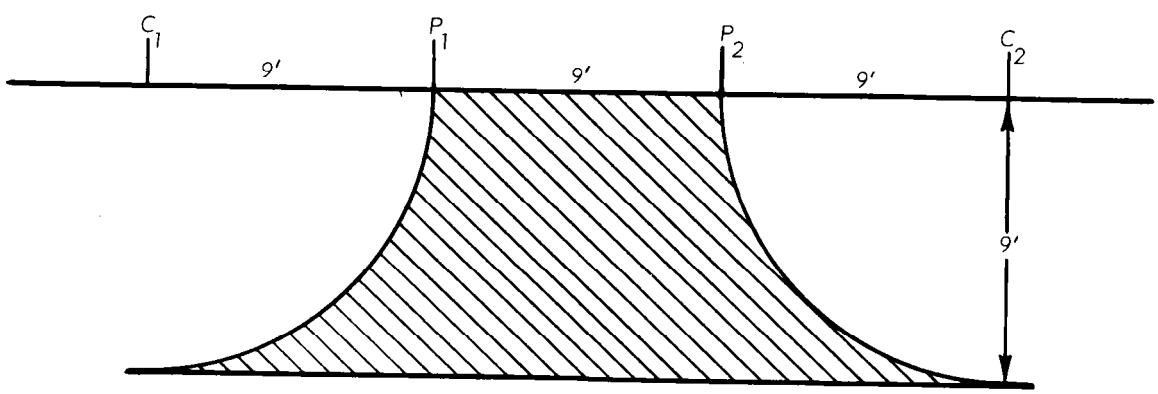

C

Figure 3-13. – Layers for 3 foot electrode increments

The data given in Table 3-5, page 3-28 , is based on a three foot incremental electrode separation. The data in this table is for the Wenner configuration and is developed in the following manner.

The electrode spacing (increment) in column 1 is determined in the field and equal increments (three feet) are used throughout. In column 2, the instrument readings of resistivity are listed for each electrode separation. Some instruments read directly in ohms (as listed in column 2) others read in mhos (column 4). Since the values in column 4 are the reciprocal of those in column 2 instrument read-out can be converted from one to the other.

The values in column 3 are the product of A (column 1) times R (column 2) times 2Π and are in ohm-feet. These values are used in the ohm-feet method of interpretation. The values in column 5 are then assumed to be the conductance of each three foot layer for each three foot electrode increment. For example 0.012 mhos in column 5 at nine foot electrode separation is the reading at nine feet minus the reading at six feet (0.087 - 0.075 = 0.012) and the reading at 12 feet in column 5 is 0.104 - 0.087 = 0.017, etc. Column 6 contains the apparent resistivity values for each layer computed from the conductance values in column 5 from the equation:

$$\rho_L = 191.5\ A\ 1/R$$

where ρ_L = apparent resistivity of layer

191.5 = a constant for 2Π times 30.48 cm/ft to convert ρ_L to ohm-cm when electrode spacing (A) is in feet.

A = electrode separation in feet

1/R = conductance (mhos) of layer.

Figure 3-14 is plotted from the data in column 1 and 6 of the table. The apparent resistivity of each three foot layer is plotted and the bar graph drawn. A resistivity "back-up" has occurred at the 3 to 6 foot interval; on the bar graph an interpreted layer is used but care must be used in the interpretation.

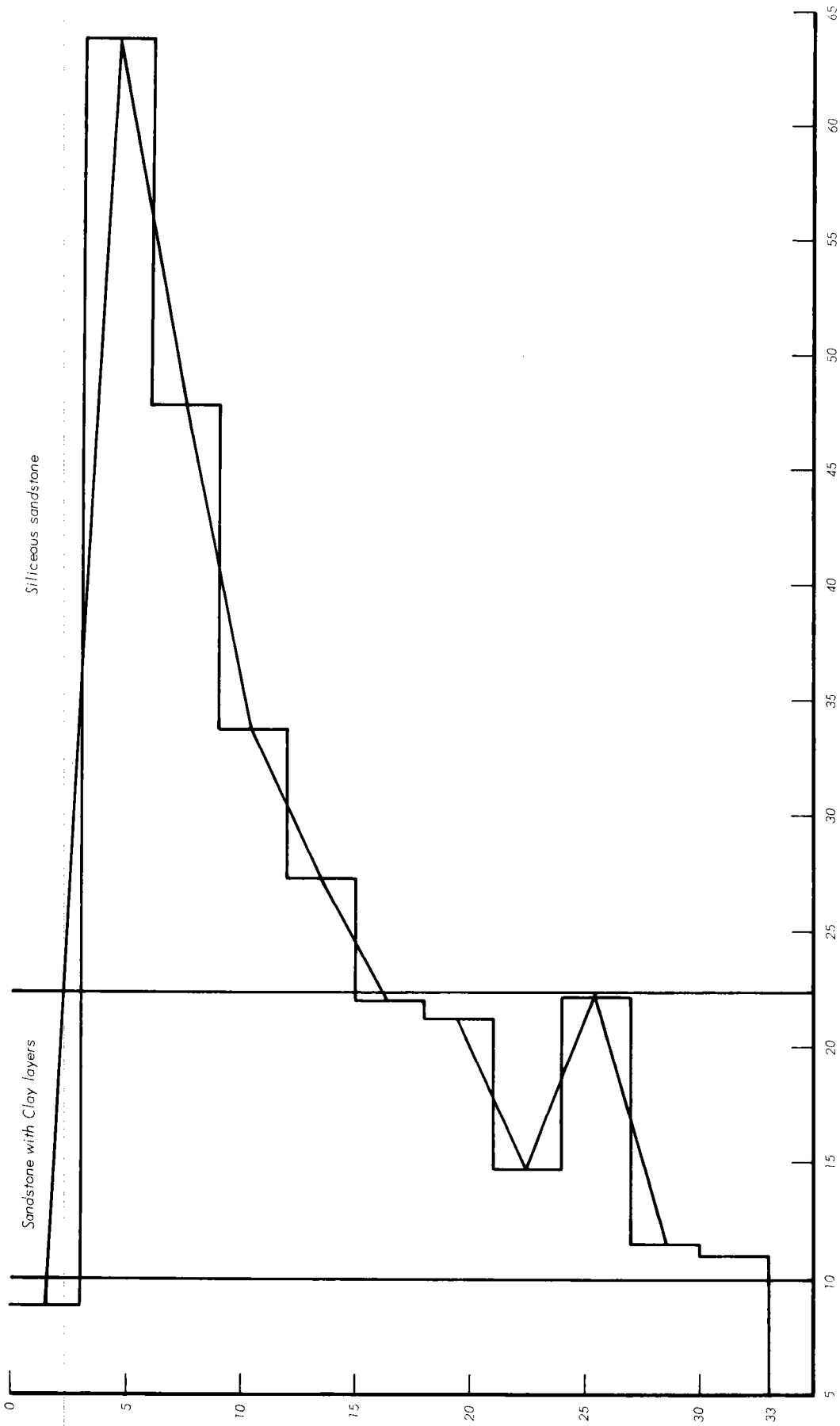

Figure 3-14. — Barnes Layer Method

Each layer value is an average for that layer, the mid-point of the layer may be considered as a representative point for that layer. These mid-points are connected by straight lines, called by Barnes (1954) "transition lines." From a knowledge of the geology of the area and correlation with test holes the range of resistivities of the various materials are known. Vertical lines separating the resistivities into the ranges of the various materials are then drawn. The intersection of the transition lines and the range lines determine the depth of the boundary between the various materials. In this example the top of the siliceous sandstone is at about 2.5 feet and the bottom 16 feet. If the ranges are unknown, group similar values into "layers."

If a resistivity contour cross section is to be drawn the resistivities at any depth can be picked from the "transition lines." The data can also be plotted as shown in Figure 3-15 with the points plotted as the resistivity at the mid-point of each layer and connected by a straight line. It may be more convenient to plot resistivity versus elevation instead of depth.

Table 3-7.is an example of vertical profiling data in a glaciated area.

Table 3-7. Vertical Profiling Data.

Electrode Spacing (A)	Conductance Total (1/R)	Conductance of Layer ($1/R_L$)	Resistivity of Layer (ρ_L)
(feet)	(mhos)	(mhos)	(ohm-cm)
3	0.0073	0.0073	78,800
6	0.0109	0.0036	159,000
9	0.0270	0.0161	35,700
12	0.0695	0.0425	13,500
15	0.120	0.0505	11,400

The bar graph is plotted and the range lines and "transition lines" are drawn in Figure 3-16. By correlation with bore holes, etc., in this area it is known that clay has resistivity range of 0 to 20,000 ohm-cm, moist sandy clay 20,000 to 50,000 ohm-cm, moist sand, silt,

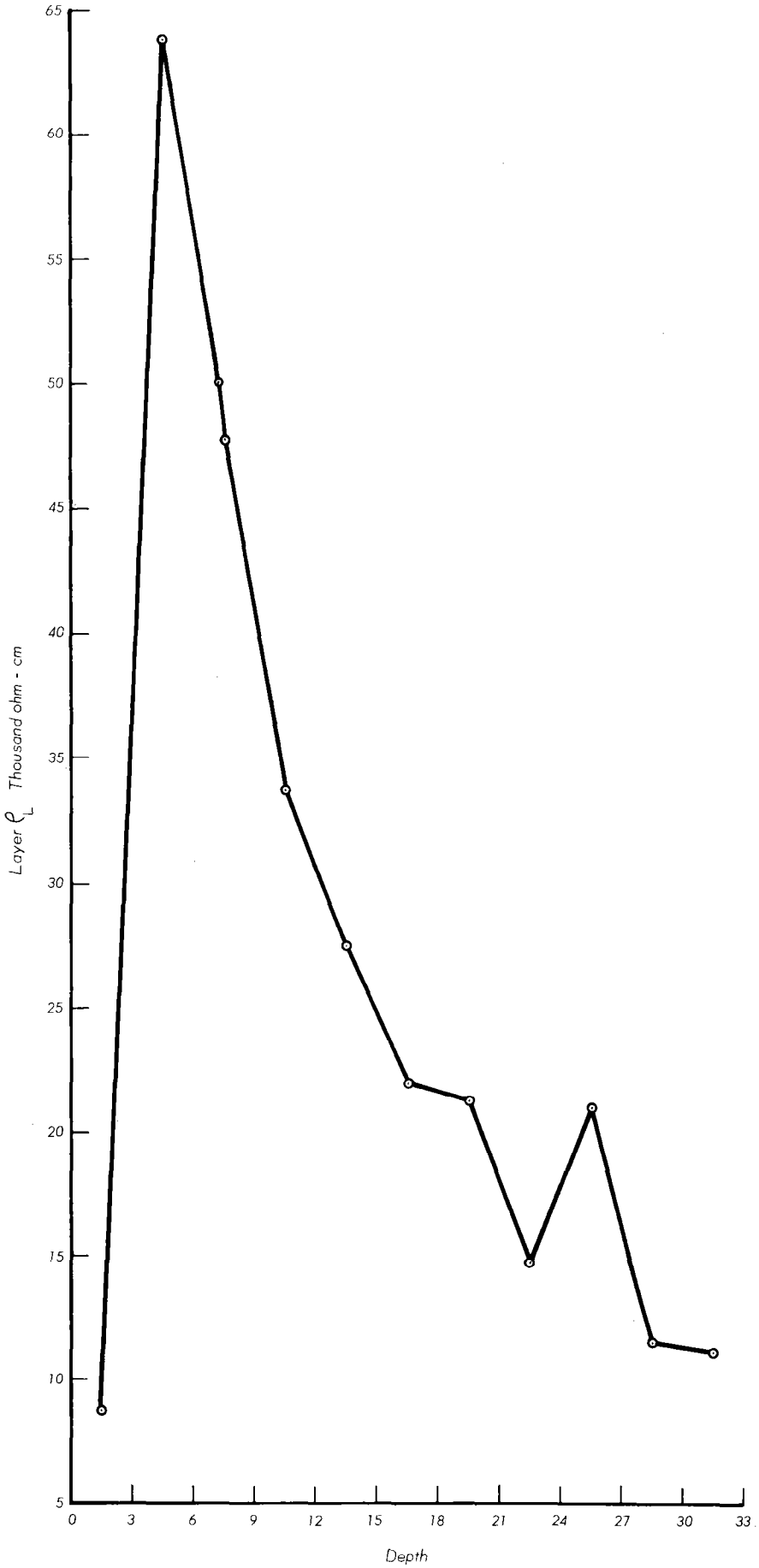

Figure 3-15. — Resistivity versus Depth

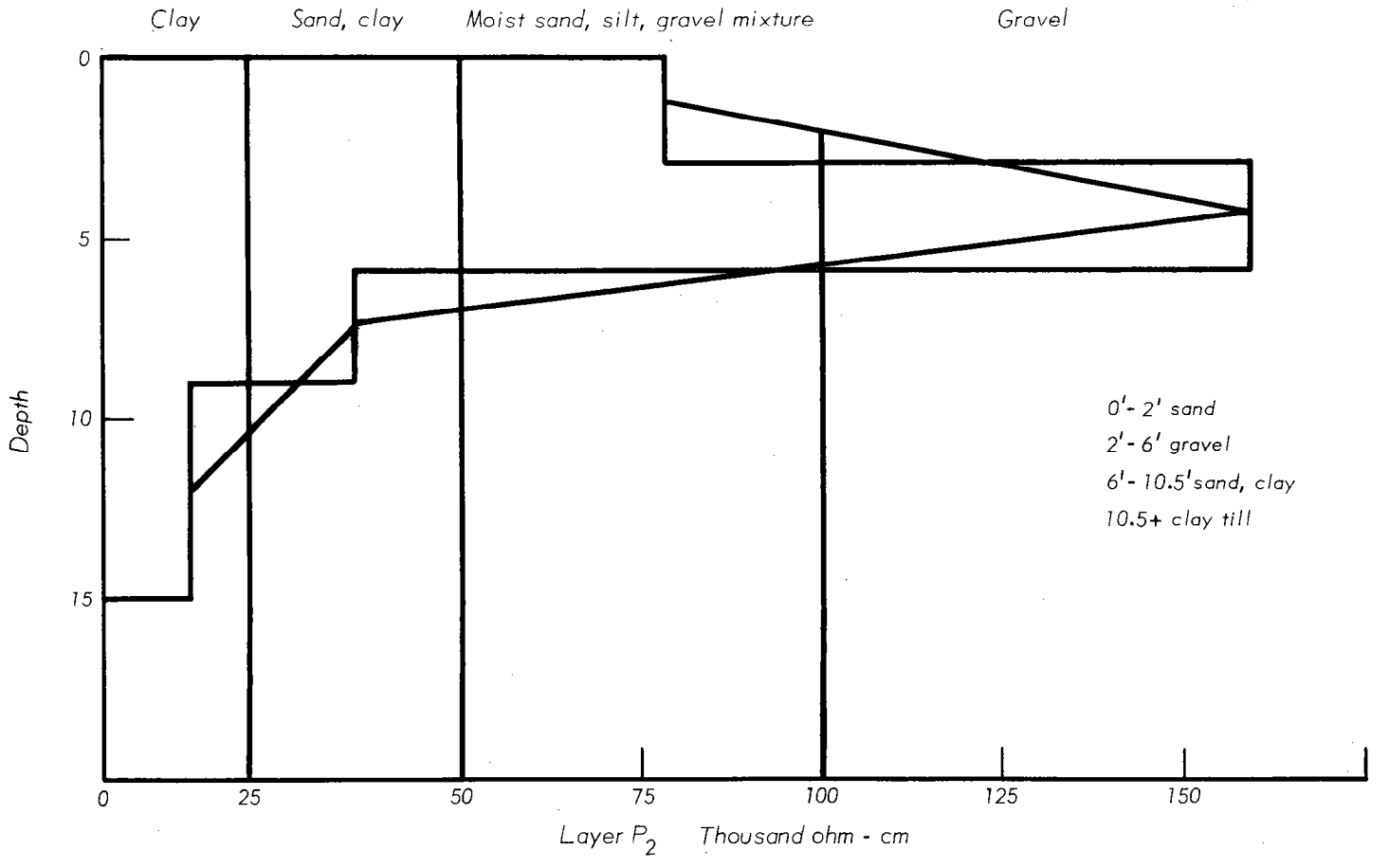

Figure 3-16. — Barnes Layer Method

gravel mixture 50,000 to 100,000 ohm-cm and coarse gravel over 100,000 ohm-cm. The intersection of the "transition lines" and range lines leads to the interpretation that 0 to 2 feet is sand, 2 to 6 feet is gravel, 6 to 10.5 feet is sandy clay (?), and below 10.5 is clay till.

Figure 3-17 is a sample form for recording and computing field data. Table 3-8 is a tabular listing of various values of conductance (GN) from 0.0001 through 0.1000 and the corresponding values of resistance (RN) for three foot layers.

According to Soiltest (1968, p. 39), "There have been theoretical objections raised concerning the Barnes Layer Method. Most of the objections arise from the warping of the electric field lines by subsurface conditions [see page 3-45]. However, in practice the Barnes Layer Method seems to work.

"The Barnes and Moore methods have been found to complement each other. In general, the Layer Method is most responsive to subsurface changes in texture. When changes occur in the electrolyte concentration in ground water, the Cumulative Method works better. In forming contoured cross sections, good correlation will usually be obtained with one of the two methods. Good boring or seismic control data is essential for correlation of this kind."

A computer program is available (Upper Darby E & WP Unit) for reducing field data for the Barnes Layer and Moore Cumulative Methods. It is suggested that the program be utilized when computations are required on more than ten vertical profiles.

Interpretations

The following discussion on interpretation should enable the reader to understand why variations in apparent resistivity readings are caused by variations both laterally and vertically in subsurface materials and how to plot and interpret by the various techniques field resistivity data.

SCS-344 5-57
Tabular Computations
3-40

U. S. DEPARTMENT OF AGRICULTURE
SOIL CONSERVATION SERVICE

EARTH RESISTIVITY PROFILING

Watershed: Operators Date

Site: Probe number:

Location of setup:

Probe Setting (ft)	Probe Separation (ft)	Meter Reading Conduct. (mhos)	Conductance (mhos)	Resistance R=1/mhos (ohms)	Apparent Resist. ρ_a (ohm-cm)	Moore Method Cumulat. Resistiv. ρ_e (ohm-cm)	Barnes Method Layer Conduct. G_n (mhos)	Barnes Method Layer Resistiv. ρ_{al} (ohm-cm)
$1\frac{1}{2}$-$4\frac{1}{2}$	3							
3-9	6							
$4\frac{1}{2}$-$13\frac{1}{2}$	9							
6-18	12							
$7\frac{1}{2}$-$22\frac{1}{2}$	15							
9-27	18							
$10\frac{1}{2}$-$31\frac{1}{2}$	21							
12-36	24							
$13\frac{1}{2}$-$40\frac{1}{2}$	27							
15-45	30							
$16\frac{1}{2}$-$49\frac{1}{2}$	33							
18-54	36							
$19\frac{1}{2}$-$58\frac{1}{2}$	39							
21-63	42							
$22\frac{1}{2}$-$67\frac{1}{2}$	45							
24-72	48							
$25\frac{1}{2}$-$76\frac{1}{2}$	51							
27-81	54							
Remarks:								

Tabulated for instrument readings in mhos or ohms and Wenner probe configurations

Figure 3–17. – Field resistivity data sample form

TABLE 3-8.- RESISTIVITY (RN) VALUES FOR CONDUCTANCE (GN) OF THREE FOOT LAYERS

CONDUCTANCE (GN) MHOS	RESISTIVITY (RN) OHMS	CONDUCTANCE (GN) MHOS	RESISTIVITY (RN) OHMS	CONDUCTANCE (GN) MHOS	RESISTIVITY (RN) OHMS
0.0001	5,745,900	0.0061	94,100	0.0121	47,400
0.0002	2,872,900	0.0062	92,600	0.0122	47,000
0.0003	1,915,300	0.0063	91,200	0.0123	46,700
0.0004	1,436,500	0.0064	89,700	0.0124	46,300
0.0005	1,149,200	0.0065	88,400	0.0125	45,900
0.0006	957,600	0.0066	87,000	0.0126	45,600
0.0007	820,800	0.0067	85,700	0.0127	45,200
0.0008	718,200	0.0068	84,500	0.0128	44,800
0.0009	638,400	0.0069	83,200	0.0129	44,500
0.0010	574,600	0.0070	82,000	0.0130	44,200
0.0011	522,300	0.0071	80,900	0.0131	43,800
0.0012	478,800	0.0072	79,800	0.0132	43,500
0.0013	442,000	0.0073	78,700	0.0133	43,200
0.0014	410,400	0.0074	77,600	0.0134	42,800
0.0015	383,000	0.0075	76,600	0.0135	42,500
0.0016	359,100	0.0076	75,600	0.0136	42,200
0.0017	338,000	0.0077	74,600	0.0137	41,900
0.0018	319,200	0.0078	73,600	0.0138	41,600
0.0019	302,400	0.0079	72,700	0.0139	41,300
0.0020	287,300	0.0080	71,800	0.0140	41,000
0.0021	273,600	0.0081	70,900	0.0141	40,700
0.0022	261,100	0.0082	70,000	0.0142	40,400
0.0023	249,800	0.0083	69,200	0.0143	40,100
0.0024	239,400	0.0084	68,400	0.0144	39,900
0.0025	229,800	0.0085	67,600	0.0145	39,600
0.0026	221,000	0.0086	66,800	0.0146	39,300
0.0027	212,800	0.0087	66,000	0.0147	39,000
0.0028	205,200	0.0088	65,200	0.0148	38,800
0.0029	198,100	0.0089	64,500	0.0149	38,500
0.0030	191,500	0.0090	63,800	0.0150	38,300
0.0031	185,300	0.0091	63,100	0.0151	38,000
0.0032	179,500	0.0092	62,400	0.0152	37,800
0.0033	174,100	0.0093	61,700	0.0153	37,500
0.0034	169,000	0.0094	61,100	0.0154	37,300
0.0035	164,100	0.0095	60,400	0.0155	37,000
0.0036	159,600	0.0096	59,800	0.0156	36,800
0.0037	155,200	0.0097	59,200	0.0157	36,500
0.0038	151,200	0.0098	58,600	0.0158	36,300
0.0039	147,300	0.0099	58,000	0.0159	36,100
0.0040	143,600	0.0100	57,400	0.0160	35,900
0.0041	140,100	0.0101	56,800	0.0161	35,600
0.0042	136,800	0.0102	56,300	0.0162	35,400
0.0043	133,600	0.0103	55,700	0.0163	35,200
0.0044	130,500	0.0104	55,200	0.0164	35,000
0.0045	127,600	0.0105	54,700	0.0165	34,800
0.0046	124,900	0.0106	54,200	0.0166	34,600
0.0047	122,200	0.0107	53,700	0.0167	34,400
0.0048	119,700	0.0108	53,200	0.0168	34,200
0.0049	117,200	0.0109	52,700	0.0169	34,000
0.0050	114,900	0.0110	52,200	0.0170	33,800
0.0051	112,600	0.0111	51,700	0.0171	33,600
0.0052	110,500	0.0112	51,300	0.0172	33,400
0.0053	108,400	0.0113	50,800	0.0173	33,200
0.0054	106,400	0.0114	50,400	0.0174	33,000
0.0055	104,400	0.0115	49,900	0.0175	32,800
0.0056	102,600	0.0116	49,500	0.0176	32,600
0.0057	100,800	0.0117	49,100	0.0177	32,400
0.0058	99,000	0.0118	48,600	0.0178	32,200
0.0059	97,300	0.0119	48,200	0.0179	32,100
0.0060	95,700	0.0120	47,800	0.0180	31,900

TABLE 3-8.- (CONTINUED)

CONDUCTANCE (GN) MHOS	RESISTIVITY (RN) OHMS	CONDUCTANCE (GN) MHOS	RESISTIVITY (RN) OHMS	CONDUCTANCE (GN) MHOS	RESISTIVITY (RN) OHMS
0.0181	31,700	0.0300	19,100	0.0420	13,600
0.0182	31,500	0.0302	19,000	0.0422	13,600
0.0184	31,200	0.0304	18,900	0.0424	13,500
0.0186	30,800	0.0306	18,700	0.0426	13,400
0.0188	30,500	0.0308	18,600	0.0428	13,400
0.0190	30,200	0.0310	18,500	0.0430	13,300
0.0192	29,900	0.0312	18,400	0.0432	13,300
0.0194	29,600	0.0314	18,200	0.0434	13,200
0.0196	29,300	0.0316	18,100	0.0436	13,100
0.0198	29,000	0.0318	18,000	0.0438	13,100
0.0200	28,700	0.0320	17,900	0.0440	13,000
0.0202	28,400	0.0322	17,800	0.0442	13,000
0.0204	28,100	0.0324	17,700	0.0444	12,900
0.0206	27,800	0.0326	17,600	0.0446	12,800
0.0208	27,600	0.0328	17,500	0.0448	12,800
0.0210	27,300	0.0330	17,400	0.0450	12,700
0.0212	27,100	0.0332	17,300	0.0452	12,700
0.0214	26,800	0.0334	17,200	0.0454	12,600
0.0216	26,600	0.0336	17,100	0.0456	12,600
0.0218	26,300	0.0338	17,000	0.0458	12,500
0.0220	26,100	0.0340	16,900	0.0460	12,400
0.0222	25,800	0.0342	16,800	0.0462	12,400
0.0224	25,600	0.0344	16,700	0.0464	12,300
0.0226	25,400	0.0346	16,600	0.0466	12,300
0.0228	25,200	0.0348	16,500	0.0468	12,200
0.0230	24,900	0.0350	16,400	0.0470	12,200
0.0232	24,700	0.0352	16,300	0.0472	12,100
0.0234	24,500	0.0354	16,200	0.0474	12,100
0.0236	24,300	0.0356	16,100	0.0476	12,000
0.0238	24,100	0.0358	16,000	0.0478	12,000
0.0240	23,900	0.0360	15,900	0.0480	11,900
0.0242	23,700	0.0362	15,800	0.0482	11,900
0.0244	23,500	0.0364	15,700	0.0484	11,800
0.0246	23,300	0.0366	15,600	0.0486	11,800
0.0248	23,100	0.0368	15,600	0.0488	11,700
0.0250	22,900	0.0370	15,500	0.0490	11,700
0.0252	22,800	0.0372	15,400	0.0492	11,600
0.0254	22,600	0.0374	15,300	0.0494	11,600
0.0256	22,400	0.0376	15,200	0.0496	11,500
0.0258	22,200	0.0378	15,200	0.0498	11,500
0.0260	22,100	0.0380	15,100	0.0500	11,400
0.0262	21,900	0.0382	15,000	0.0502	11,400
0.0264	21,700	0.0384	14,900	0.0504	11,400
0.0266	21,600	0.0386	14,800	0.0506	11,300
0.0268	21,400	0.0388	14,800	0.0508	11,300
0.0270	21,200	0.0390	14,700	0.0510	11,200
0.0272	21,100	0.0392	14,600	0.0512	11,200
0.0274	20,900	0.0394	14,500	0.0514	11,100
0.0276	20,800	0.0396	14,500	0.0516	11,100
0.0278	20,600	0.0398	14,400	0.0518	11,000
0.0280	20,500	0.0400	14,300	0.0520	11,000
0.0282	20,300	0.0402	14,200	0.0522	11,000
0.0284	20,200	0.0404	14,200	0.0524	10,900
0.0286	20,000	0.0406	14,100	0.0526	10,900
0.0288	19,900	0.0408	14,000	0.0528	10,800
0.0290	19,800	0.0410	14,000	0.0530	10,800
0.0292	19,600	0.0412	13,900	0.0532	10,800
0.0294	19,500	0.0414	13,800	0.0534	10,700
0.0296	19,400	0.0416	13,800	0.0536	10,700
0.0298	19,200	0.0418	13,700	0.0538	10,600

TABLE 3-8.- (CONTINUED)

CONDUCTANCE (GN) MHOS	RESISTIVITY (RN) OHMS	CONDUCTANCE (GN) MHOS	RESISTIVITY (RN) OHMS	CONDUCTANCE (GN) MHOS	RESISTIVITY (RN) OHMS
0.0540	10,600	0.0660	8,700	0.0780	7,300
0.0542	10,600	0.0662	8,600	0.0782	7,300
0.0544	10,500	0.0664	8,600	0.0784	7,300
0.0546	10,500	0.0666	8,600	0.0786	7,300
0.0548	10,400	0.0668	8,600	0.0788	7,200
0.0550	10,400	0.0670	8,500	0.0790	7,200
0.0552	10,400	0.0672	8,500	0.0792	7,200
0.0554	10,300	0.0674	8,500	0.0794	7,200
0.0556	10,300	0.0676	8,500	0.0796	7,200
0.0558	10,200	0.0678	8,400	0.0798	7,200
0.0560	10,200	0.0680	8,400	0.0800	7,100
0.0562	10,200	0.0682	8,400	0.0802	7,100
0.0564	10,100	0.0684	8,400	0.0804	7,100
0.0566	10,100	0.0686	8,300	0.0806	7,100
0.0568	10,100	0.0688	8,300	0.0808	7,100
0.0570	10,000	0.0690	8,300	0.0810	7,000
0.0572	10,000	0.0692	8,300	0.0812	7,000
0.0574	10,000	0.0694	8,200	0.0814	7,000
0.0576	9,900	0.0696	8,200	0.0816	7,000
0.0578	9,900	0.0698	8,200	0.0818	7,000
0.0580	9,900	0.0700	8,200	0.0820	7,000
0.0582	9,800	0.0702	8,100	0.0822	6,900
0.0584	9,800	0.0704	8,100	0.0824	6,900
0.0586	9,800	0.0706	8,100	0.0826	6,900
0.0588	9,700	0.0708	8,100	0.0828	6,900
0.0590	9,700	0.0710	8,000	0.0830	6,900
0.0592	9,700	0.0712	8,000	0.0832	6,900
0.0594	9,600	0.0714	8,000	0.0834	6,800
0.0596	9,600	0.0716	8,000	0.0836	6,800
0.0598	9,600	0.0718	8,000	0.0838	6,800
0.0600	9,500	0.0720	7,900	0.0840	6,800
0.0602	9,500	0.0722	7,900	0.0842	6,800
0.0604	9,500	0.0724	7,900	0.0844	6,800
0.0606	9,400	0.0726	7,900	0.0846	6,700
0.0608	9,400	0.0728	7,800	0.0848	6,700
0.0610	9,400	0.0730	7,800	0.0850	6,700
0.0612	9,300	0.0732	7,800	0.0852	6,700
0.0614	9,300	0.0734	7,800	0.0854	6,700
0.0616	9,300	0.0736	7,800	0.0856	6,700
0.0618	9,200	0.0738	7,700	0.0858	6,600
0.0620	9,200	0.0740	7,700	0.0860	6,600
0.0622	9,200	0.0742	7,700	0.0862	6,600
0.0624	9,200	0.0744	7,700	0.0864	6,600
0.0626	9,100	0.0746	7,700	0.0866	6,600
0.0628	9,100	0.0748	7,600	0.0868	6,600
0.0630	9,100	0.0750	7,600	0.0870	6,600
0.0632	9,000	0.0752	7,600	0.0872	6,500
0.0634	9,000	0.0754	7,600	0.0874	6,500
0.0636	9,000	0.0756	7,600	0.0876	6,500
0.0638	9,000	0.0758	7,500	0.0878	6,500
0.0640	8,900	0.0760	7,500	0.0880	6,500
0.0642	8,900	0.0762	7,500	0.0882	6,500
0.0644	8,900	0.0764	7,500	0.0884	6,500
0.0646	8,800	0.0766	7,500	0.0886	6,400
0.0648	8,800	0.0768	7,400	0.0888	6,400
0.0650	8,800	0.0770	7,400	0.0890	6,400
0.0652	8,800	0.0772	7,400	0.0892	6,400
0.0654	8,700	0.0774	7,400	0.0894	6,400
0.0656	8,700	0.0776	7,400	0.0896	6,400
0.0658	8,700	0.0778	7,300	0.0898	6,300

Note: Resistivity values in the units and tens columns have been truncated - not rounded

Two Layer Case $\rho_1 < \rho_2$

Assume a simple two layer case in which a laterally homogeneous layer of resistivity ρ_1 is underlain by another laterally homogeneous layer of resistivity ρ_2. Further assume that the resistivity of ρ_1 is less than ρ_2.

At small electrode spacings (Wenner configuration) the current flow lines are all uniform in layer ρ_1 (Figure 3-18A) and the apparent resistivity equal to the true resistivity. As the electrode spacing is increased the ρ_2 layer affects the current flow lines. Since ρ_2 has a higher resistivity than ρ_1 the current flow lines are compressed into the ρ_1 layer (further apart in ρ_2 layer) as in Figure 3-18B. As was shown in the theory section on page 3-6 the apparent resistivity is directly proportional to the current density and true resistivity and inversely proportional to the current. $\rho \propto (i/I)\, \rho_0$

As the current density i increases the apparent resistivity increases and the true resistivity and current are unchanged. Figure 3-18C is a plot of apparent resistivity versus electrode spacing for this two layer case. Point A_1 would represent the apparent resistivity for the small electrode spacing and point A_2 would represent the apparent resistivity for the large electrode spacing.

As can be seen from the curve, sharp breaks in resistivity such as the boundary between ρ_1 and ρ_2 show as a gradual change in apparent resistivity because the current density is only changed gradually as the electrode spacing is increased.

Two Layer Case $\rho_1 > \rho_2$

Assume this simple two layer case in which a high resistivity layer overlies a low resistivity layer (reverse of Figure 3-18).

Figure 3-19A shows the current flow lines essentially unaffected by the underlying low resistivity layer at small electrode spacing. When the

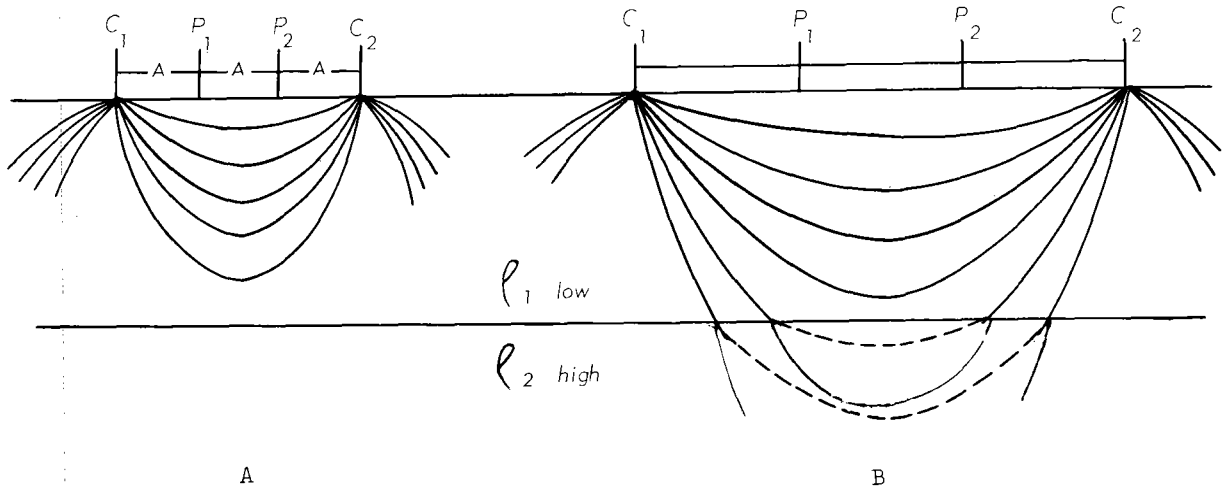

A B

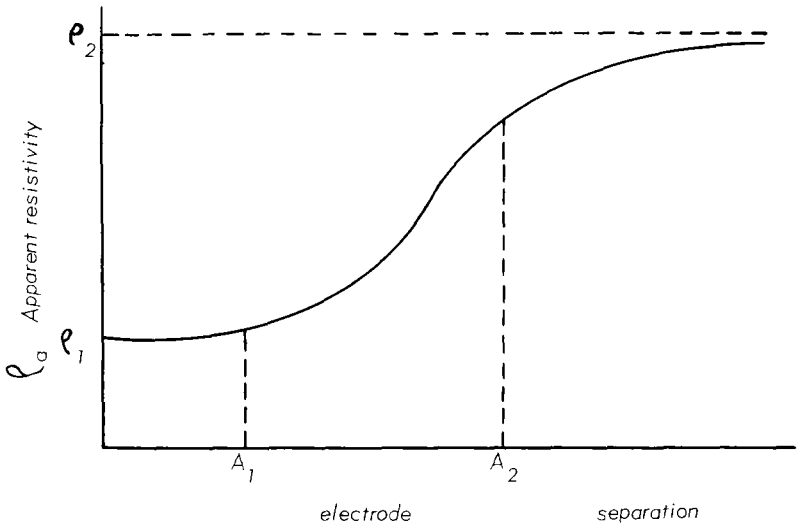

C

Figure 3-18. – Current flow lines and plot for two layer case (adapted from Soiltest, 1968.)

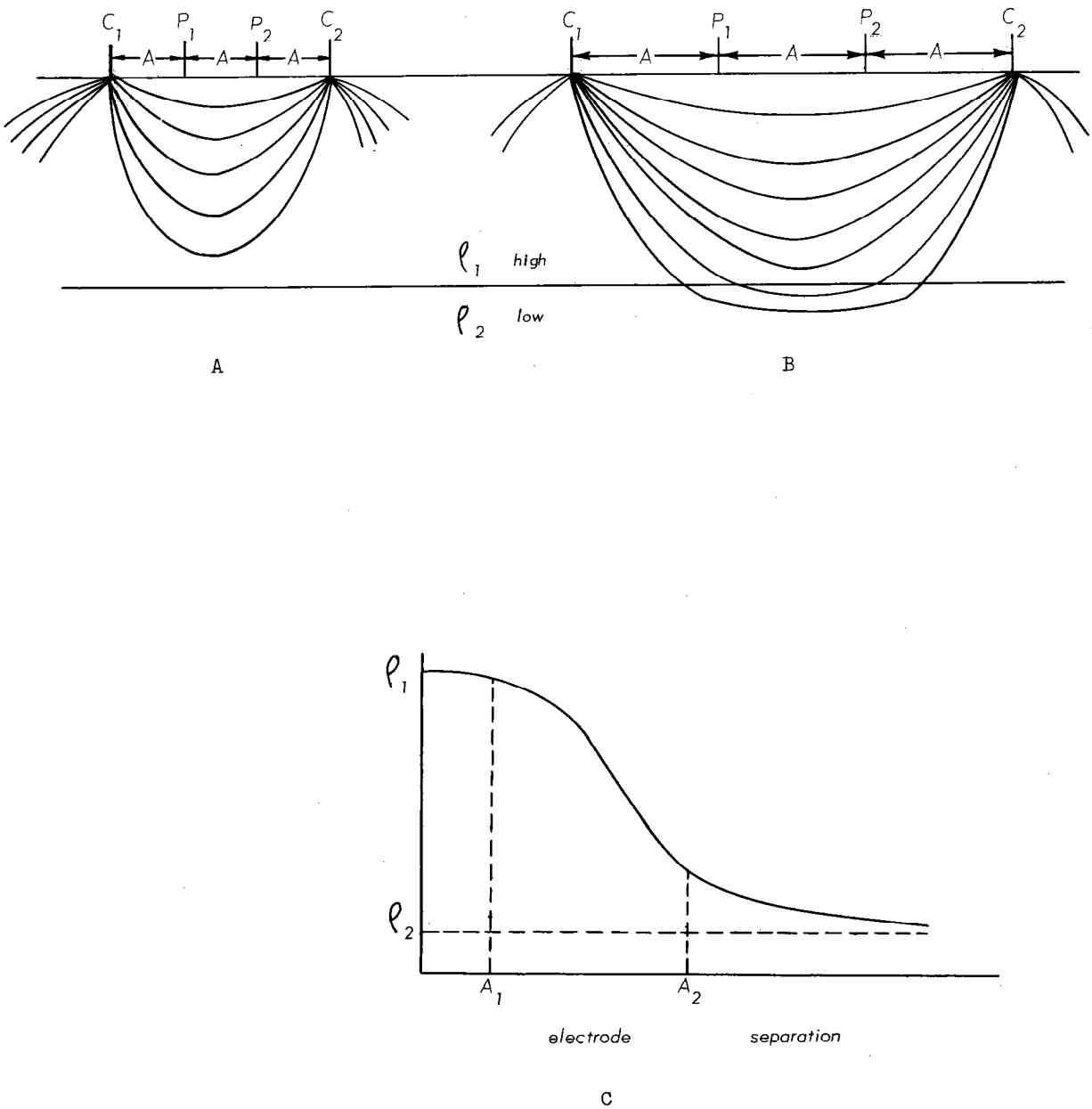

Figure 3-19. – Current flow lines and plot for two layer case (adapted from Soiltest, 1968.)

electrode spacing is increased, Figure 3-19B, the underlying layer affects the current flow lines. They are closer together in the low resistivity layer and further apart in the high resistivity layer. Therefore, the apparent resistivity is less. Figure 3-19C is a plot of apparent resistivity versus electrode spacing.

According to Soiltest (1968, p. 16), "The effect on resistivity readings of a thin, horizontal deposit near the surface is much greater than its physical volume suggests it should be. Often such discontinuities are interpreted as being more massive deposits lying at greater depths or as vertical changes. If sudden changes occur in the readings, near-surface horizontal discontinuities or vertical changes should be suspected. Only rarely will material lying at depth produce sudden variations in electrical readings made on the surface."

Effect of Topographic Features

Topographic features such as cliffs, road cuts, hills, etc. affect the current flow lines and current density between current electrodes. The quantitative effect of these features is very difficult to calculate but the following graphical representations will illustrate the effect of these topographic features on current flow lines.

Figure 3-20 illustrates how a cliff or steep road cut affects the current flow lines. As the electrode spacing increases in vertical profiling or as the spread approaches the cliff in horizontal profiling the current flow lines (in cross-section view) are compressed near the cliff because the air has infinite resistivity. The current density is increased and the apparent resistivity will show an increase. Notice in the plan view the current flow lines when a resistivity spread is run parallel to a cliff. The current flow around both current electrodes on the cliff side are compressed resulting in an increase in current density and erroneous increase in apparent resistivity.

Effect of High Resistivity Lenticular Deposits

Figure 3-21 illustrates the effect of a high resistivity lenticular deposit (such as gravel) surrounded by low resistivity material.

In Figure 3-21A the electrode spacing is small and the lens has no appreciable effect on the current density. As the electrode spacing is increased the current flow lines and current density are affected and compressed upward giving an increase in apparent resistivity (Figure 3-21B).

The optimum electrode spacing or spacings to detect this lenticular deposit is determined from knowledge of local geology and vertical profiling. The horizontal profiling technique using this optimum electrode spacing or spacings can be used to delineate the lens.

Profiling across Vertical Contacts

The following figures illustrate the effect a vertical contact between materials of different resistivity has on plots of apparent resistivity versus electrode location. These vertical contacts could be faults, dikes, breccia zones, the steep side of a buried stream channel in bedrock, etc. These are typical plots for horizontal profiling.

Figure 3-22 illustrates horizontal profiling across a vertical fault with resistivities on opposite sides of 1 and 5 ohm-meters. The solid line is the plot of field data using the Wenner configuration with constant electrode spacing "a", and an interval between stations of "a/2." The dashed line is a continuous theoretical plot.

When the center of the spread is at locations in the vicintiy of -3 from the fault, the fault is not affecting the current flow lines and the apparent resistivity (1.0 + ohm-meters) is approximately equal to the true resistivity (1.0 ohm-meter). When the lead electrode nears the fault the apparent resistivity shows a gradual increase (plotted point -1.8, lead electrode at -0.3). When the lead electrode crosses the

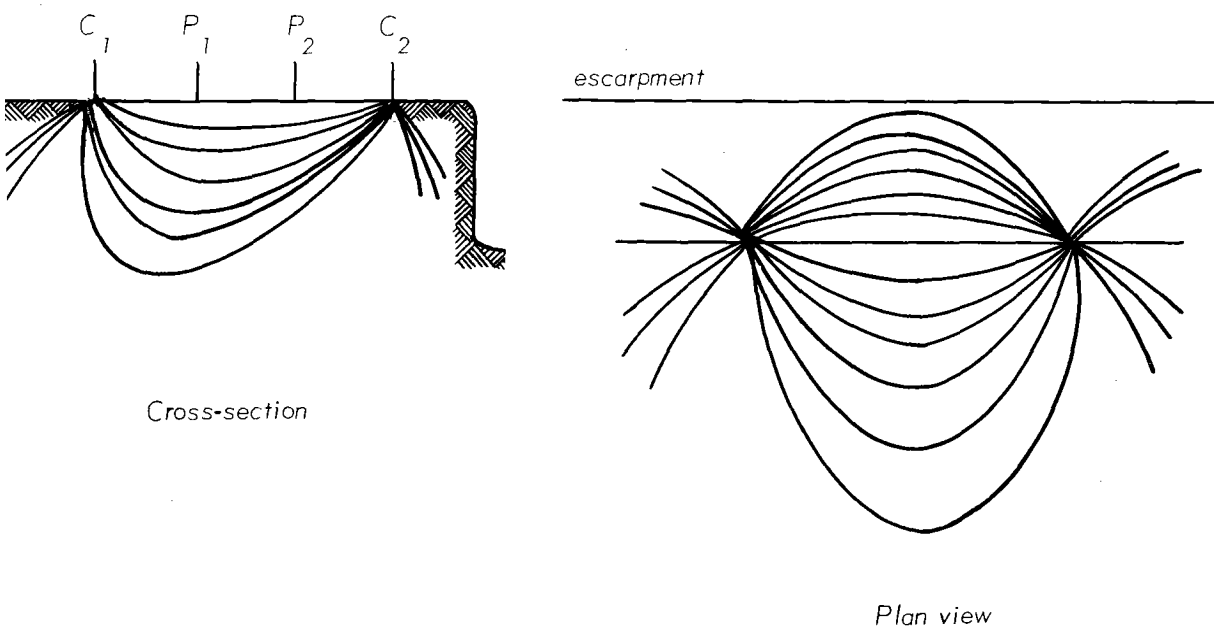

Figure 3-20. – Effect of cliff or road cut on current flow lines (adapted from Soiltest, 1968.)

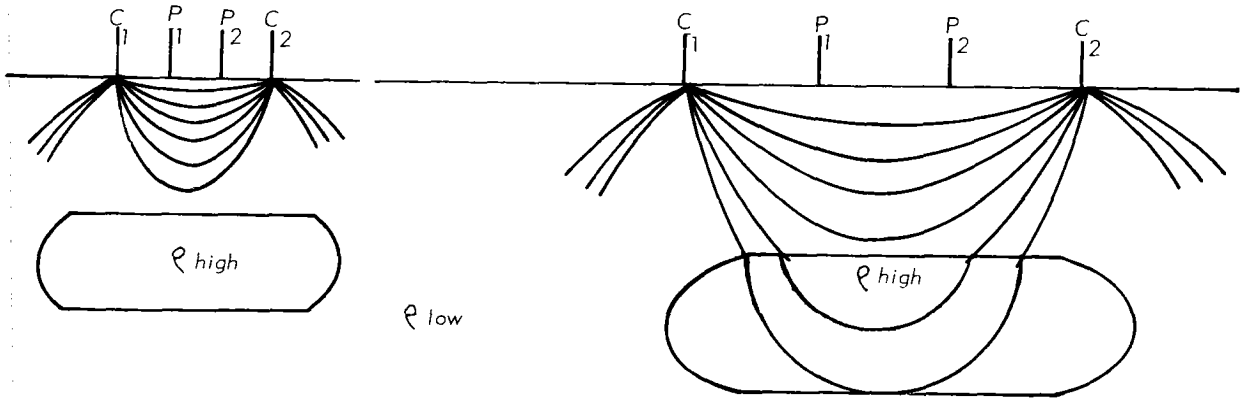

Figure 3-21. – Effect of high resistivity deposit on current flow lines (Adapted fron Soiltest, 1968)

fault the apparent resistivity decreases slightly because of redistribution of current flow lines (plotted point -0.8). When one current and one potential electrode cross the fault and the center of the spread (plotted point) is exactly on the fault, the apparent resistivity would be 3.0 ohm-meters. If these two electrodes cross the fault but the center of the spread is not on the fault the apparent resistivity is a weighted average depending on the distance the electrodes are from the fault and the resistivity of the material on both sides of the fault. As profiling across the fault continues a sharp break occurs as each electrode crosses the fault such as A' when the second potential electrode crosses the fault and B' when the second current electrode crosses.

The sharp maximum A in the continuous plot is subdued and is displaced to the right to A' in the field plot and the minimum peak B is displaced to the left to B'. This displacement of the actual plot with respect to the theoretical plot is caused by the electrode separation and the location of the electrodes for each reading. If by chance the location of the electrodes had been closer to the fault the field plot would have approached the theoretical plot much closer. Another problem is that if these peaks are used to locate the fault exactly the displacement of peaks will lead to error.

Figure 3-22A is a vertical resistivity profile across high-resistivity, steeply dipping beds using the Lee Configuration.

Figure 3-23 shows several theoretical plots of Wenner configuration horizontal profiling across a brecciated zone separating materials with a resistivity of 1:5. The six plots show the different curves when the brecciated area with a width of a/2 has resistivities of ∞, 10, 0, 4, 3, and 2.

For a brecciated zone of infinite resistivity a pronounced peak lies vertically over the axis of the zone (Figure 3-23A). For a brecciated zone with a resistivity which is greater than the resistivity of the material to the right of the zone (in this case 10 units) it also

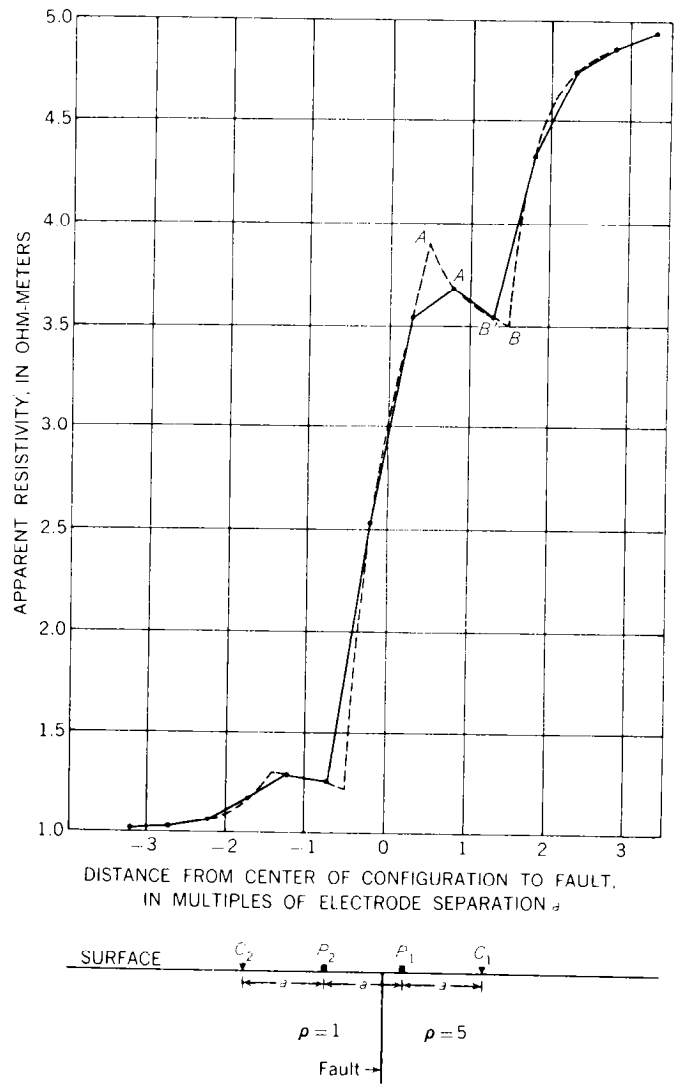

Wenner horizontal resistivity profile over a vertical fault. Comparison of a theoretical field plot (solid line) and a continuous theoretical-resistivity curve (dashed line).

Figure 3–22. – Horizontal profile across a vertical contact (From Van Nostrand and Cook, 1966)

produces a peak vertically over the axis of the zone (Figure 3-23B), but less than the true resistivity of the material to the right of the zone. For zones with small resistivities (Figures 3-23 C, E and F) the peak shifts to the right and occurs a distance of a/2 to the right of the right edge of the brecciated zone. In Figure 3-23D the peak occurs over the right edge of the brecciated zone. The brecciated zones with high resistivity in Figure 3-23A and B produce pronounced peaks that can be interpreted as brecciated zones. The

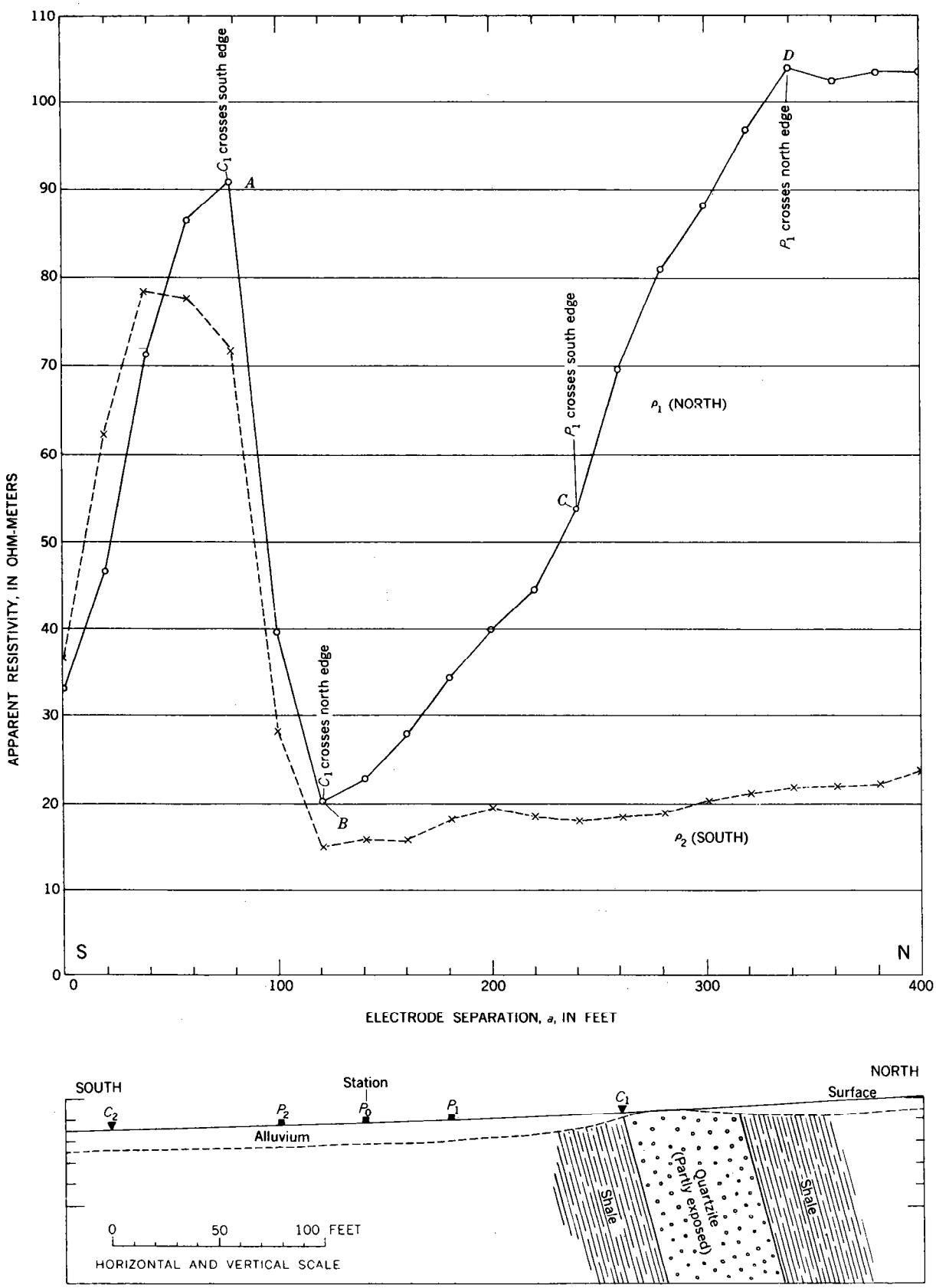

Vertical resistivity profile across high-resistivity steeply dipping quartzite bed, Mountain City copper district, Elko County, Nev., Lee configuration. Adapted from C. H. Sandberg and K. L. Cook (1945), unpublished data.

Figure 3–22A. – Vertical resistivity profile (From Van Nostrand and Cook, 1966)

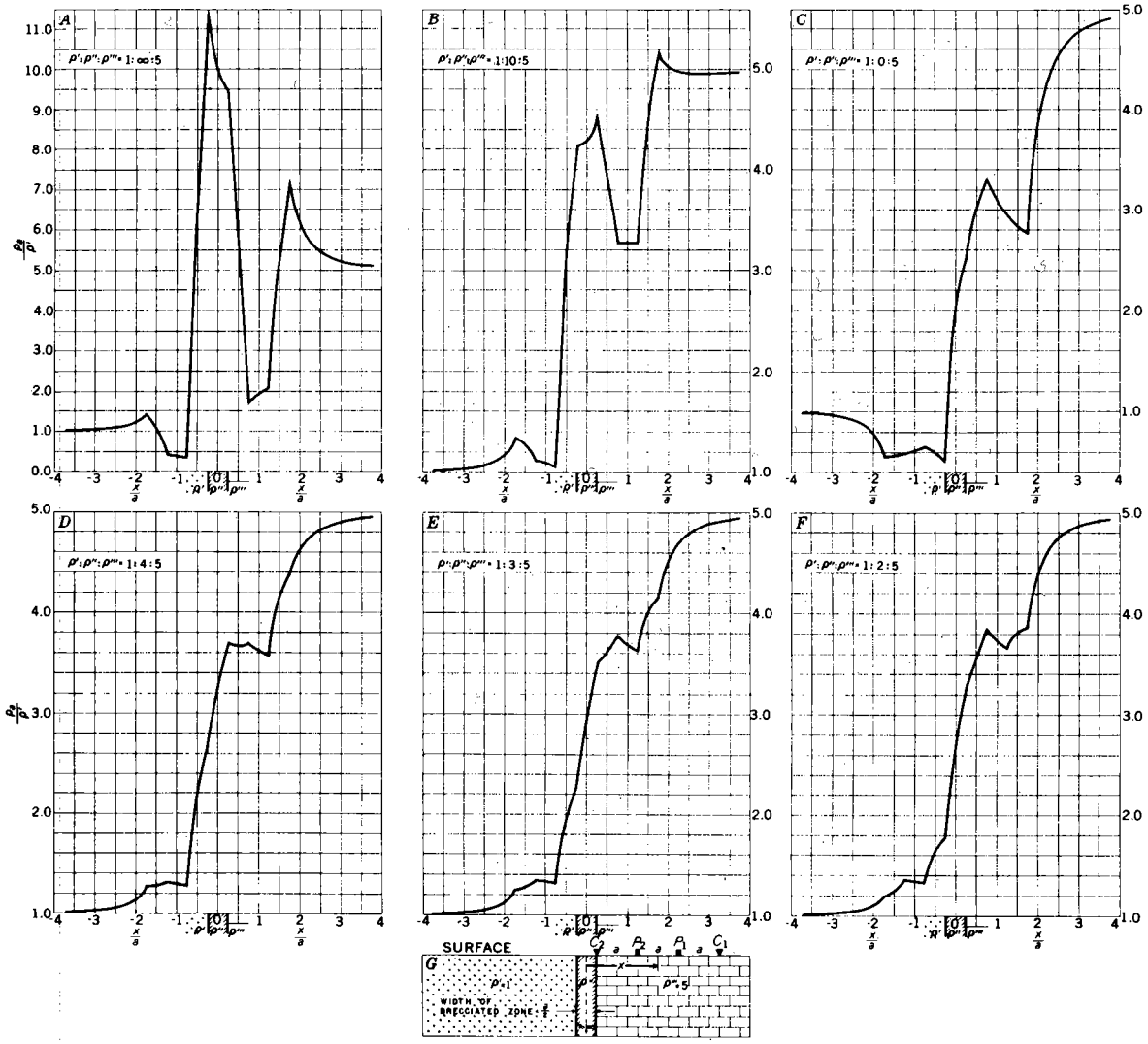

Horizontal resistivity profiles across brecciated zone of different resistivities, Wenner configuration. For all diagrams $\rho'/\rho''' = 1/5$ and width is a/2.

Figure 3–23. – Horizontal profiling across brecciated zone (From Van Nostrand and Cook, 1966)

remaining plots (Figure 3-23C, D, E and F) produce peaks that are similar to those obtained over a single fault and it would be difficult to recognize in field data any evidence of the brecciated zone as such.

Resistivity "Back-ups"

The normal sequence of readings when vertical profiling is a decrease in resistance (R) or an increase in conductance (G = 1/R) as the electrode interval is increased.

Occasionally this normal sequence of readings is reversed or "backs-up" for one or two readings (R increases or G decreases). Care must be exercised in interpreting this condition. Usually these "back-ups" occur when the equipotential surface induced around one current

electrode encompasses a material of much higher resistivity than the material around the other current electrode. This distorts the current flow lines, increases the current density, and results in an abnormally high resistance reading.

The following figures illustrate some of the surface and subsurface conditions that can cause resistivity "back-ups" when using the Wenner configuration.

Figure 3-24 shows the effect of varying amounts of material around the current electrodes on the current flow lines (and current density). In Figure 3-24A the additional material to the left end above the left current electrode has greater conductance (less resistance) than the air (infinite resistance) above the right current electrode. Thus the current flow lines are deflected to the left resulting in greater resistance measurements than would be measured on a horizontal surface. Figure 3-24B shows the same result as A due to the infinite resistance of air to the right of the right electrode.

Figure 3-25 shows the distortion of current flow lines when the spread is run across the slope instead of on the contour. Some distortion of current flow lines would occur even if the hill was not underlain by highly resistant bedrock. The bedrock causes further distortion that results in a resistivity "back-up". This points out again the desirability of running resistivity spreads on level ground or on the contour if at all possible.

Figure 3-26 illustrates how a lens or localized high resistivity material (in comparison to surrounding material) near one current electrode distorts the current flow lines resulting in increased current density and resistivity "back-ups". An additional spread perpendicular to the first would help delineate the cause of the "back-ups".

Seating a current electrode on a boulder or in a coarse aggregate can cause distortion of the current flow lines (Figure 3-27). If the

electrode must be moved to avoid a boulder, etc., it should be moved in an arc using the distance from the electrode to the center of the

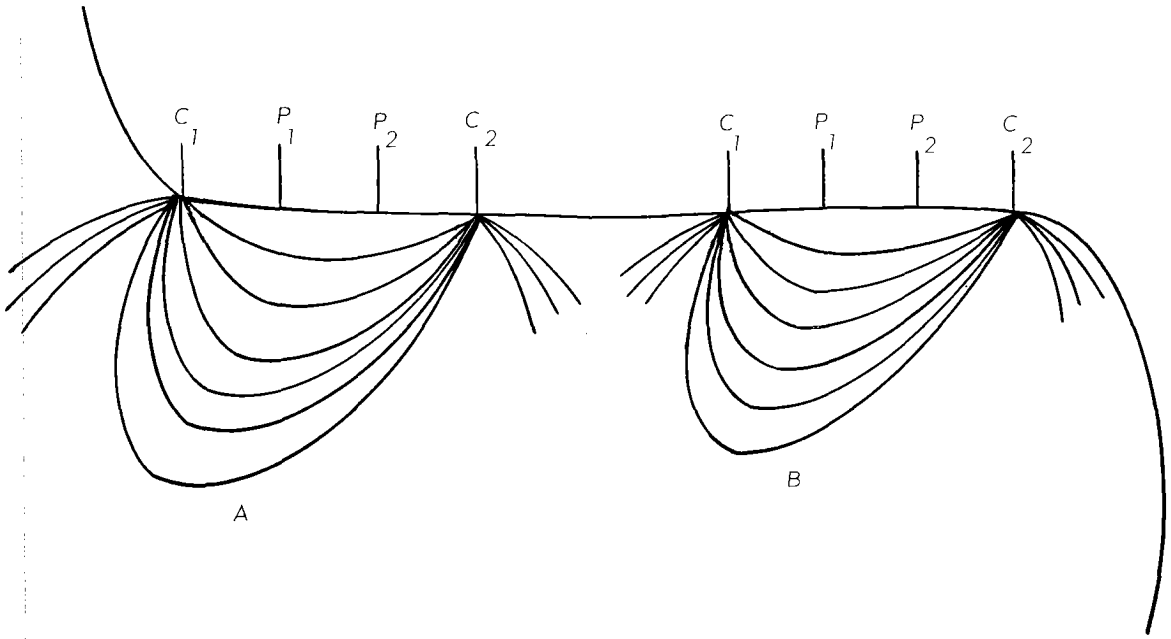

Figure 3-24. – Effect of topographic features on resistivity back-ups (adapted from Soiltest, 1968.)

spread as the radius. For moves that are small in comparison to the radius, the electrode can be moved perpendicular to the line of the spread.

Curve Matching

The last interpretative procedure to be discussed is curve matching. Van Nostrand and Cook (1966, pp. 89-99) have an excellent discussion of curve matching. A portion of their discussion including figures is quoted directly on the following 13 pages.

Theoretical Curves

"Our approach to the subject of theoretical curves of horizontal bedding problems is objective. Literally hundreds of apparent-reisitivity curves have been published for the two-, three-, and four-layer cases (Mooney and Wetzel, 1956). Our principal objectives, therefore, are

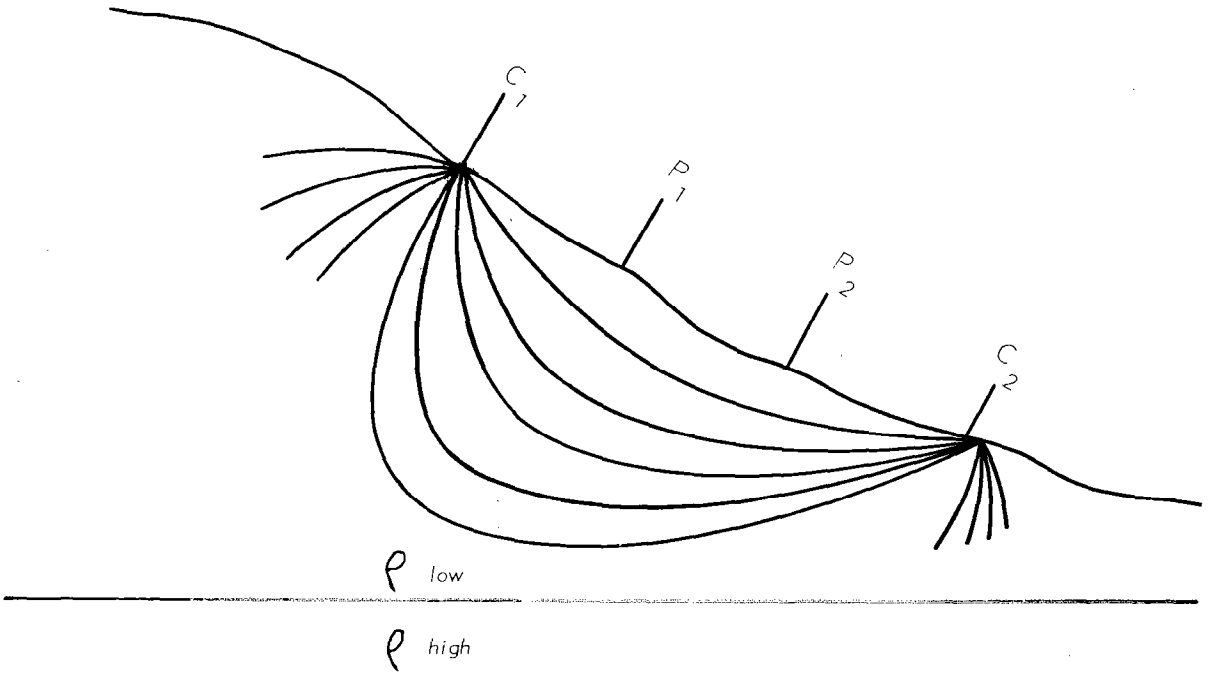

Figure 3-25. – Resistivity back-up caused by running spread on slope (adapted from Soiltest, 1968)

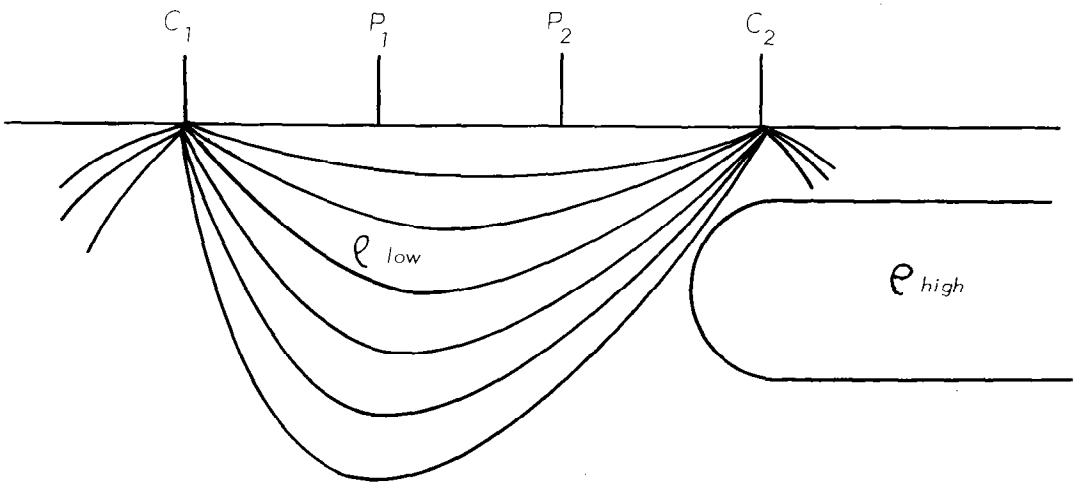

Figure 3-26. – Resistivity back-up caused by high resistivity material near one electrode (adapted from Soiltest, 1968.)

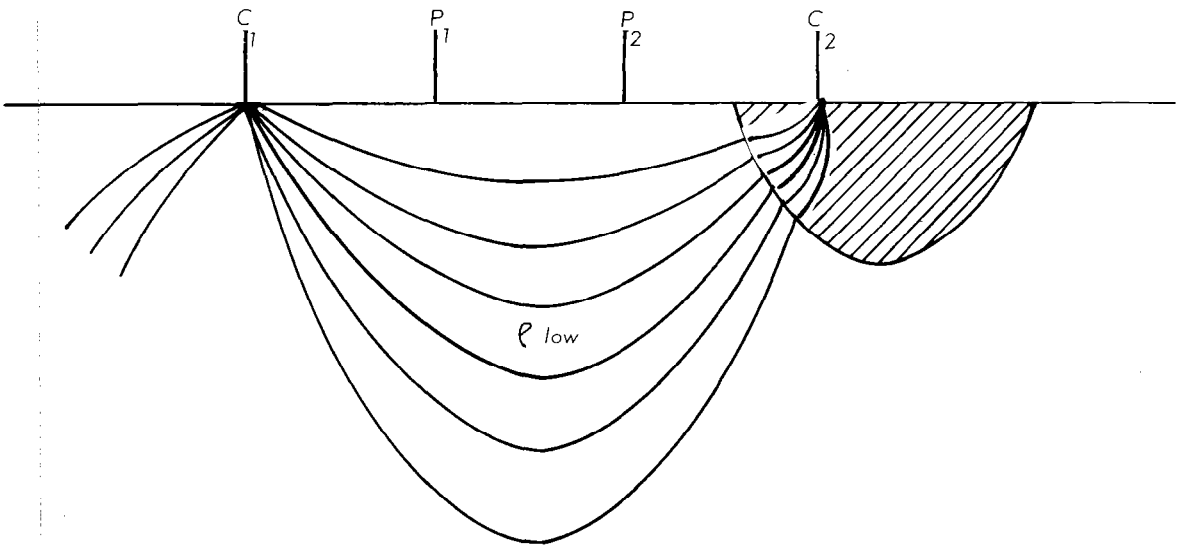

Figure 3-27. – Resistivity back-up caused by one electrode seated in high resistivity material (Adapted from Soiltest, 1968)

to digest and analyze the works of others on the horizontal-bed problems, and to give an evaluation of the best solutions available and the best methods to use in actual field problems. It should be emphasized that the key to the interpretation of the horizontal-bed problem lies in the recognition of the practical limitations of the resistivity method to solve the problem.

"The most serious limitation is one of depth. We normally find that the electrode separation in the Wenner configuration, for example, must be of the order of two or three times the depth to the beds of interest. Thus, even though current penetration can be obtained, the great electrode separations needed for the effects of deep layers to manifest themselves usually result in lateral effects superposed on the depth effects. Exceptions to this rule are rare in the field, and consequently the quantitative interpretation of horizontal-bed problems is usually restricted to relatively shallow depths.

"Other limitations are sufficient resistivity contrasts and compatible thicknesses. Although the restrictions imposed by resistivity contrasts are fortunately not very stringent, the vast range of resistivities is not as important as it appears. As we found in the previous section on theory, the resistivity contrast invariably enters the problem in the form of the reflection factor $k_{ij}=(\rho_i-\rho_j)/(\rho_i+\rho_j)$. The absolute value of the reflection factor ranges only from zero to unity. If the resistivity of a given bed is twice that of a neighboring bed, the reflection factor is one-third--which is already one-third of its entire range. If the resistivity of a given bed is 5 times the resistivity of an adjacent bed, the reflection factor is two-thirds. As the resistivity contrast rises above this value of 5 to 1, the reflection factor increases very slowly toward unity. For all practical purposes, a resistivity contrast of the order to 10 to 1 gives an anomaly of the same order of magnitude as an infinite resistivity contrast. This rule applies to almost all types of structures.

"The thicknesses of the beds also govern our approach to the problem of horizontal beds. For example, if there exist three layers and if the middle layer is of sufficient thickness, the three-layer problem can be solved by the successive use of methods normally applied to solve two-layer problems. As the thickness of the middle layer decreases, we find a stage in which the theroetical three-layer curves must be consulted; for an expanding electrode configuration, the effect of the bottommost bed appears in the apparent resistivity almost as soon as the effect of the middle layer. Finally, when the thickness of the middle layer becomes even smaller, the problem reduces to a simple two-layer case because the effect of the middle layer is no longer important at any electrode separation. It is obvious that the critical thicknesses of the middle layer in this hypothetical case are dependent on the resistivity contrasts.

"A working knowledge of what can or cannot be accomplished with resistivity techniques for the horizontal-bed problem is predicated upon a practical viewpoint of the manner in which these parameters of depth,

thicknesses, and resistivity contrasts are interrelated.

Two-Layer Case

"For the plotting of vertical resistivity profiles in horizontal-bed problems, logarithmic plotting for both the apparent resistivity and the electrode separation is preferable to linear plotting. When both the observed and theoretical curves are plotted on the same type of logarithmic paper, the effect of scale is eliminated; and once a satisfactory match between the observed and theoretical curves is made, the parameters can be determined. For the observed curves, the apparent resistivity ρ_α is plotted as the ordinate, and the electrode separation α is plotted as the abscissa. For the theoretical curves, the ratio of the apparent resistivity ρ_α to the true resistivity ρ_0 of the top layer is usually plotted as the ordinate, and the ratio of the electrode separation α to the thickness z_1 of the top layer is plotted as the abscissa; it is convenient to plot the theoretical curves on transparent material to facilitate curve matching.

"Figure 33[Figure 3-28] shows a master set of such theoretical curves for the two-layer case (adapted from Roman, 1941). The values of the reflection factor k are shown for intervals of 0.1 between +1.0 and -1.0. The theoretical curves are applicable for either the Wenner or Lee configurations. Assuming that a satisfactory fit occurs between the observed apparent resistivity curve and one of the curves in figure 33[Figure 3-28], the following factors may be readily obtained when the curves are in superposition. (See Figure 34)[Figure 3-29].

1. The reflection factor k, which equals $(\rho_1-\rho_0)/(\rho_1+\rho_0)$ is read immediately off the theoretical curve that fits the data. If an observed curve fits, but lies intermediate between the ones drawn on the master curves in Figure 33 [Figure 3-28], the estimated value of k can be obtained by interpolation from the chart.
2. The resistivity ρ_0 of the top layer is obtained by noting where the horizontal "resistivity index" line on the master chart intersects the axis of ordinates of the observed curve. This results from the fact that the resistivity index is the line (axis of abscissas) on

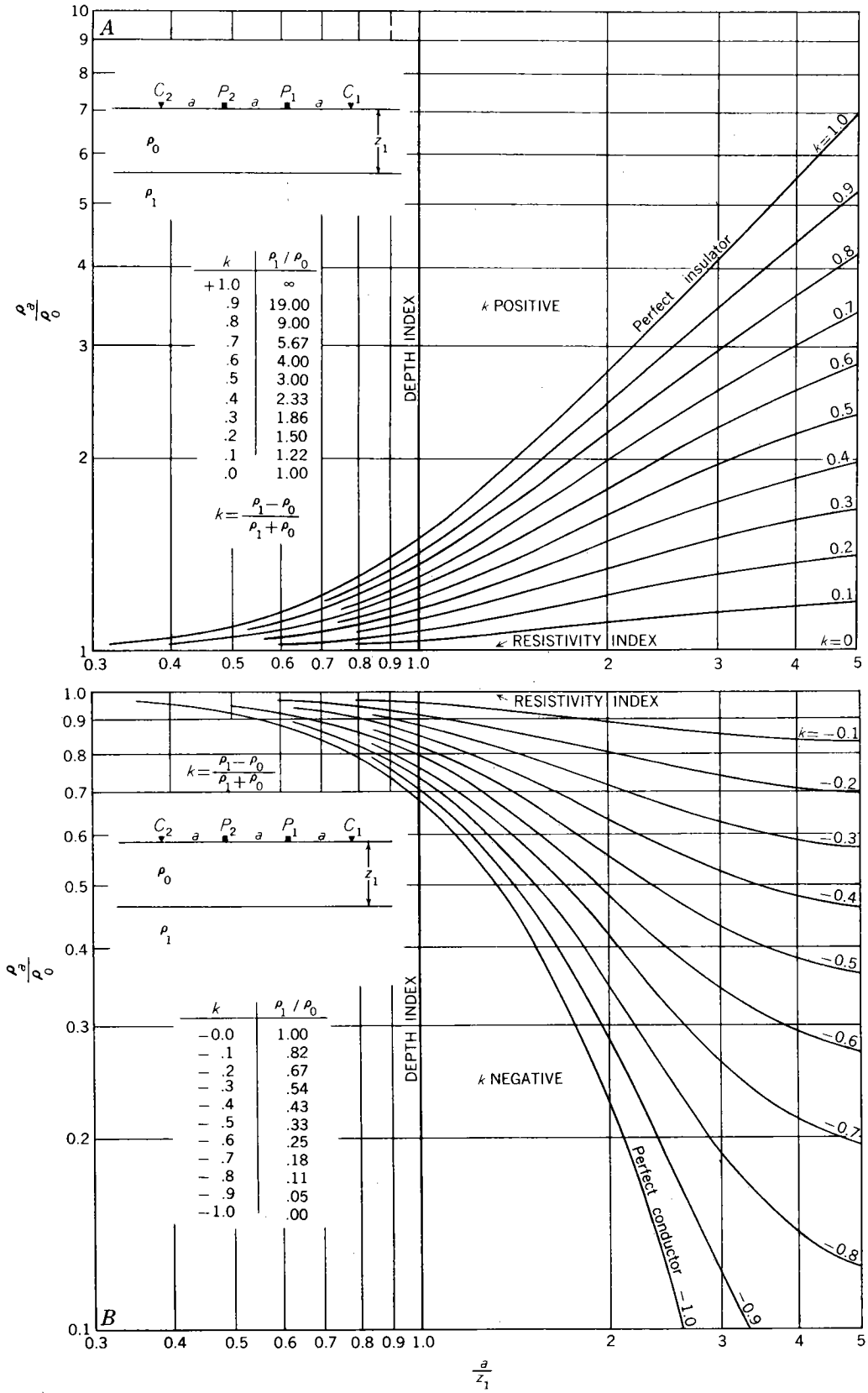

FIGURE 33.—Apparent-resistivity curves for two-layer case, logarithmic plotting. (*A*) Positive and (*B*) negative values, respectively, of reflection factor $k = (\rho_1-\rho_0)/(\rho_1+\rho_0)$ Adapted from Roman (1941).

Figure 3–28. – Apparent resistivity curves

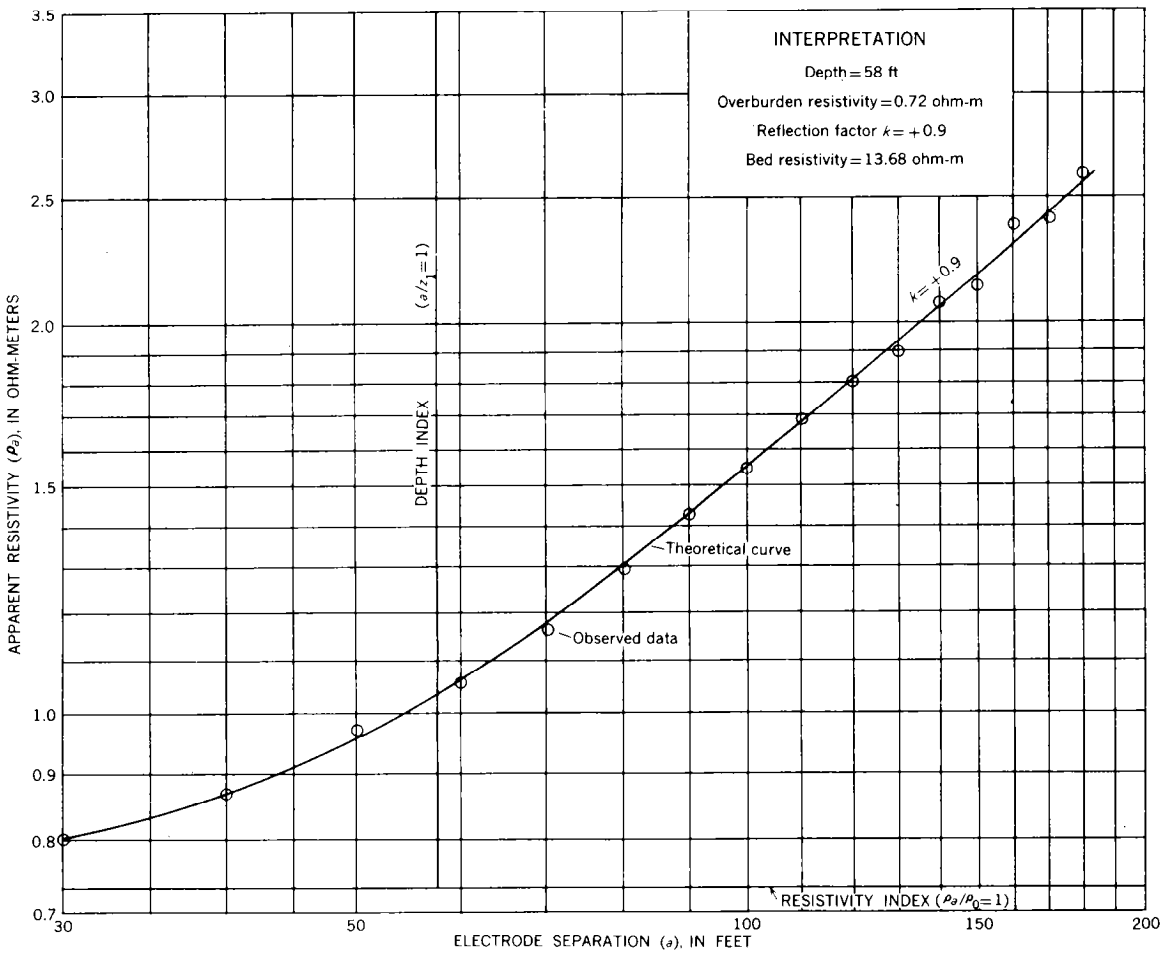

FIGURE 34.—Example of resistivity interpretation by curve matching, two-layer case, logarithmic plotting. Adapted from Irwin Roman (1952, unpublished data).

Figure 3–29. – Curve matching

the master chart representing k=0, which means that $\rho_\alpha/\rho_0 = 1$, and consequently log ρ_α = log ρ_0. The fundamental reason for the validity of superposition in this manner, however, lies in the facts that log (ρ_α/ρ_0) = log ρ_α - log ρ_0 and log (a/z_1) = log a-log z_1 and because both log ρ_0 and log z_1 are constant. Thus the sliding of the master chart up and down, or back and forth to the right and left, does not affect the scale.

3. The depth z_1 to the bottom layer is obtained by noting where the vertical "depth index" line (axis of ordinates) on the master chart intersects the axis of abscissas (values of electrode separation α) on the observed curve. This results from the fact that the depth

index is the line on the master chart representing log $(\alpha/z_1)=0$, which means that $\alpha/z_1=1$ and that, therefore, $\alpha=z_1$. The fact that this electrode separation α is equal to the depth z_1 has nothing to do with the Gish-Rooney empirical rule mentioned earlier.

4. The resistivity ρ_1, of the bottom bed is determined directly from the relationship

$$\rho_1 = \frac{1 + k}{1 - k} \rho_0$$

"In the example shown in figure 34 [Figure 3-29], the values of the factors listed above are given in the diagram.

"Though we recommend curve matching as the best procedure for quantitative resistivity interpretation, there are certain generalizations that assist the interpreter in making a preliminary analysis of observed apparent-resistivity curves for the two-layer case. The fact that larger anomalies are obtained for negative reflection factors than for positive reflection factors (see figure 33[Figure 3-28]) indicates that a bed of better conducting material at depth can be detected more readily than a poorly conducting one, other things being equal. The most valuable generalizations, however, apply to situations in which the resistivity of the bottom bed is assumed to be great, because usually the resistivity does increase with depth. When the bottom bed in the two-layer case is a perfect insulator, the apparent-resistivity curve for a vertical profile gives a limiting straight-line curve which passes through the origin of coordinates (for linear plotting) and which has an inclination $\tan \alpha = 1.386$. A limiting straight line also occurs with logarithmic plotting. For this limiting case the limiting value of the slope will be reached when $\alpha/z_1 = 1.5$; this is also approximately true for other resistivity constrasts that exceed about $\rho_1/\rho_0 = 10{:}1$. This property, which is important also in considering the analysis of three- and four-layer cases discussed later, implies that in a two-layer region in which the bottom bed is ten or more times resistive than the top bed, the configuration will need to be expanded to only about two or three times the suspected depth to obtain the thickness z_1 of the top layer. In

addition, for large values of ρ_1/ρ_0, the apparent resistivity ρ_a is 1.5 times the true resistivity ρ_0 of the upper layer when $a=z_1$, that is, when the electrode separation is equal to the thickness of the top layer. As the true resistivity of the ordinary alluvium is usually much lower than that of the bedrock below it, a valuable indication of the depth of the bedrock can frequently be obtained by this relationship in simple two-layer depth-to-bedrock problems. Of course, this assumes that a determination of ρ_0 can be obtained from the value of the apparent resistivity at small electrode separations.

Multiple-Layer Case

"The three-layer case comprises a top layer of thickness z_1, a middle layer of thickness d, and a bottommost layer at depth z_2 (z_2 is defined by the equation $z_2=z_1+d$) that theoretically extends to infinity (see figure 38 [Figure 3-30]). As there are an infinite number of permutations and combinations of the factors of electrode separations, thicknesses of beds, and resistivity contrasts of the three beds, it is helpful in the analysis of the three-layer problem to first systematize the conventions and practices that will suffice for practical needs and at the same time keep the problem from being unwieldly. Our conventions and reasonings for the three-layer case follow those of Wetzel and McMurry (1937) with some modifications. The thickness z_1 of the top layer is always taken as our unit of length. Except in special cases, the assumed resistivity contrasts will be in ratios of $1/\infty$, 1/100, 1/10, 1/3, 3/1, 10/1, 100/1, and $\infty/1$. There are three main groups of possibilities concerning the resistivity of the middle bed in relation to that of the others; its resistivity may be higher than, lower than, or intermediate between the resistivities of the top and bottommost beds. The assumed thicknesses of the layers are either equal or are simple multiples of each other. Thin beds of thickness less than one unit will not be considered because, for all practical purposes, they will not be detectable in the field unless they are either nearly perfectly conducting or perfectly insulating; and if they are so, they fall into the category of special limiting cases of the three-layer problem that can be recognized from the families of theoretical curves that will be

shown later. It should be emphasized, however, that the presence of undetectable thin beds can still cause erroneous interpretations.

"As in the two-layer case, logarithmic plotting is recommended, because it renders the shape of the curves independent of the field units used and allows the interpreter to become familiar with the curve trends. This is difficult to do if linear plots are used. Provided the three-layer assumption is correct and the beds are homogeneous, a unique solution, is possible, as in the two-layer case; but to obtain a unique solution, the electrode configuration must generally be expanded to much larger electrode separations than for the two-layer case. Great care must also be used in obtaining the apparent resistivity for small electrode separations.

"The best depth determinations that can ordinarily be expected with the resistivity method for the three-layer case is to within an accuracy of only 10 percent. When reference is made to obtaining an "accurate" depth estimate in this paper, the inherent limitation of the method is still implied.

"For the special three-layer cases in which the bottommost bed is either a perfect insulator or perfect conductor, the mathematics is greatly simplified, and the properties are therefore easily obtainable. When the bottommost layer is a perfect insulator, the asymptotic curve for large electrode separations passes through the origin of coordinates (for linear plotting), and its slope is identical to that for the two-layer case in which the bottom layer is a perfect insulator.

"Figure 38 [Figure 3-30] shows the effect on the apparent resistivity of varying ratios of the top-layer thickness z_1 to middle-layer thickness d for the Wenner or Lee configuration (Wetzel and McMurry, 1937). The ratios of resistivities are $\rho_0:\rho_1:\rho_2::1:1/3:1$. The ratio $z_1:d::0:8$ is identical to a two-layer case, and the ratio $z_1:d::8:0$ is the homogeneous case. Because for large separations the slopes of the curves approach that for the two-layer case, it is clear that a family of logarithmic two-layer curves can be used to obtain approximately the

depth z_2 of the bottommost bed. The same is true in this case for the depth z_1.

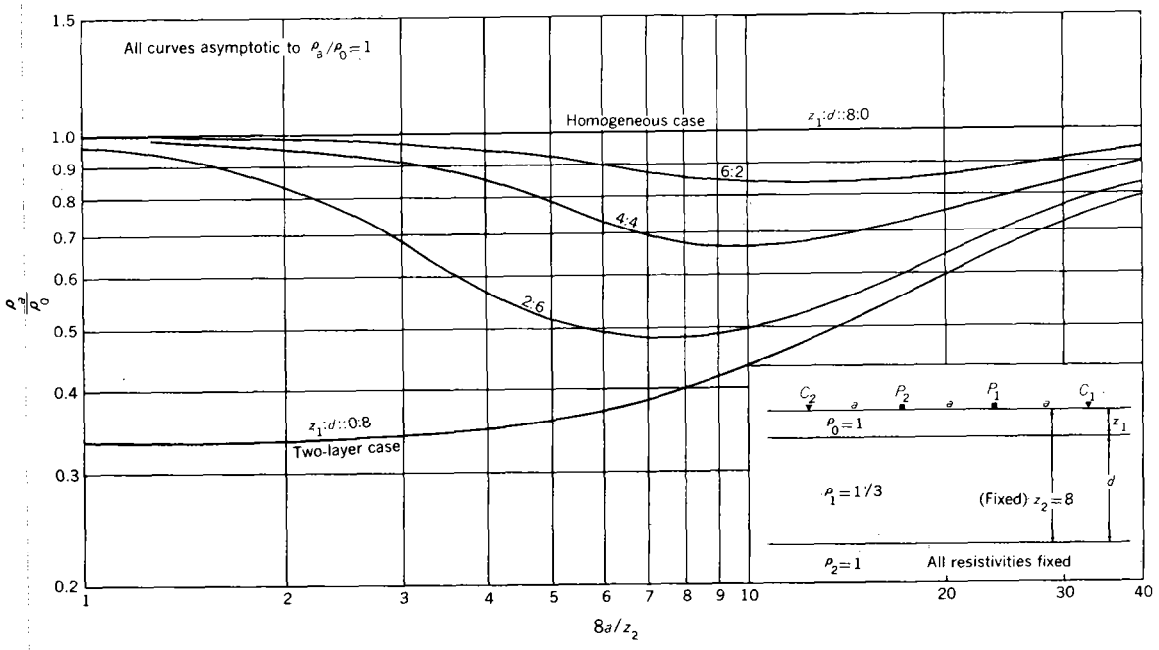

FIGURE 38.—Diagram of three-layer case showing the effect on the apparent resistivity ρ_a of varying ratios of top-layer thickness z_1 to middle-layer thickness d, Wenner or Lee configuration. $\rho_0:\rho_1:\rho_2::1:1/3:1$. Adapted from Wetzel and McMurry (1937).

Figure 3–30. – Three layer case

"Figure 39 [Figure 3-31] shows the effect on the apparent resistivity of varying the resistivity ρ_1 of the middle layer, all other factors remaining constant (Wetzel and McMurry, 1937). The resistivities of the top and bottommost beds are equal, and $z_1:d::3:1$. All curves are asymptotic to the value $\rho_\alpha/\rho_0 = 1$. In this case the logarithmic two-layer curves can be used to obtain approximately the thickness z_1 of the top layer, but they cannot be used to obtain the depth z_2 of the bottommost layer because the curves on the right-hand side of the diagram are not close enough to asymptotic values to allow the two-layer approximation to be applied. [Figure 3-32].

"Figure 40 [Figure 3-32] shows the effect on the apparent resistivity of variations in the resistivity ρ_2 of the bottommost layer, all other factors remaining constant (Wetzel and McMurry, 1937). the fixed resistivities are such that $\rho_1=3\rho_0$, and $z_1:d::1:3$. The curve labeled $\rho_2=3\rho_0$ is for the two-layer case; and it fits the other curves so closely

for abscissa values less than 3 that in this case also the thickness z_1 of the top layer can obviously be obtained approximately from the two-layer logarithmic curves for all resistivity contrasts involved.

"Figure 41 [Figure 3-33] shows the behavior of certain types of resistivity curves by comparing three-layer curve A for $z_1:d::4:4$ with various limiting curves. The resistivities for curve A are $\rho_0:\rho_1:\rho_2::1:10:1/3$; thus the resistivity of the middle layer is greater than that of either the top or bottommost layers, and the resistivity of the bottommost layer is least of all three. Asymptotic curve D is for the two-layer case in which the resistivities of the upper-two layers have been averaged according to Hummel's (1929 c,d) method. Curve A approaches this asymptotic curve for much larger electrode separations than shown in the figure. Within the region of the chart shown, however, this asymptotic value cannot be used as a guide in the analysis of curve A. In this example the logarithmic two-layer curves, therefore, cannot be used to obtain even approximately the depth z_2 to the bottommost layer. An attempt to do so in this example would involve a 400-percent error in the determination of depth z_2.

"The mathematical expression for the apparent resistivity of the three-layer case reduces continuously to the expression for the two-layer case if either z_1 or d is allowed to approach zero. Applying this to our present example in figure 41 [Figure 3-33] curve B is obtained when z_1 approaches zero, and curve C is obtained when d approaches zero. It should be emphasized that the apparent-resistivity curves B and C for the limiting two-layer cases are not enevelopes for the families of three-layer curves similar to curve A, as might normally be expected. In addition, it is possible for members of these multiple-layer resistivity curve families to cross; this fact makes the task of extrapolation of curve families difficult.

"Figure 42 [Figure 3-34] shows an example of the interpretation of a three-layer case by superposition of the logarithmic theoretical (solid lines) and hypothetical observed (dashed line) curves (Wetzel and McMurry,

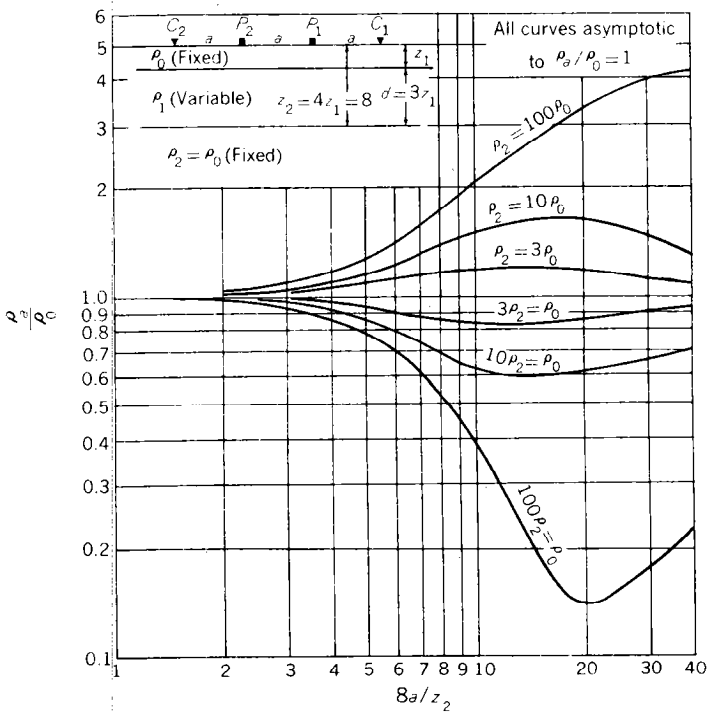

FIGURE 39.—Diagram of three-layer case showing the effect on the apparent resistivity ρ_a of varying resistivity ρ_1 of the middle layer, all other factors remaining constant, Wenner or Lee configuration; $z_1:d::3:1$; $\rho_0=\rho_2=1$. Adapted from Wetzel and McMurry (1937).

Figure 3–31. – Three layer case

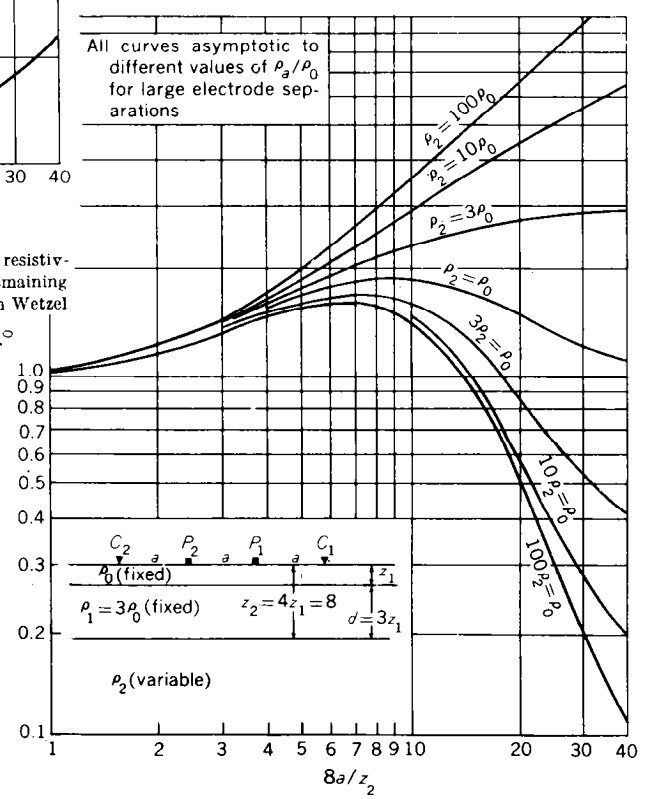

FIGURE 40.—Diagram of three-layer case showing the effect on the apparent resistivity ρ_a of variations in resistivity ρ_2 of bottommost layer, all other factors remaining constant, Wenner or Lee configuration; $z_1:d::1:3$; $\rho_0=1$; $\rho_1=3$. Adapted from Wetzel and McMurry (1937).

Figure 3–32. – Three layer case

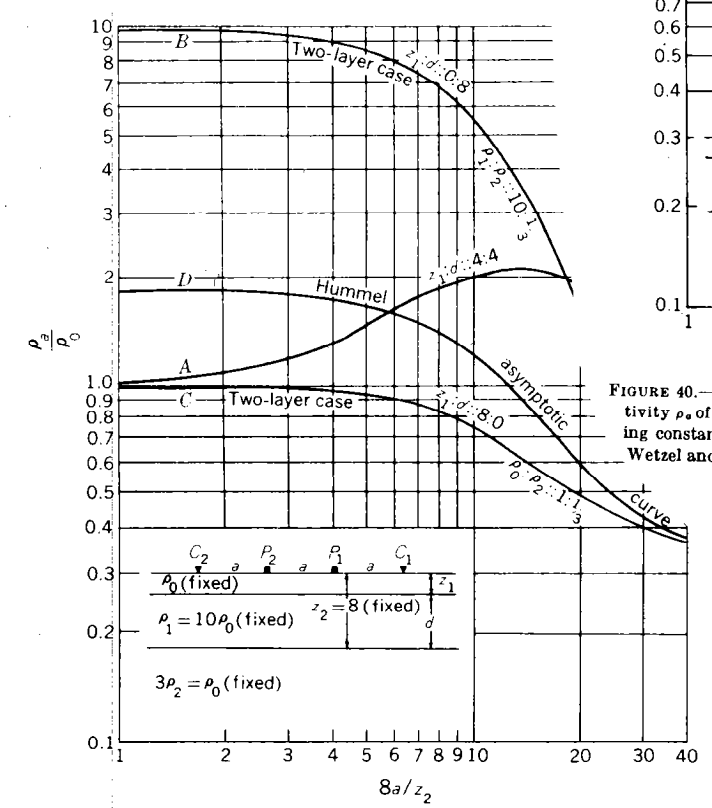

FIGURE 41.—Comparison of three-layer curve A with limiting two-layer curves B and C and Hummel asymptotic curve D (for the top layers only), Wenner or Lee configuration. $\rho_0:\rho_1:\rho_2::1:10:1/3$; various values of $z_1:d$. Adapted from Wetzel and McMurry (1937).

Figure 3–33. – Comparison of three layer and two layer curves

1937). The family of theoretical curves are for fixed resistivities $\rho_0:\rho_1:\rho_2::1:3:10$ and for various values of z_1:d. The "resistivity index" line, which is defined as the axis of abscissas on the theoretical chart for which $\rho_\alpha/\rho_0 = 1$, is extended to the left to intersect the ordinate value of ρ_α on the observed logarithmic chart; this gives the value of ρ_0, which in the present example is 33 ohm-centimeters. The fact that the observed curve matches a theoretical curve in this family, whose theoretical ratio is $\rho_0:\rho_1:\rho_2::1:3:10$ indicates that the field resistivity values are $\rho_0:\rho_1:\rho_2::33:99:330$. The "depth index" line, which is defined in the three-layer case as the electrode separation equal to the depth of the bottommost layer--that is, $\alpha=z_2$--, corresponds in the Wetzel-McMurry charts with the abscissa point $8\alpha/z_2=8$, and is found on the diagram to be z_2 = 330 feet. Finally the z_1:d ratio is read by noting that the field curve lies about halfway between the theoretical curves whose ratios are 2:2 and 1:3; therefore, the z_1:d ratio for the field curve corresponds to about 3:5. Using the relationship $z_2=z_1+d$ and knowing that $z_2=330$ feet, we readily obtain the thickness of the top layer z_1 = 124 feet. The problem is thus completely solved.

"The members of the Schlumberger school have pointed out the advantages of logarithmic curve matching and themselves have used it as a standard procedure for many years for both two- and three-layer problems. During 1933 to 1936 the Schlumberger organization in Paris, la Compagnie Generale de Geophysique, computed an album of 480 master curves for two- and three-layer cases that were recently published (Compagnie Generale de Geophysique, 1955). Figure 43 [Figure 3-35] shows the values of the parameters used in the Schlumberger album and the generalized character of the apparent-resistivity curves in each category with the Schlumberger configuration. The resistivity ρ_2 of the bottommost layer is assumed to have only four separate values, namely, $\rho_2=0, \rho_0, \rho_1/\rho_0$, and ∞."

"The four-layer case comprises a top layer of thickness z_1 and resistivity ρ_0 and two successively deeper layers of respective thickness d_1 and d_2 whose bottoms lie at successive depths of z_2 and z_3, respectively, below the earth's surface [Figure 3-36]. The bottommost layer, at depth z_3, is assumed to extend to great depth.

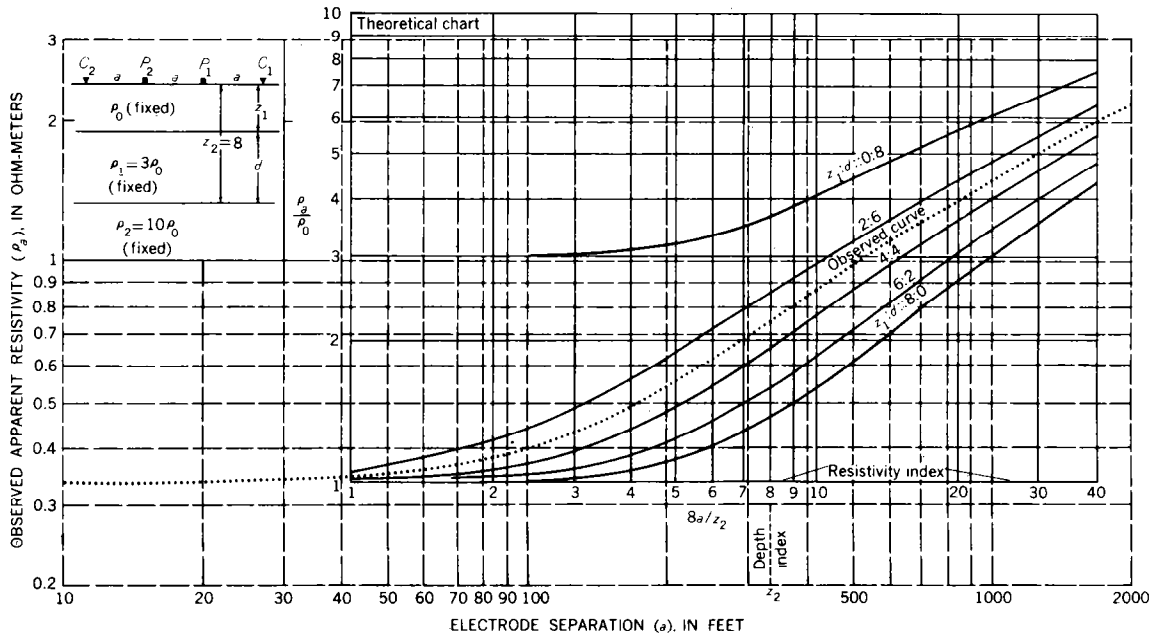

FIGURE 42.—Example of interpretation of three-layer case by superposition of logarithmic theoretical (solid lines) and hypothetical observed (dashed line) curves, Wenner or Lee configuration. $\rho_0:\rho_1:\rho_2::1:3:10$; various values of $z_1:d$; $z_2=8$ units (depth index). Adapted from Wetzel and McMurry (1937).

Figure 3–34. – Interpretation of three layer case by superposition

At the outstart, we repeat our contention that, except for ideal and very rare field problems, lateral variations interfere too much for the four-layer case analysis to be applied with much degree of certainty."

Tables 3-9 and 3-10 are from Roman (1960,pp. 10-11) and furnish the data to plot the two-layer theoretical curves discussed by Van Nostrand and Cook (1966) above.

Cost Data

The cost of electrical resistivity surveys is composed of several parts. They are: the instrument, travel, survey line, correlation test holes and interpretation, and preparation of a report.

The cost of the various types of resistivity instruments has been discussed in a previous section of this TR. Travel expenses depend on location, distance from headquarters, etc., and have to be evaluated separately for each site.

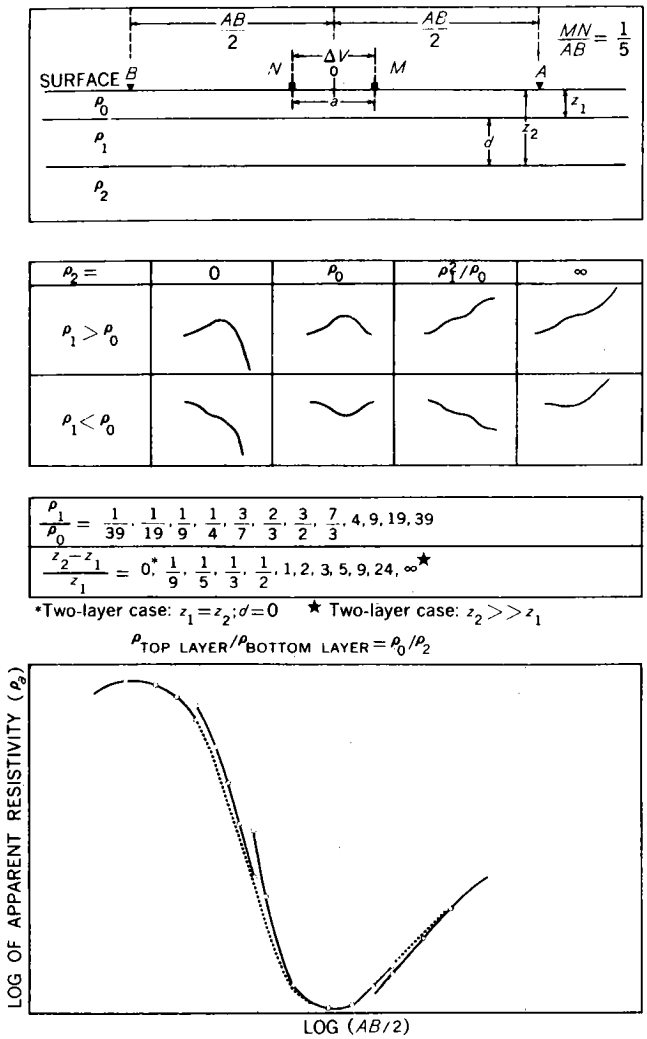

FIGURE 43.—Diagram showing values of parameters used in the Schlumberger album of 480 master two- and three-layer curves and the generalized character of the apparent-resistivity curves in each category for vertical profiles, Schlumberger configuration. Adapted from Compagnie Générale de Géophysique (1955).

Figure 3–35. — Examples of Schlumberger curves

Actual field survey time for a two man crew using Wenner configuration, three foot electrode increments for vertical profiling to a depth of 30 feet would on the average take about 1/2 hour for each survey point. Considering time to pick up electrodes, wire, instruments, etc., to move to next survey point, an average of three spreads every two hours would be good. If site conditions are difficult, for example, steep topography, very wooded, rocky soils, or dry soils that have to be moistened at each electrode considerable more field time could be required for each set up.

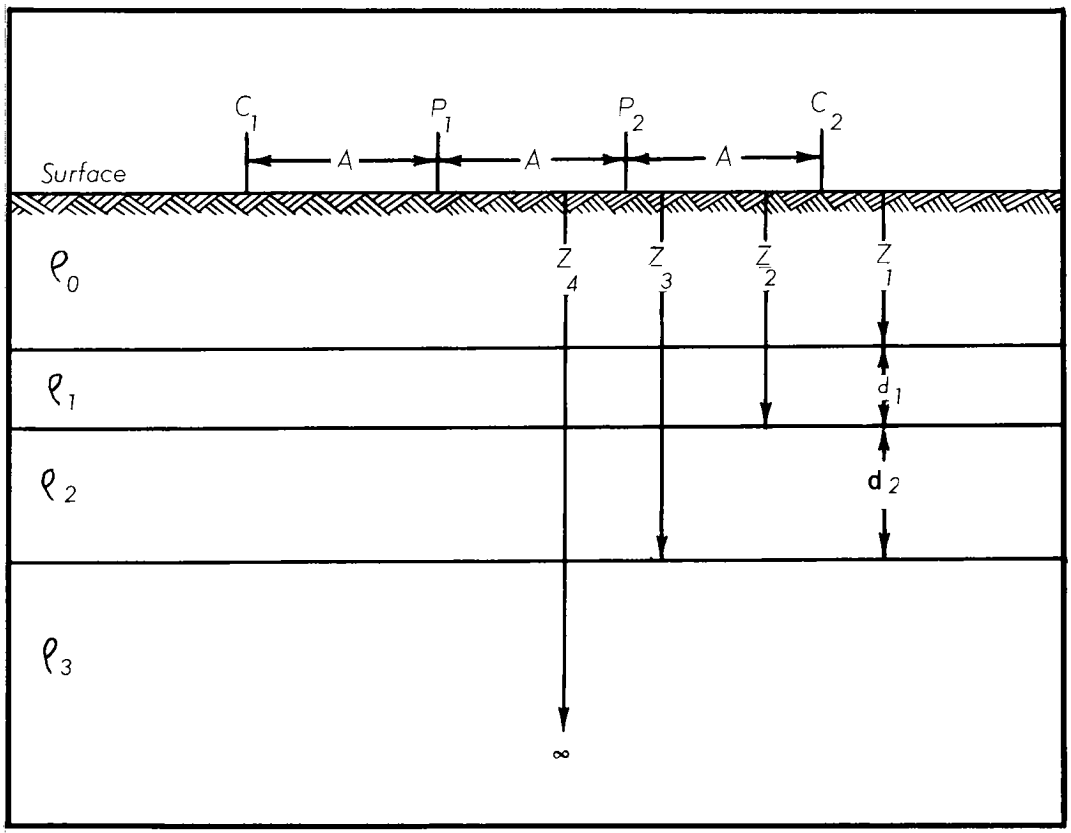

Figure 3-36. – Four layer case

Correlation test holes are required at every site to enable valid interpretations to be made. These test holes can be hand auger holes, test pits, power auger, or core holes depending on site conditions and equipment available.

Interpretation of the field data and preparation of the report of investigation require about 1/2 the man days that the field investigation required. If the geologist and one helper spend one week in the field gathering the data, it will require about one week of the geologist's time to make the computations, interpretations and prepare the report.

Table 3-9 - Disturbing factor, Wenner or Lee configuration, buried conductor (From Roman, 1960)

l/h	Disturbing factor for indicated values of Q									
	−0.1	−0.2	−0.3	−0.4	−0.5	−0.6	−0.7	−0.8	−0.9	−1.0
0.2	(*)	(*)	(*)	(*)	(*)	(*)	(*)	(*)	(*)	0. 9948
0.4	(*)	(*)	(*)	(*)	0. 9804	(*)	(*)	(*)	(*)	. 9629
0.6	(*)	(*)	0. 9654	(*)	. 9439	(*)	(*)	0. 9134	(*)	. 8942
0.8	0. 9768	0. 9543	. 9326	0. 9114	. 8909	0. 8710	0. 8516	. 8326	0. 8141	. 7960
1.0	. 9633	. 9279	. 8938	. 8609	. 8290	. 7981	. 7682	. 7391	. 7108	. 6833
1.2	. 9490	. 9002	. 8534	. 8084	. 7650	. 7233	. 6829	. 6439	. 6061	. 5696
1.4	. 9350	. 8732	. 8142	. 7579	. 7039	. 6522	. 6024	. 5546	. 5085	. 4640
1.6	. 9220	. 8482	. 7783	. 7118	. 6485	. 5881	. 5304	. 4751	. 4222	. 3714
1.8	. 9101	. 8257	. 7462	. 6711	. 5999	. 5324	. 4682	. 4071	. 3488	. 2932
2.0	. 8996	. 8059	. 7182	. 6358	. 5582	. 4850	. 4157	. 3502	. 2880	. 2289
2.2	. 8904	. 7887	. 6940	. 6056	. 5229	. 4452	. 3723	. 3036	. 2387	. 1773
2.4	. 8823	. 7738	. 6734	. 5801	. 4934	. 4124	. 3367	. 2657	. 1991	. 1364
2.6	. 8753	. 7610	. 6558	. 5587	. 4689	. 3854	. 3078	. 2354	. 1677	. 1044
3.0	. 8639	. 7406	. 6283	. 5256	. 4316	. 3452	. 2655	. 1918	. 1236	. 0604
3.2	. 8593	. 7324	. 6175	. 5130	. 4176	. 3304	. 2503	. 1766	. 1085	. 0457
3.6	. 8519	. 7195	. 6005	. 4934	. 3965	. 3083	. 2282	. 1548	. 0876	. 0259
4.0	. 8461	. 7097	. 5882	. 4794	. 3817	. 2935	. 2136	. 1412	. 0751	. 0146
4.4	. 8416	. 7022	. 5790	. 4693	. 3712	. 2833	. 2041	. 1323	. 0674	. 0082
5	. 8366	. 6941	. 5691	. 4587	. 3607	. 2733	. 1950	. 1245	. 0610	. 0034
6	. 8311	. 6856	. 5590	. 4483	. 3508	. 2644	. 1874	. 1186	. 0567	. 0008
7	. 8278	. 6804	. 5532	. 4425	. 3455	. 2598	. 1838	. 1159	. 0550	. 0002
8	. 8255	. 6771	. 5496	. 4390	. 3423	. 2572	. 1818	. 1146	. 0543	. 0000
9	. 8240	. 6749	. 5471	. 4366	. 3402	. 2555	. 1805	. 1137	. 0539	. 0000
10	. 8229	. 6733	. 5454	. 4350	. 3388	. 2544	. 1797	. 1132	. 0536	. 0000
12	. 8215	. 6712	. 5432	. 4330	. 3371	. 2530	. 1787	. 1125	. 0533	. 0000
14	. 8206	. 6700	. 5419	. 4318	. 3361	. 2522	. 1781	. 1121	. 0531	. 0000
16	. 8200	. 6692	. 5411	. 4310	. 3354	. 2516	. 1777	. 1119	. 0530	. 0000
18	. 8196	. 6687	. 5406	. 4305	. 3350	. 2513	. 1774	. 1117	. 0529	. 0000
20	. 8194	. 6683	. 5402	. 4301	. 3346	. 2510	. 1772	. 1116	. 0529	. 0000
22	. 8192	. 6680	. 5399	. 4298	. 3344	. 2509	. 1771	. 1115	. 0528	. 0000
24	. 8190	. 6678	. 5396	. 4296	. 3342	. 2507	. 1770	. 1114	. 0528	. 0000
26	. 8189	. 6676	. 5395	. 4295	. 3341	. 2506	. 1769	. 1114	. 0528	. 0000
30	. 8187	. 6674	. 5392	. 4293	. 3339	. 2505	. 1768	. 1113	. 0527	. 0000
50	. 8184	. 6669	. 5387	. 4288	. 3335	. 2502	. 1766	. 1112	. 0527	. 0000
100	. 8182	. 6667	. 5385	. 4286	. 3334	. 2500	. 1765	. 1111	. 0526	. 0000
∞	. 8182	. 6667	. 5385	. 4286	. 3333	. 2500	. 1765	. 1111	. 0526	. 0000

Table 3-10.- Disturbing factor, Wenner or Lee configuration, buried insulator
(From Roman 1960)

l	Disturbing factor for indicated values of Q									
	+0.1	+0.2	+0.3	+0.4	+0.5	+0.6	+0.7	+0.8	+0.9	+1.0
0.2	(*)	(*)	(*)	(*)	(*)	(*)	(*)	(*)	(*)	1. 0070
0.4	(*)	(*)	(*)	(*)	1. 0226	(*)	(*)	(*)	(*)	1. 0511
0.6	(*)	(*)	1. 0380	(*)	1. 0658	(*)	(*)	1. 1131	(*)	1. 1512
0.8	1. 0241	1. 0490	1. 0750	1. 1022	1. 1307	1. 1607	1. 1926	1. 2268	1. 2640	1. 3062
1.0	1. 0383	1. 0782	1. 1200	1. 1639	1. 2104	1. 2596	1. 3123	1. 3694	1. 4322	1. 5044
1.2	1. 0534	1. 1095	1. 1686	1. 2312	1. 2977	1. 3689	1. 4458	1. 5298	1. 6235	1. 7329
1.4	1. 0685	1. 1408	1. 2176	1. 2995	1. 3872	1. 4819	1. 5851	1. 6991	1. 8278	1. 9810
1.6	1. 0828	1. 1708	1. 2649	1. 3660	1. 4753	1. 5942	1. 7251	1. 8713	2. 0385	2. 2410
1.8	1. 0959	1. 1987	1. 3094	1. 4292	1. 5597	1. 7031	1. 8624	2. 0424	2. 2510	2. 5083
2.0	1. 1078	1. 2243	1. 3505	1. 4883	1. 6395	1. 8072	1. 9954	2. 2103	2. 4627	2. 7799
2.2	1. 1186	1. 2475	1. 3882	1. 5429	1. 7143	1. 9059	2. 1230	2. 3737	2. 6721	3. 0540
2.4	1. 1281	1. 2683	1. 4225	1. 5932	1. 7838	1. 9989	2. 2450	2. 5321	2. 8782	3. 3294
2.6	1. 1367	1. 2871	1. 4536	1. 6395	1. 8486	2. 0865	2. 3613	2. 6852	3. 0808	3. 6056
3.0	1. 1508	1. 3190	1. 5077	1. 7210	1. 9646	2. 2462	2. 5772	2. 9757	3. 4743	4. 1593
3.2	1. 1567	1. 3325	1. 5309	1. 7567	2. 0164	2. 3189	2. 6776	3. 1133	3. 6653	4. 4364
3.6	1. 1668	1. 3558	1. 5715	1. 8200	2. 1096	2. 4518	2. 8640	3. 3746	4. 0360	4. 9907
4.0	1. 1748	1. 3747	1. 6053	1. 8737	2. 1905	2. 5698	3. 0338	3. 6184	4. 3922	5. 5452
4.4	1. 1813	1. 3903	1. 6336	1. 9199	2. 2613	2. 6751	3. 1886	3. 8464	4. 7348	6. 0997
5	1. 1888	1. 4091	1. 6683	1. 9775	2. 3517	2. 8130	3. 3965	4. 1614	5. 2250	6. 9315
6	1. 1976	1. 4313	1. 7110	2. 0506	2. 4702	3. 0003	3. 6898	4. 6252	5. 9839	8. 3177
7	1. 2034	1. 4465	1. 7411	2. 1039	2. 5599	3. 1475	3. 9306	5. 0251	6. 6787	9. 7041
8	1. 2074	1. 4573	1. 7630	2. 1439	2. 6292	3. 2653	4. 1308	5. 3728	7. 3171	11. 090
9	1. 2103	1. 4652	1. 7794	2. 1745	2. 6838	3. 3609	4. 2990	5. 6771	7. 9055	12. 477
10	1. 2124	1. 4711	1. 7919	2. 1985	2. 7275	3. 4396	4. 4418	5. 9452	8. 4495	13. 863
12	1. 2153	1. 4792	1. 8095	2. 2329	2. 7922	3. 5599	4. 6691	6. 3941	9. 4421	16. 636
14	1. 2170	1. 4844	1. 8210	2. 2559	2. 8369	3. 6463	4. 8402	6. 7527	10. 265	19. 408
16	1. 2182	1. 4879	1. 8288	2. 2720	2. 8688	3. 7101	4. 9720	7. 0439	11. 002	22. 181
18	1. 2190	1. 4903	1. 8343	2. 2836	2. 8924	3. 7586	5. 0754	7. 2834	11. 650	24. 953
20	1. 2196	1. 4921	1. 8384	2. 2923	2. 9103	3. 7961	5. 1580	7. 4827	12. 223	27. 726
22	1. 2201	1. 4934	1. 8415	2. 2989	2. 9242	3. 8257	5. 2250	7. 6502	12. 732	30. 498
24	1. 2204	1. 4944	1. 8439	2. 3040	2. 9351	3. 8495	5. 2800	7. 7923	13. 187	33. 271
26	1. 2207	1. 4952	1. 8458	2. 3081	2. 9439	3. 8688	5. 3254	7. 9138	13. 596	36. 044
30	1. 2211	1. 4964	1. 8486	2. 3141	2. 9569	3. 8980	5. 3959	8. 1091	14. 296	41. 589
50	1. 2218	1. 4987	1. 8540	2. 3262	2. 9837	3. 9602	5. 5554	8. 5961	16. 387	69. 315
100	1. 2221	1. 4997	1. 8563	2. 3315	2. 9958	3. 9897	5. 6367	8. 8825	18. 060	138. 63
∞	1. 2222	1. 5000	1. 8571	2. 3333	3. 0000	4. 0000	5. 6667	9. 0000	19. 000	∞

TECHNICAL RELEASE

NUMBER 44

SEISMIC AND RESISTIVITY METHODS OF GEOPHYSICAL EXPLORATION

CHAPTER 4. COMPLEMENTARY USAGE AND GEOPHYSICAL REPORTS

Contents

Figures

CHAPTER 4. COMPLEMENTARY USAGE AND GEOPHYSICAL REPORTS

A knowledge of the structural, lithologic, geomorphic, and ground water conditions in the study area is of prime importance for seismic and resistivity surveys. Drill hole logs, deep quarries, road cuts, or gullies are needed for checking and correlating the seismic or resistivity characteristics of the soil and rock horizons in the vicinity. Hand augering may be used to verify types of materials and depths to rock, water table, or gravel beds. Difficulties in interpretation may be expected in areas with steeply dipping rocks, sink holes, caverns, and faults. Abnormal velocities and resistivities are good indicators of these conditions. The ability to locate these problems may be valuable in selecting the exact locations where drilling is needed, and they may be good indicators of construction problems requiring further intensive studies.

Both the seismic and resistivity methods have limitations in field application. Fortunately, these methods often supplement each other, and where one method gives uncertain results the other may verify or correct it. Areas with high noise, or vibrations from traffic, planes, or wind may make data from the seismograph questionable. However, in instruments with cathode ray tubes or recorders, the interferences often can be identified and ignored. Resistivity equipment may get the desired information, or if a seismic correlation is needed, a quiet day may be selected later for a recheck.

Two or three layers with distinct increases in density will give excellent results in depth and velocity determinations with the seismograph. However, a low velocity layer underneath a higher velocity layer cannot be detected with the refraction seismograph but can sometimes be detected by resistivity methods.

Examples of some materials which may cause difficulty in interpretation are:

	Resistivity	Seismic (P wave) Velocity
dry gravel	high	low
dense rock	high	high
pure water	high	medium
saline water	very low	medium
dry compact boulders and cobbles	very high	moderately high
saturated boulders and cobbles	moderate	moderately high

From these few examples it is obvious that (1) moisture content usually makes a difference both in resistivity and velocity, except in massive rock; (2) most dry materials (soil and rock) usually have high resistivity, but the velocities may vary extremely; (3) the purity or salinity of water will give extreme differences in resistivity, but will have little effect on velocity. It is therefore advisable to use both kinds of equipment where there is some doubt as to the results obtained with one or the other. This is especially true if greater accuracy is needed or if reliable information is required in areas not accessible to power drilling equipment. Figure 4-1 is an example of a summary form for comparing results of resistivity and seismic surveys.

It should be kept in mind that one type of equipment or a single survey will not always give conclusive answers to geologic problems in soils and rocks. The investigator must know what he is looking for, the capabilities of the equipment, and the general geology of the area. He should make some correlation tests on logged drill holes if available or nearby deep cuts where profiles of the soils and rocks are exposed.

A knowledge of the soils, rocks, and ground water is essential to properly interpret geophysical data. This is especially true for premliminary exploration in areas where requirements, time, and cost limit the use of large exploration equipment. Geophysical surveys are a valuable supplement to detailed drilling investigations by spacing drill holes farther apart and filling in between with geophysical surveys.

SEISMIC AND RESISTIVITY TEST SUMMARY

Location _____ State _____ Date _____

Geology of Area _____

Subsurface Conditions _____

Depth (Ft)	Type of Material	Resistivity (1000's ohms/cu.cm.)	Seismic Velocity (Ft./sec.)

Interpretation of Seismic (SM) and Resistivity (RN) Data

Remarks

Signature _____

Figure 4–1. – Sample summary form

In preliminary investigations for dam sites or channel relocations the geologist, having become acquainted with the area, can gain valuable and probably adequate information on the presence, depth, and hardness of rock, the depth to ground water, and whether or not unusual geologic problems exist. A seismograph or resistivity meter may indicate whether adequate borrow material is available near a dam site. Also short-cut methods may be used to determine whether hard rock occurs within the limits of proposed channels and emergency spillways.

The depth to ground water often may be determined if the geologist knows that pervious soils exist in the horizon that may include the water table. Gravel beds and sometimes buried channels may often be detected with geophysical instruments. Both the seismograph and resistivity equipment should be used to obtain more reliable results where there is is any doubt in proper interpretations.

In case geophysical surveys do not give conclusive results, its use will help to locate accurately any abnormalities which should be investigated in greater detail by drilling or excavating deep pits. Faults, buried sinkholes, buried channels, gravel beds, and ground water often may be located where a normal drilling program might not find some of these conditions.

To summarize, it should be emphasized that resistivity and seismic methods of subsurface exploration cannot logically be compared. Earth resistivity is based on the contrasts and comparisons of electrical resistances in various soil, gravel, and rock materials. On the other hand, the seismic method is based on the contrasts and comparisons of the transmission velocities of percussion waves through various soil and rock materials. Consequently, the seismic and resistivity methods can not be substituted for one another for conclusive data. It should be considered that one supplements the other. When geophysical data are calibrated to proven test data, considerable savings in time, costs, detailed investigations, and testing will result.

Contracting for Geophysical Surveys

Where there is a need for extensive geophysical surveying and SCS personnel and equipment are not available, arrangements may be made for contracting this work to a consulting firm. Some contracts have shown that a considerable saving in expense and much useful information have been gained by contracting this work. The consultants usually require a few logged drill holes on the site for correlation purposes, and this provides a good check for the accuracy of the survey.

Geophysical Report

A report will be prepared on the results of the geophysical investigation. The report must set forth clearly the methods of investigation and the information obtained. Include copies of plans, profiles, time-distance graphs, logs of any test holes, etc. A section of the report will contain interpretations, recommendations, and conclusions. Figure 4-2 is an example of a plan view showing the location of seismic and resistivity lines. Figure 4-3 is a profile showing how seismic and resistivity information is plotted.

The purpose of a report is to inform the reader. To do this three things must be fulfilled (Sypherd, et al., 1943, p. 226).

"1. Ascertain the necessary facts.
2. Digest these facts and draw the correct conclusions. . .
3. Present these conclusions so clearly and concisely that they can be grasped without effort or delay."

Outline for Geophysical Investigation Report

This outline may be modified as necessary and only those items that are pertinent to the investigation and report should be used.

I. Summary
II. Introduction
    A. Name of watershed or area

B. Purpose of investigation

C. Scope of investigation

D. Previous studies or investigations (include plans and profiles) also logs of any test holes and show locations

III.. Geology and Basic Data of Study Area and Source

IV. Method of Investigation

A. Personnel

B. Equipment (be specific - e.g. brand name and model)

C. Procedures and techniques (outline in detail) such as Lee Wenner etc., phone spacings, shot depths, type of energy. etc.)

D. Costs

E. Weather (an important factor in considering subsurface readings)

V. Interpretations and Conclusions

VI. Recommendations

VII. Date and signatures of persons making the survey

VIII. Attachments

A. Geologic maps

B. Profiles, cross-sections, and other diagrams

C. Time-Distance graphs and computations.

D. Logs of test holes and results of field tests

E. Plan map showing location and extent of all geophysical tests.

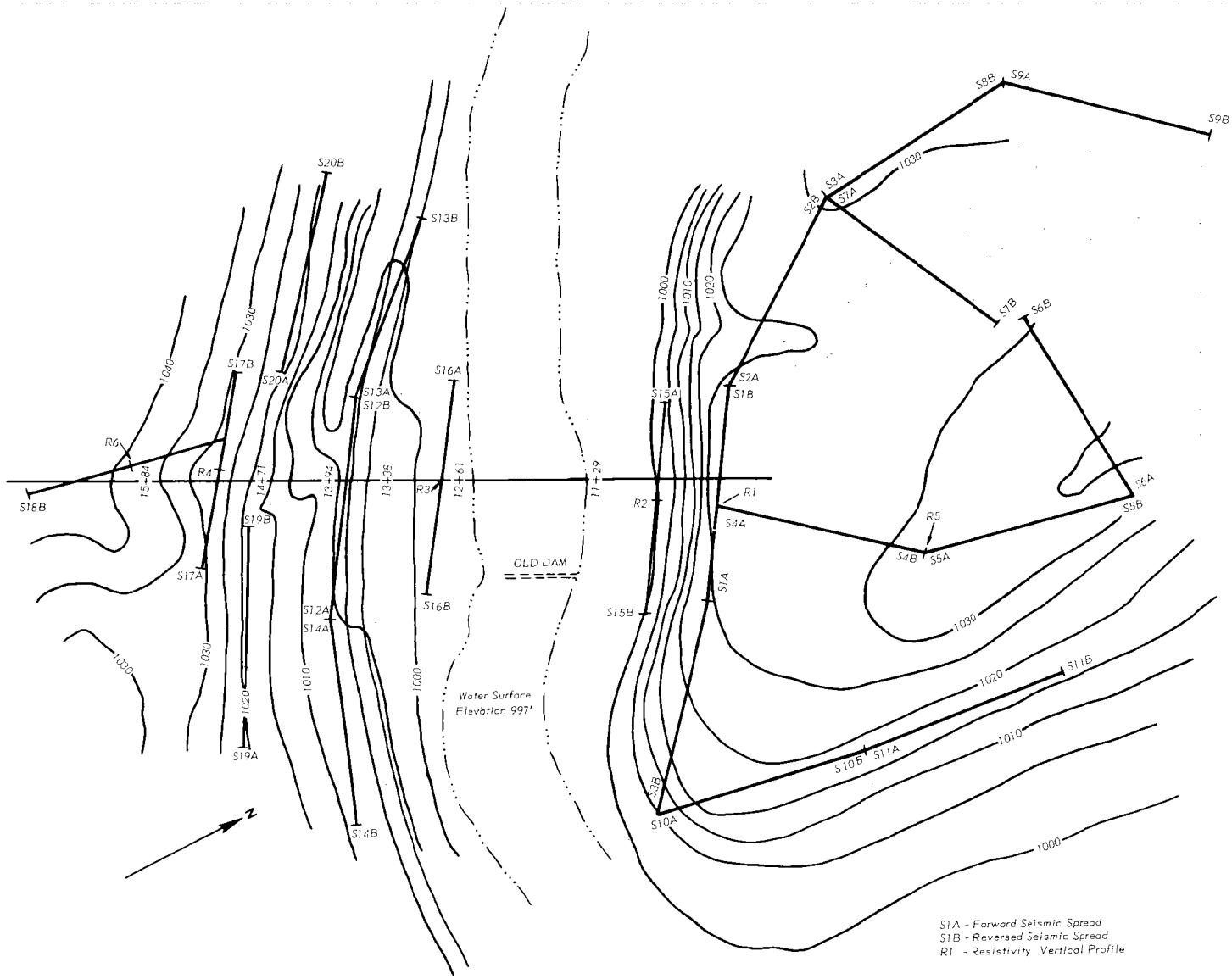

Figure 4-2. – Example of a plan view showing location of seismic and resistivity measurements

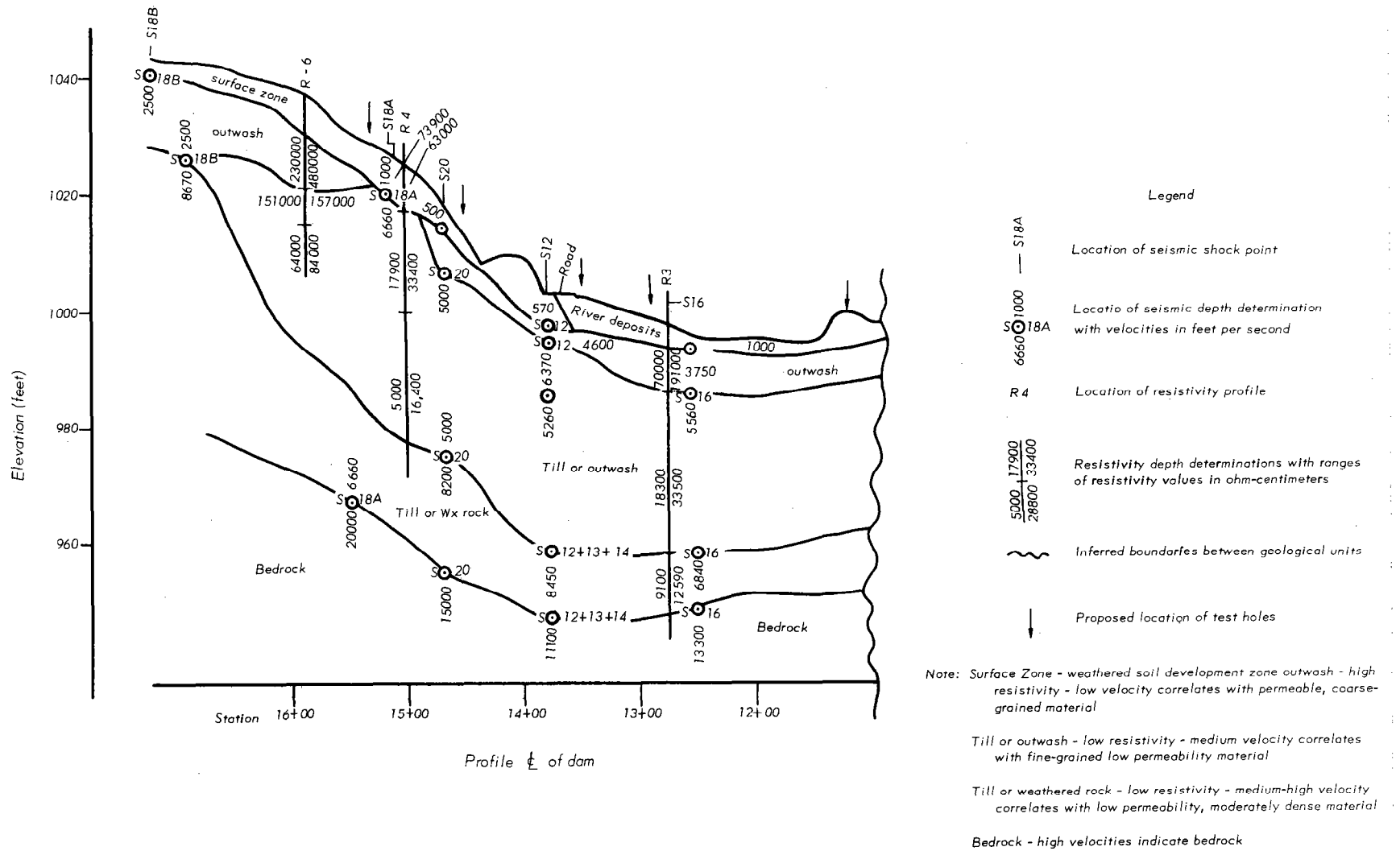

Figure 4-3. — Example of a profile constructed using seismic and resistivity information

REFERENCES

American Society for Testing Materials
1916 Race Street
Philadelphia, Pa. 19103

Symposium on Surface and Subsurface Reconnaissance, STP No. 122, 1951, 228 p.

Symposium on Dynamic Testing of Soils, STP No. 156, 1953, 261 p.

Barnes, H. E., 1952. Soil Investigation Employing a New Method of Layer-Value Determination for Earth Resistivity Interpretation. Highway Research Bulletin 65, pp. 25-36.

Belcher, Cuykendall, and Sack, 1950. The Measurement of Soil Moisture and Density by Neutron and Gamma-Ray Scattering. CAA Tech. Dev. Report 127.

Birch, F., J. F. Schairer, and H. C. Spicer (eds.), 1942, Handbook of Physical Constants: Geol. Soc. Am. sp. Papers No. 36.

Burroughs, E. R., Hughes, Hicks, and Haupt, 1965. Geophysical Exploration in Watershed Studies. Journal Soil and Water Conservation, January - February 1965. pp. 3-7.

Criner, J. H., 1966. Seismic Surveying With Firecrackers. U. S. Geological Survey Professional Paper 550-B, pp. 104-107.

Compagnie Generale de Geophysique, La, 1955, Abaques de sondage electrique [Curves of electric profiling]; Geophys. Prosp., v. 3, supp. no. 3, 7 p. Many charts for three-layer case with explanation of Schlumberger configuration.

Currier, L. W., "The Seismic Method in Subsurface Exploration of Highway and Foundation Sites in Massachusetts," Geol. Sur. Cir. 426, 1960, 8 p.

Denham, D., "The Use of Geophone Groups to Improve the Signal-to-Noise Ratio of the First Arrival in Refraction Shooting", Geoph. Prosp., 1963, p. 389.

Dix, C. H., Refraction and Reflection of Seismic Waves II - Discussion of the Physics of Refraction Prospecting," Geoph., 1939, p. 238.

Dobrin, M. B., 1960. Introduction to Geophysical Prospecting. McGraw-Hill, New York.

Dobrin, M. B. and Dunlap, H. F. 1957. Geophysical Research and Progress in Exploration. Geophysics, Vol. 22, pp. 412-433.

Domzalski, W., "Some Problems of Shallow Refraction Investigations," Geoph. Prosp., 1956, p. 140.

Donato, R. J., "Measurements on the Arrival Refracted from a Thin, High-Speed Layer, Geoph. Prosp., 1965, p. 387.

Drake, C. L., "Geophysics, GEOPHYSICS, and Engineering." Geoph., vol. 27, April 1962, pp. 193-197.

DuPont, 1967. Blasters' Handbook. Fifteenth Edition. E. I. DuPont de Nemours and Co., Wilmington, Delaware, 19898.

Dyna Metric, Inc., 330 W. Holly St., Pasadena, California, 91103 Instruction manuals for the operation and interpretation of their siesmic timers.

Electro-Technical Labs., Division of Mandrel Industries, 6909 Southwest Freeway, P. O. Box 36306, Houston, Texas, 77036 A manual entitled: The Refraction Method of Seismic Prospecting.

Gish, O.H., and Rooney, W. J., 1925, Measurements of Resistivity of Large Masses of Undisturbed Earth; Terrestrial Magnetism Atmos. Electricity, v. 30, pp. 161-188 Resistivity.

Goguel, J. M., "Seismic Refraction with Variable Velocity," Geoph., 1951, p. 81

Green, R., "The Hidden Layer Problem," Geoph. Prosp., 1962, p. 166.

Hagedoorn, J. G., "The Elusive First Arrival (Refraction Signal-to-Noise), Geoph. 1964, p. 806.

Hawkins, L. V., "The Reciprocal Method of Routine Shallow Seismic Refraction Investigations, Geoph., 1961, p. 806. (Discussion and Reply in Geoph., 1962, p. 534.)

Heilbig. K., "Refraction Seismics with an Anisotropic Overburden - A Graphical Method of Interpretation," Geophys. Prosp., 1964, p. 383.

Hubbert, M. King, 1934. Locations of Faults in Hardin County, Illinois, by Earth Resistivity Method. Transactions, American Inst. of Mining and Metallurgical Engineers, Vol. 110, 1934.

Hughes, D. S., and Kelly, J. L., 1952. Variation of Elastic Wave Velocity With Saturation in Sandstone. Geophysics, Vol. 17, pp. 739-752.

Huntec Limited, 1450 O'Connor Drive, Toronto 16, Ontario, Canada, Instruction manuals for the use of the Huntec seismographs, including "Dynamic Testing of Soil With the Seismic Method" by Tsvi Meidav, and "On the Hammer Seismograph Model FS-2 and its Use in Finland" by Stig Johansson.

Institute of Makers of Explosives. Pamphlet 17 Safety in the Handling of Explosives, and Pamphlet 20, Radio Frequency Energy.

Jones, R., "Non-Destructive Dynamic Testing of Soils and Highway Pavements," Highway Res. Board Bull. 277, Wash., D.C., 1960.

Kisslinger, C., E. J. Mateker and T. V. McEvilly, "SH Motion from Explosions in Soil," Jour. Geoph. Res., vol. 66, 1961, pp. 3487-3496.

Knox, W. A., "A Slide Rule for Near-Surface Refraction Problems," Geoph., 1958, p. 154.

Krynine, D. P., and W. R. Judd, 1957. Principles of Engineering Geology and Geotechnics. McGraw-Hill, New York. pp. 259-268.

Lennox, D. H. and V. Carlson, 1967. Geophysical Exploration for Buried Valleys in an Area North of Two Hills, Alberta. Geophysics, Vol. 32, No. 2, pp. 331-362.

Linehan, S. J., D. and V. J. Murphy, "Engineering Seismology Applications in Metropolitan Areas," Geoph., vol. 27, April 1962, pp. 213-220.

McDonal, F. J., F. A. Angona and R. L. Mills, "Attention of Shear and Compressional Waves in Pierre Shale," Geoph., 1958, p. 421.

McGuinness, W. T., W. C. Beckman, and C. B. Officer, "The Application of Various Geophysical Techniques to Specialized Engineering Projects," Geoph., vol. 27, April, 1962. pp. 221-236.

Meidav, T., "Nomograms to Speed Up Seismic Refraction Computations," Geoph., 1960, p. 1035. (Correction in Geoph., 1961, p. 102.)

Meidav, Tsvi, 1960. An Electrical Resistivity Survey for Ground Water. Geophysics, 25(5), pp. 1077-1093.

Meidav, Tsvi, (About 1966). Dynamic Testing of Soil With the Seismic Method. A 20-page reprint available from Huntec, Ltd., Toronto, Canada.

Mooney, H. M. and R. A. Kaasu, "Air Waves in Engineering Seismology," Geoph. Prosp., 1962, p. 84.

Mooney, H. M., and Wetzel W.W., 1956, The Potentials About a Point Electrode and Apparent Resistivity Curves for a two-three-, and four-layer Earth; Minneapolis, Univ. Minnesota Press, 146 p. and 243 loose sheets of reference curves. GA 166-144.

Moore, R. W. 1944. Prospecting for Gravel Deposits by Resistivity Methods. Public Roads, July, August, September 1944, Vol. 24, No. 1

Moore, R. W., 1945, An Empirical Method of Interpretation of Earth Resistivity Measurements; Trans. Amer. Inst. Min. Met. Eng. v. 164, pp. 197-223.

Moore, R. W., 1950. Geophysical Methods of Subsurface Exploration in Highway Construction. Public Roads, Vol. 26, No. 3, Aug. 1950.

Mota, L., "Determination of Dips and Depths of Geological Layers by the Seismic Refraction Method," Geoph., vol. 19, 1954, p. 242.

Neale, R. N., "The Use of Isochron Charts in Seismic Refraction Interpretation," Geoph. Prosp., 1964, p. 214.

Nettleton, L. L., 1940, Geophysical Prospecting for Oil; McGraw-Hill Book Co. Inc., New York.

Obert, Leonard, and Duvall, "Generation and Propagation of Strain Waves in Rock," Part 1: Bur. of Mines Rpt. of Inv. 4683, 1950, 19 pp.

O'Brien, P.N.S., "Model Seismology - the Critical Refraction of Elastic Waves," Geoph., 1955, p. 227.

-------, "The Variation with distance of the Amplitude of Critically Refracted Waves," Geoph. Prosp., 1957, p. 300.

-------, "The Use of Amplitudes in Refracting Shooting - A Case History," Geoph. Prosp., 1960, p. 417.

Officer, Jr., C. B., "The Refraction Arrival in Water-Covered Areas," Geoph., 1953, p. 805.

Pakiser, L. C., and R. A. Black "Exploring for Ancient Channels with the Refraction Seismograph," Geoph., 1946, p. 32.

Paterson, N. R., and T. Meidav," Geophysical Methods in Highway Engineering," Huntec Ltd., Toronto, Canada. Paper presented at 48th Ann. Conv. of the Canadian Good Roads Assoc., Sept. 1965.

Phelps, J. M., 1964. Applied Shallow Seismology for Engineering, Construction, and Research. Manual No. 4611-641. Joseph M. Phelps and Associates, 2955 E. Colorado Blvd., Pasadena, California, 91107.

Prill, R. C. and W. R. Meyer, 1968. Neutron Moisture Measurements by Continuous- and Point-Logging Procedures. U. S. Geological Survey Prof. Paper 600-B, pp. 226-230.

Quarles Miller, Jr., 1950. Fault Interpretation in Southwest Texas. Geophysics, Vol. 15, pp. 462-476.

Roman, Irwin, 1960, Apparent Resistivity of a Simple Uniform Overburden; U. S. Geol. Survey Prof. Paper 365.

Rosenbaum, J. H., "Refraction Arrivals through Thin High-Velocity Layers (Attenuation Wave)," Geoph., 1965, p. 204.

Scholen, Douglas E., (about 1963). The Seismic Timer and Road Design. U.S.D.A. Forest Service, Arcadia, California. (Discusses rippability of rock and the use of the shear geophone).

Sendlein, Lyle V. A., 1967. Seismic Refraction and Electrical Resistivity: Tools in Groundwater Exploration. Paper No. 67-726, American Society of Agricultural Engineers. December 1967.

Slotnick, M. M., "A Graphical Method for the Interpretation of Refraction Profile Data," Geoph., 1950, p. 163.

Smythe, Richard E., (about 1964). Utilization of the Seismograph in the Construction Industry. Geo Space Corporation, 5803 Glenmont Drive, Houston, Texas, 77036.

Soiltest, Inc., 2205 Lee St., Evanston, Illinois, 60202. Instruction manuals for the operation and interpretation of their equipment, including the MD, the Terra-Scout, and the Michimho Resistivity Meter.

Soiltest, Inc., 1968, Earth Resistivity Manual, Soiltest, Inc., Evanston, Ill., 52 pp.

Sypherd, W. O., A. M. Fountain, and S. Brown, 1943. the Engineers Manual of English; Scott, Foresman and Co., New York.

Soske, J. L., "Discussion on the Blind Zone Problem in Engineering Geophysics (Refraction,")Geoph., 1949, p. 359.

Stam, J. C., "Modern Developments in Shallow Seismic Refraction Techniques," Geoph., vol. 27, April 1962, pp. 198-212.

Tapp, W. N., 1960. Resistivity Method Scans Geologic Conditions. Johnson National Drillers' Journal. September - October 1960, pp. 3-6.

Tarrant, L. H., "A Rapid Method of Determining the Form of a Seismic Refractor from Line Profile Results," Geoph. Prosp., 1956, p. 131.

Todd, D. K. 1955. Investigating Ground Water by Applied Geophysics. American Society Civil Engineers Trans. v. 81, separate 625, 13 p.

Todd, D. K., 1959, Ground Water Hydrology., John Wiley & Sons, Inc., New York, pp. 219-244.

U. S. Army Corps of Engineers., 1948. Geophysical Exploration. Engineering Manual, Civil Works Construction, Part CXVIII, Chapter 2.

U. S. Dept. Agriculture, Soil Conservation Service, 1968. Guide to Geologic Site Exploration, South RTS Area. EWP Technical Guide No. 4, Fort Worth, Texas, 76110.

U. S. Department Agriculture, Soil Conservation Service, 1963. Section 8, Engineering Geology. National Engineering Handbook. Washington, D. C. 20250.

U. S. Forest Service. Construction Handbook, Blastir Section.

Van Nostrand, R. G., and K. L. Cook, 1966. Interpretation of Resistivity Data. Geol. Survey Prof. Paper 499. U. S. Dept. of Interior, Washington, D. C., 310 pp. illus. Govt. Printing Office $2.75.

Van Zelst, Th. W., 1965. Geophysical Instruments in Highway Planning. Soiltest, Inc., Evanston, Illinois.

Warner, Don L., 1969, Preliminary Field Studies Using Earth Resistivity Measurements for Delineating Zones of Contaminated Ground Water; Ground Water, v. 7, no. 1, pp. 9-16.

Warrick, R. E., and J. D. Winslow, "Application of Seismic Methods to a Ground-Water Problem in Northeastern Ohio," Geoph., 1960, p. 505.

West, S. S., "Dependence of Seismic Velocity upon Depth and Lithology," Geoph., 1950, p. 653.

Wetzel, W. W., and McMurry, H. V., 1937, A Set of Curves to Assist in the Interpretation of the Three-layer Resistivity Problem; Geophysics, v. 2, pp. 329-341.

White, J. E., and R. L. Sengbush, "Velocity Measurements in Near-Surface Formations," Geoph., 1953, p. 54.

White, J. E., and R.L. Sengbush, "Shear Waves from Explosive Sources," Geoph., 1963, p. 1001.

Wilson, S. D., and R. T. Dietrich, "Effect of Consolidation Pressure on Elastic and Strength Properties of Clay," ASCE Res. Conf. on Shear Strength of Cohesive Soils, Boulder, Colo., 1960, pp. 419-435.

Wyllie, M. R., A. R. Gregory and L. W. Gardner, "Elastic Wave Velocities in Heterogeneous and Porous Media," Geoph., 1956, p. 41.

------, "An Experimental Investigation of Factors Affecting Elastic Wave Velocities in Porous Media," Geoph. 1953, p. 459.

Wyrobek, S. M., "Application of Delay and Intercept Times in the Interpretation of Multi-layer Refraction Time-Distance Curves," Geoph. Prosp., 1956, p. 112.

GENERAL INDEX